



# Instituto Universitário de Lisboa

Departamento de Ciências e Tecnologias de Informação

## Propagation model for cellular mobile networks used in UAVs communications environments

André de Sousa Silvério

Dissertação submetida como requisito parcial de obtenção do grau de

Mestre em Engenharia de Telecomunicações e Informática

Orientador:

Prof. Pedro Joaquim Amaro Sebastião,

Professor Auxiliar, ISCTE-IUL

Co-orientador:

Prof. Alexandre Almeida,

Professor Auxiliar, ISCTE-IUL

Agosto 2017



## ABSTRACT

Recognizing the growth of the drone market in recent years, it is crucial to evaluate the capacity of the mobile communications technologies as well as their infrastructure to verify if these are capable to support various applications and services that may associate with these type of vehicles, achieving lower costs to the users. The type of application chosen for this thesis is a video streaming that is able to assume different qualities depending on the RF conditions, in order to overcome the limitation of radio communications, in which the user is only able to communicate with the drone when in his line of sight.

It was necessary to take into account a propagation model that considered the unique characteristics of an UAV, since the most commonly used models only consider a typical mobile user moving below the level of the BSs and their respective antennas using a short/medium frequency interval that is not able to consider the third and fourth generation technologies at once. In order to choose the ideal model, a theoretical study was carried out, which allowed to conclude that Lisbon University Institute Model is the most accurate since it is able to fulfill the requirements associated to a flying drone, considering a larger frequency spectrum, allowing the use of third and fourth generation technologies that are fundamental to support multimedia services, such as video streaming.

To verify the viability of mobile communications, measurements were made in three real scenarios in rural areas using a spectrum analyzer carried by a flying drone, in order to monitor, read and write the data related to the signal's behavior into a file, during the flight route.

Based on this approach, it was possible to analyze the viability of mobile communications for a video streaming service using a drone, in a rural environment and considering UMTS and LTE technologies. In addition, evaluate the signal's performance when the drone is above the antennas where the "hole phenomenon" occurs, theoretically.

**Keywords:** Cellular/Wireless Networks, Mobile Communications, UAV, Propagation Models, LTE, UMTS, Drones

*This page was intentionally left in blank*

## RESUMO

Tendo em conta o crescimento que o mercado de drones tem tido nos últimos anos, é importante considerar as tecnologias de comunicações móveis assim como as respectivas infraestruturas e verificar se estas são capazes de suportar diversas aplicações que podem estar associadas a estes veículos, permitindo isto um custo inferior para os utilizadores dos mesmos. O tipo de aplicação escolhida para esta tese foi uma streaming de vídeo, com o objetivo de ultrapassar a limitação das comunicações rádio, em que o utilizador apenas consegue comunicar com o drone caso este se encontre no seu campo de visão.

Foi necessário ter em conta um modelo de propagação que considerasse as características únicas de movimentação dum drone, uma vez que os modelos mais utilizados apenas consideram um utilizador móvel comum que se desloque abaixo do nível das estações base e respetivas antenas para um espectro de frequências curto/médio. Para a escolha deste modelo, foi realizado um estudo teórico que permitiu concluir que o *Lisbon University Institute Model* é o mais acertado, uma vez que é capaz de cumprir os requisitos associados a um drone, considerando um intervalo de frequências maior, permitindo a utilização das tecnologias de terceira e quarta geração, que são fundamentais para suportar aplicações multimedia, como é o caso da streaming de vídeo. Para verificar a viabilidade das comunicações móveis, foram feitas medições em três cenários reais em zona rural recorrendo a um analisador de espectros transportado por um drone, com o objetivo de monitorizar, fazer a leitura e gravação de dados associados ao comportamento do sinal para um ficheiro durante a rota de voo.

Com esta abordagem, foi possível analisar a viabilidade das comunicações móveis para a aplicação de *streaming* de vídeo num drone, em cenário rural, considerando as tecnologias UMTS (3G) e LTE (4G). Para além disso, foi ainda possível avaliar o comportamento do sinal quando o drone se encontra acima do eixo vertical das antenas, onde o “fenómeno do buraco” ocorre.

**Palavras-chave:** Redes celulares, Comunicações móveis, Modelos de propagação, LTE, UMTS, Drones

*This page was intentionally left in blank*

## ACKNOWLEDGMENTS

I will take this opportunity to express my gratitude to my supervisor Prof. Pedro Sebastião for the support, patience, motivation, availability and shared knowledge throughout the year. His guidance helped me to follow the correct path with the right thoughts, the correct attitude and without his help, I wouldn't be able to reach the right persons and companies to supply the necessary instruments for this thesis.

Furthermore, I would like to give a special thanks to Eng. Ricardo Freitas from Rohde & Schwarz, for trusting me and giving me the responsibility to take care of an expensive instrument since without it, I wouldn't be able to get such reliable results.

I would like to thank my colleague, Ricardo Silva, for providing a drone capable of lifting the spectrum analyzer and for all the effort on preparing, adjusting and controlling it to recreate a real-world scenario, in order to obtain a successful measurement campaign. Also, I would like to thank António Raimundo from IT for the interest and availability to help me and Ricardo S. during the measurements week.

At last, but not least, I would like to thank my loved ones, specially my mom, who kept me motivated and focused during my academic path.

*This page was intentionally left in blank*



# TABLE OF CONTENTS

ABSTRACT .....	III
RESUMO .....	V
ACKNOWLEDGMENTS .....	VII
TABLE OF CONTENTS .....	IX
TABLE OF FIGURES .....	XI
TABLE OF TABLES .....	XII
TABLE OF GRAPHICS .....	XIII
SYMBOLS .....	XV
ACRONYMS & ABBREVIATIONS .....	XVII
CHAPTER 1 INTRODUCTION.....	1
1.1 Overview .....	2
1.2 Motivation .....	3
1.3. Objectives .....	4
1.4. Contributions .....	5
1.5. Dissertation Structure .....	5
CHAPTER 2 CONCEPTS .....	7
2.1 Cellular Networks.....	8
2.1.1 GSM .....	9
2.1.2 UMTS .....	12
2.1.3 LTE.....	13
2.1.3 Handover .....	15
2.2. Drone .....	18
2.3. Spectrum Analyzer .....	19
2.4. Frequency bands .....	21
CHAPTER 3 PROPAGATION MODELS AND PROPOSED MODEL.....	22
3.1. Overview .....	23
3.2. Propagation models .....	23
3.2.1. Okumura Model.....	23
3.2.2. Hata Model .....	28
3.2.3. Cost 231-Hata Model.....	29
3.2.4. COST 231 – Walfish-Ikegami Model .....	30
3.2.5. Erceg Model (or basic SUI model).....	31
3.2.6. LUI Model .....	33
CHAPTER 4 MEASUREMENTS .....	40
4.1. Overview .....	41
4.2. Measurement campaign requirements .....	43
4.3. Locations and flight routes .....	45
4.4. Measurement results .....	48
4.4.1. Scenario A .....	52
4.4.2. Scenario B .....	60

4.4.3. Scenario C .....	65
CHAPTER 5 CONCLUSIONS .....	71
5.1. Main conclusions .....	72
5.2 Future Work.....	74
ANNEX A ROMES SOFTWARE .....	76
ANNEX B MEASUREMENT RESULTS .....	93
B.1. Scenario A: .....	94
• LTE (796 MHz Channel) .....	94
• UMTS (2152.4 MHz Channel): .....	96
• UMTS (2157.4 MHz Channel): .....	97
B.2. Scenario B:.....	99
• LTE (796 MHz Channel):.....	99
• UMTS (2152.4 MHz Channel): .....	101
B.3. Scenario C:.....	103
• LTE (806 MHz Channel):.....	103
• UMTS (2117.8 MHz Channel): .....	106
ANNEX C ADDITIONAL STATISTIC .....	108
Overview .....	109
C.1. Scenario A.....	109
LTE.....	109
UMTS .....	113
C.2. Scenario B.....	117
LTE.....	117
UMTS .....	120
C.3. Scenario C.....	123
LTE.....	123
UMTS .....	126
REFERENCES .....	130

## TABLE OF FIGURES

Figure 2- 1. Cellular Networks technologies evolution, Source: [4].....	9
Figure 2- 2. GSM Coverage Worldwide, Source: [5] .....	10
Figure 2- 3. GSM Architecture, Source: [6].....	11
Figure 2- 4. UMTS Architecture, Source: [8] .....	12
Figure 2- 5. Network infrastructure from GSM to LTE, Source: [11] .....	14
Figure 2- 6. OFDMA (DL) and SC-FDMA (UL), Source: [11] .....	14
Figure 2- 7. Hard Handover, Source: [13] .....	16
Figure 2- 8. Soft Handover, Source: [13].....	17
Figure 2- 9. Softer Handover, Source: [13].....	17
Figure 2- 10. Inter-LTE/RAT Handover, Source: [15] .....	18
Figure 2- 11. Intra-LTE Handover, Source: [15] .....	18
Figure 2- 12. Octocopter (drone) with TSMA attached (under it) .....	19
Figure 2- 13. Spectran HF-60100, Source: [16].....	19
Figure 2- 14. R&S TSME scanner connected to a PC, Source: [18].....	20
Figure 2- 15. R&S TSMA scanner and TSMA-BP (battery pack), Source: [20].....	21
Figure 3- 1 - Median attenuation related to free space (Okumura model), Source: [23] .....	25
Figure 3- 2. BS Effective Height gain, Source: [23] .....	25
Figure 3- 3. Mobile height gain factor, Source: [23].....	26
Figure 3- 4. Correction factor for different types of terrain, Source: [23] .....	27
Figure 3-5. Rectangular function, Source: [1].....	35
Figure 3-6. Unit step function, Source: [1] .....	36
Figure 3-7. Angles associated to the antenna, Source: [1] .....	37
Figure 3-8. Sectorial choice and identification, Source: [1].....	38
Figure 4- 1. Proposed flight plan: X(distance) and Y(altitude) axes.....	41
Figure 4-2. R&S TSMA accessories, Source: [32] .....	43
Figure 4-3. R&S TSMA - Rear Panel, Source: [32] .....	43
Figure 4-4. R&S TSMA and TSMA-BP with some accessories connected, Source: [32].....	44
Figure 4-5. Equipment attached below the drone with velcro tape .....	44
Figure 4-6. Base Station A (MEO).....	45
Figure 4-7. Scenario A (BS A) and respective flight route .....	46
Figure 4-8. Scenario B (BS A) and respective flight route .....	46
Figure 4-9. Base Station B (Vodafone).....	47
Figure 4-10. Scenario C and respective flight route.....	48
Figure 4-11. 5 MHz channels UMTS Band I (DL) .....	51
Figure 4-12. 10 MHz channels LTE Band 20 .....	51
Figure 4-13. 20 MHz channels LTE Band 3 .....	51
Figure 4-14. Different SC associated to each NodeB plan [36].....	56
Figure 7- 1. Radiation pattern example vertical plane (Kathrein 742215), Source: [37] .....	73
Figure A- 1. Remote Desktop Connection to access TSMA UI.....	77
Figure A- 2. WLAN connection between TSMA and laptop.....	77
Figure A- 3. ROMES software icons .....	78
Figure A- 4. StartUp window of ROMES software .....	78
Figure A- 5. User levels .....	79
Figure A- 6. Empty workspace .....	79

Figure A- 7. List of devices connected to TSMA connected to ROMES, Source: [34].....	80
Figure A- 8. Add/Remove drivers, Source: [34] .....	80
Figure A- 9. Available and loaded drivers (example), Source: [34] .....	81
Figure A- 10. Generated view areas labels.....	81
Figure A- 11. RAT selection, Source: [34] .....	82
Figure A- 12. Frequency interval, Source: [34] .....	82
Figure A- 13. Frequency bands available, Source: [34].....	82
Figure A- 14. ACD view area (before and during measurement) .....	83
Figure A- 15. ROMESMAP Route Track View area (during measurement) .....	83
Figure A- 16. GSM Scanner Top N View during measurement .....	84
Figure A- 17. GSM Scanner Top N Configuration, Source: [34] .....	84
Figure A- 18. GSM Scanner BCH Tree View during measurement.....	85
Figure A- 19. Power Spectrum Overview .....	86
Figure A- 20. Details of the selected sweep.....	86
Figure A- 21. Spectrum History of the selected sweep .....	86
Figure A- 22. Available signals.....	86
Figure A- 23. Tools menu .....	87
Figure A- 24. General settings .....	87
Figure A- 25. Performance tab settings.....	88
Figure A- 26. TSMA connections settings.....	88
Figure A- 27. Save workspace file .....	88
Figure A- 28. Start recording button, Source: [34] .....	89
Figure A- 29. Stop button, Source: [34].....	89
Figure A- 30. Export measurement file to another extension .....	89
Figure A- 31. Export measurement data menu.....	90
Figure A- 32. Measurement file to export.....	90
Figure A- 33. Available devices in selected measurement file .....	90
Figure A- 34. ScannerData Export settings.....	91
Figure A- 35. Measurement file (* .rscmd).....	91
Figure A- 36. Scanner data export result (folder and KML file).....	91
Figure A- 37. Folder content .....	91

## TABLE OF TABLES

Table 2- 1. Frequency of the carrier according to region, Source: [9] .....	13
Table 2- 2. Major differences between UMTS and LTE (theoretical), Source: [12] .....	15
Table 3- 1. K value according to d and f units .....	24
Table 3- 2. Parameter values for different types of terrain, Source: [27].....	32
Table 3- 3. LUI model parameters for three different technologies, Source: [30] .....	34
Table 4-1. Recommended bit rates for video streaming, Source: [31].....	42
Table 4- 2. RSRP limits for LTE, Source: [35].....	50
Table 4-3. RSSI limits for GSM/3G(UMTS)/HSPA, Source: [35].....	50
Table 4-4. Parameter differences between UMTS and LTE .....	52
Table 4-5. Nr. of samples and respective percentage for the defined thresholds .....	54
Table 4-6. Main parameters for all sectors in reference BS .....	55
Table 4-7. Nr. of samples and respective percentage for the defined thresholds .....	57
Table 4-8. Nr. of samples and respective percentage for the defined thresholds .....	58

Table 4-9. Main parameters for all sectors in reference BS .....	60
Table 4-10. Nr. of samples and respective percentage for the defined thresholds .....	61
Table 4- 11. Main parameters for all sectors in reference BS .....	62
Table 4-12. Nr. of samples and respective percentage for the defined thresholds .....	63
Table 4- 13. Main parameters for all sectors in reference BS .....	64
Table 4- 14. Nr. of samples and respective percentage for the defined thresholds .....	66
Table 4- 15. Main parameters for all sectors in reference BS .....	67
Table 4- 16. Nr. of samples and respective percentage for the defined thresholds.....	69
Table 4- 17. Main parameters for all the cells from reference BS .....	70

## TABLE OF GRAPHICS

Graphic 3 - 1. "Below BS antenna difference using <i><math>\chi</math>angles</i> ", Source: [1] .....	38
Graphic B - 1. All sectors/cells from reference BS (eNodeB: 1675) .....	94
Graphic B - 2. Reference sector below the highest quality threshold .....	94
Graphic B - 3. Throughput vs RSRP from the reference sector .....	94
Graphic B - 4. Order 2 polynomial trendlines for every sector in reference BS .....	95
Graphic B - 5. RSRP vs Height vs Distance to BS (PCI_177) .....	95
Graphic B - 6. RSRP vs Height vs Distance to BS (PCI_178) .....	95
Graphic B - 7. RSRP vs Height vs Distance to BS (PCI_179) .....	96
Graphic B - 8. Throughput vs Time [All sectors, reference BS].....	96
Graphic B - 9. Reference sector throughput below minimum threshold.....	96
Graphic B - 10. Throughput vs RSSI [reference sector] .....	97
Graphic B - 11. Order 2 polynomial trendlines for every cell in reference BS.....	97
Graphic B - 12. Throughput vs Time [All sectors, reference BS].....	97
Graphic B - 13. Signal strength from reference sector below minimum threshold.....	98
Graphic B - 14. Order 2 polynomial trendlines for every cell in reference BS.....	98
Graphic B - 15. RSSI vs Height vs Distance to BS (Reference cell: 34164) .....	98
Graphic B - 16. RSSI vs Height vs Distance to BS (Cell 34163) .....	99
Graphic B - 17. RSSI vs Height vs Distance to BS (Cell 34162) .....	99
Graphic B - 18. Throughput vs Time considering all sectors from reference BS .....	99
Graphic B - 19. Reference sector results below VQ5 threshold.....	100
Graphic B - 20. Throughput vs RSRP for all sectors from reference BS.....	100
Graphic B - 21. RSRP vs Height vs Distance to BTS for sector 177 (adjacent).....	100
Graphic B - 22. RSRP vs Height vs Distance to BTS for sector 179 (adjacent).....	101
Graphic B - 23. RSRP vs Height vs Distance to BTS for sector 178 (reference) .....	101
Graphic B - 24. Throughput vs Time for all sectors from the reference BS .....	101
Graphic B - 25. Reference sector throughput below poorest quality threshold .....	102
Graphic B - 26. RSRP vs Height vs Distance to BTS for sector 34162 (adjacent).....	102
Graphic B - 27. RSRP vs Height vs Distance to BTS for sector 34164 (adjacent).....	102
Graphic B - 28. RSRP vs Height vs Distance to BTS for sector 34162 (reference) .....	103
Graphic B - 29. Throughput vs Time considering all the cells from the reference BS .....	103
Graphic B - 30. Reference sector throughput below the HQ threshold.....	104
Graphic B - 31. Throughput vs RSRP for reference eNodeB/BS .....	104
Graphic B - 32. RSRP vs Height vs Distance to BTS for sector 474 (adjacent).....	104
Graphic B - 33. RSRP vs Height vs Distance to BTS for sector 475 (reference) .....	105
Graphic B - 34. RSRP vs Height vs Distance to BTS for sector 476 (adjacent).....	105
Graphic B - 35. Throughput vs Time considering sector from adjacent BS .....	105
Graphic B - 36. Throughput vs Time relation – sectors from ref. and adj. BS .....	106

Graphic B - 37. Reference sector below minimum VQ threshold .....	106
Graphic B - 38. Throughput vs RSSI for every sector in reference BS .....	106
Graphic B - 39. RSRP vs Height vs Distance to BTS for sector 44894 (adjacent).....	107
Graphic B - 40. RSRP vs Height vs Distance to BTS for sector 44896 (adjacent).....	107
Graphic B - 41. RSRP vs Height vs Distance to BTS for sector 44895 (reference) .....	107
Graphic C - 1. PDF of RSRP; LTE: 796 MHz; Sc: A.....	109
Graphic C - 2. CDF of RSRP; LTE: 796 MHz; Sc: A .....	111
Graphic C - 3. CDF of Throughput; LTE: 796 MHz; Sc: A .....	112
Graphic C - 4. PDF of Throughput; LTE: 796 MHz; Sc: A.....	113
Graphic C - 5. CDF of RSSI; UMTS: 2152.4 MHz; Sc: A .....	113
Graphic C - 6. PDF of RSSI; UMTS: 2152.4 MHz; Sc: A .....	115
Graphic C - 7. CDF of Throughput; UMTS: 2152.4 MHz; Sc: A .....	116
Graphic C - 8. PDF of Throughput; UMTS: 2152.4 MHz; Sc: A.....	116
Graphic C - 9. CDF of RSRP, LTE: 796 MHz; Sc: B.....	117
Graphic C - 10. PDF of RSRP, LTE: 796 MHz; Sc: B .....	117
Graphic C - 11. CDF of Throughput; LTE: 796 MHz; Sc: B .....	119
Graphic C - 12. PDF of Throughput; LTE: 796 MHz; Sc: B .....	119
Graphic C - 13. CDF of RSSI; UMTS: 2152.4 MHz; Sc: B .....	120
Graphic C - 14. PDF of RSSI; UMTS: 2152.4 MHz; Sc: B.....	121
Graphic C - 15. CDF of Throughput; UMTS: 2152.4 MHz; Sc: B.....	121
Graphic C - 16. PDF of Throughput; UMTS: 2152.4 MHz; Sc: B .....	122
Graphic C - 17. CDF of RSRP; LTE: 806 MHz; Sc: C.....	123
Graphic C - 18. PDF of RSRP; LTE: 806 MHz; Sc: C.....	124
Graphic C - 19. CDF of Throughput; LTE: 806 MHz; Sc: C.....	125
Graphic C - 20. PDF of Throughput; LTE: 806 MHz; Sc: C.....	125
Graphic C - 21. CDF of RSSI; UMTS: 2117.8 MHz; Sc: C.....	126
Graphic C - 22. PDF of RSSI; UMTS: 2117.8 MHz; Sc: C.....	127
Graphic C - 23. CDF of Throughput; UMTS: 2117.8 MHz; Sc: C.....	127
Graphic C - 24. PDF of Throughput; UMTS: 2117.8 MHz; Sc: C .....	128

## SYMBOLS

$h_r$	Receiver antenna height
$h_t$	Transmitter antenna height
$C_H$	Antenna height correction factor
$L_0$	Free space propagation loss, which comes from FSPL formula
$L_{LOS}$	Path loss in Line of Sight situation (Walfish-Ikegami)
$L_{NLOS}$	Path loss in Non-Line of Sight situation (Walfish-Ikegami)
$L_O$	Path loss considering an open area
$L_U$	Path loss result for small city considering urban environment equation
$d_{bp}$	Breakpoint distance
$k_{TEC}$	Constant that assumes a different value according to the size of the cell
$\chi_{angles}$	Correction factor that use several parameters related to the antennas
$\chi_{\theta+\psi}$	Correction factor considering the elevation and the tilt of the antenna
$\chi_{\varphi+\beta}$	Correction factor that considers azimuth ( $\varphi$ ) and $\beta$
$A_{MU}(\mathbf{f}, \mathbf{d})$	Median attenuation related to free space
$d$	Distance between transmitter and receiver
$d_0$	Reference distance that vary according to the technology in use
$f$	Frequency of signal transmission
$G(\mathbf{h}_r)$	Mobile antenna height gain factor (receiver)
$G(\mathbf{h}_t)$	BS antenna height gain factor (transmitter)
$G_{area}$	Gain depending on the type of environment/terrain
$L_{msd}$	Multiscreen diffraction related to urban rows of buildings
$L_{rts}$	Correction factor related to diffraction and scattering from rooftop to street
$\Delta L_{b,f}$	Frequency correction factor (Basic SUI Model)
$\Delta L_{bh}$	Receiver/terminal antenna height correction factor
$B$	Channel Bandwidth
$C$	Channel Capacity/Throughput
$L$	Median value of propagation path loss
$a(\mathbf{h}_R)$	UE antenna height correction factor as described in the Hata Model for urban areas
$c$	Speed of light in vacuum ( $\sim 3 \times 10^8$ [m/s] )
$\beta$	Angle that determines in which sector the terminal station is located

$\gamma$  Path loss exponent

$\theta$  Elevation angle

$\varphi$  Azimuth

$\psi$  Tilt of the antenna



## ACRONYMS & ABBREVIATIONS

<b>2D</b>	Two coordinates system (two dimensions)
<b>3D</b>	Three coordinates system (three dimensions)
<b>3G</b>	Third Generation technologies
<b>3GPP</b>	Third Generation Partnership Project (3GPP)
<b>4G</b>	Fourth Generation technologies
<b>AuC</b>	Authentication Center
<b>BS</b>	Base Station
<b>BSC</b>	Base Station Controller
<b>BSS</b>	Base Station Subsystem
<b>BTS</b>	Base Transceiver Station
<b>CI</b>	Cell Identity
<b>CDF</b>	Cumulative Density Function
<b>CN</b>	Core Network
<b>DCS</b>	Digital Cellular System
<b>DD</b>	Digital Dividend
<b>DDF</b>	Dirac Delta Function
<b>DL DC</b>	Downlink Dual Carrier
<b>EDGE</b>	Enhanced Data rates for Global Evolution
<b>FDD</b>	Frequency Division Duplex
<b>GPS</b>	Global Positioning System
<b>GSM</b>	Global System for Mobile Communications
<b>HLR</b>	Home Location Register
<b>HSPA</b>	High Speed Packet Access
<b>IN</b>	Intelligent Network
<b>LAC</b>	Location Area Code
<b>LoS</b>	Line of Sight
<b>LTE</b>	Long Term Evolution
<b>LUI</b>	Lisbon University Institute
<b>MCC</b>	Mobile Country Code
<b>MNC</b>	Mobile Network Code
<b>MSC</b>	Mobile Switching Centre

<b>NLoS</b>	No line of sight
<b>NSS</b>	Network subsystem
<b>OFDMA</b>	Orthogonal Frequency-Division Multiple Access
<b>OS</b>	Operating System
<b>PAPR</b>	Peak to Average Power Ratio
<b>PC</b>	Personal Computer
<b>PCI</b>	Physical Cell Identity
<b>PDF</b>	Probability Density Function
<b>QoE</b>	Quality of Experience
<b>QoS</b>	Quality of Service
<b>RC</b>	Radio Communications
<b>RF</b>	Radio Frequency
<b>RNC</b>	Radio Network Controller
<b>RSCP</b>	Received Signal Code Power
<b>RSRP</b>	Reference Signal Received Power
<b>RSRQ</b>	Reference Signal Received Quality
<b>RSSI</b>	Received Signal Strength Indication
<b>SC</b>	Satellite Communication
<b>SC-FDMA</b>	Single-Carrier Frequency-Division Multiple Access
<b>SINR</b>	Signal to Interference Plus Noise Ratio
<b>SMS</b>	Short Message Service
<b>SNR</b>	Signal to Noise Ratio
<b>SUI</b>	Stanford University Interim
<b>TDD</b>	Time Division Duplex
<b>UAV</b>	Unmanned Air Vehicles
<b>UE</b>	User Equipment
<b>UMTS</b>	Universal Mobile Telecommunications System
<b>UTC</b>	Universal Time Coordinated
<b>UTRAN</b>	UMTS Terrestrial Radio Access Network
<b>VLR</b>	Visitor Location Register
<b>VQ</b>	Video Quality
<b>WCDMA</b>	Wide Band Code Division Multiple Access
<b>WLAN</b>	Wireless Local Area Networking

# **CHAPTER 1**

## **INTRODUCTION**

Overview, motivation, objectives, contributions  
and dissertation structure are available in this chapter

## 1.1 Overview

Ten years ago, it was unthinkable that UAVs could reach such success in civil and even in commercial industries. Nowadays, it is mandatory to think that not only smartphones or laptops can depend on cellular mobile networks, but also these vehicles. However, the existent propagation models do not yet consider this possibility, which is why it is so important to create or redefine some of these models to establish a solution since the UAV's market is growing exponentially, justified by the large amount of applications related to it.

Actually, most of these UAVs establish a connection to the user provided by radio communication (RC) but it is not reliable when there is no line of sight (LoS) between the two intervenient. However, it is possible to establish a link between both but only by using satellite communication (SC) that is extremely expensive and only reachable for military purposes. To overtake this problem, cellular mobile networks are an alternative to RC and SC, where the LoS and high costs will no longer be an obstacle.

The cellular mobile networks considered use UMTS and LTE technologies since they are capable to reach faster data rates and permit lower latency, which is extremely important when applications like streaming is used, since it requires large sets of data in a short period.

One of the main focus of this thesis considers the “*hole phenomenon*” that occurs above the antennas where the radiation pattern is not reachable. Considering this, it is important to examine the signal strength based on measurement campaigns since it's a crucial parameter to confirm if in a problematic situation (e.g., *weak signal strength*) it's still possible to maintain vital services for a specific application (e.g., *video streaming*) appealing to handover, or if it's not even necessary to consider this option. It is also mandatory to verify if the service provider infrastructure is prepared to solve this problem by establishing communication with another base station (*handover*) whenever it is necessary to keep providing a good signal strength to maintain an acceptable QoS when considering video streaming application.

It is possible to maintain acceptable signal strength values for video streaming application when considering an outdoor scenario and variations in 2D coordinates (e.g., altitude or distance vs signal strength) [1]. One of the challenges proposed in this reference was to study the signal's propagation when the variation between two crucial parameters occur

simultaneously (distance and altitude) in suburban and rural scenarios. In this dissertation, only rural scenarios are considered.

Besides that, it is necessary to examine a propagation model that fits the UAV's demands, its own characteristics and capabilities since these are different from the usual UEs. Lisbon University Model (LUI Model) is a possibility because it is able to support UMTS and LTE when considering correction factors and the use of experimental results [2].

## **1.2 Motivation**

Drones have a fundamental role in society based on its increasing impact in the most diverse areas. About ninety percent (90%) of the investment made in this market was only for military purposes [3], but this number tends to decrease in medium/long term since these vehicles are already in use for civil and industrial purposes with several interesting applications, whose description is below:

- Inspection and monitoring:
  - o Inspection of oil and gas platforms;
  - o Inspection of infrastructures like bridges, roads, railways, etc.;
  - o Preventive action or emergency cases.
- Surveying and mapping:
  - o Land cover classification and mapping;
  - o Surveying and mapping for cartography, topography, cadastral surveys and urban and regional development;
  - o Archeological surveys and excavation monitoring.
- Precision agriculture:
  - o Ecological and agronomic rural cultivation;
  - o Analysis of soil, health and vigor of crops.
- Condition Survey and Civil Engineering;
- Aerial Imaging – HR Photos;
- HD Film and Video.

Based on all the applications mentioned above, a well-implemented network infrastructure is crucial to guarantee a stable communication between the user and the drone. To guarantee a reliable connection, the signal's propagation conditions and the adequate propagation model are crucial parameters of analysis. To choose a certain model, several aspects are studied:

- Scenarios:
  - o Rural, suburban or urban
  - o Outdoor or indoor
- Frequency range;
- Antenna description and its characteristics: bandwidth, gain, polarization, (ir)radiation pattern, physical (e.g., transmitter/receiver antenna height) and mechanical characteristics.

### 1.3. Objectives

Considering the cellular networks potential for UAVs communication environment, it is important to upgrade or develop a new propagation model that considers all the factors that might affect the link between the controller and the vehicle by providing a good QoS in video streaming service. UMTS and LTE are the main technologies since these are capable to provide higher data rates, which are fundamental to this function. LUI is an empirical propagation model, which main concern is the urban scenario but only considering 2D and not 3D coordinates, which is necessary in this dissertation. Having this, it is mandatory to study all the scenarios using three dimensions, in order to achieve a sustainable and reliable propagation model proposal.

Besides that, the *hole* phenomenon over the antennas is also considered to conclude if we can still maintain a good signal strength, since theoretically this parameter values drop dramatically and might not guarantee an acceptable quality of service depending on the application. If that happens, it is possible to answer if the actual infrastructure for a specific service provider (e.g., NOS, Vodafone and MEO) in a certain environment and location is prepared to support this event or not.

It is possible to synthesize all this information in five topics:

1. Analyze the equipment and conclude which one meets the measurement campaigns requirements;
2. Measurement campaigns in a specific scenario (outdoor and rural) using the equipment attached to the UAV and considering a specific and controlled flight route;
3. Filter all the information provided by the instrument by studying how signal propagation behaves along the flight considering fundamental parameters (e.g., signal strength, quality, etc.), which might lead to several conclusions:

- a. Is it possible to maintain a good QoS for video streaming in every single coordinate of UAV's flight?
  - b. Is the actual infrastructure from a specific service provider prepared to handle *handover* considering UAVs characteristics (e.g., height, distance, etc.)?
4. Propose or sustain an existent propagation model (e.g. LUI model) that considers UAVs unique characteristics when compared with general UEs (e.g. smartphone, laptop, etc.), which are considered by other models (e.g. Okumura);
  5. Comparison between theoretical and empirical approaches about the "*hole phenomenon*".

#### 1.4. Contributions

This dissertation proposes to develop or sustain empirically an already existent propagation model considering cellular networks (UMTS and LTE technologies) in a 3D coordinates system where the drone changes its distance and altitude simultaneously during its flight route. Besides that, it also analyzes the capacity of a specific service provider infrastructure to handle a *handover* event, if necessary. For example, if the antennas from the reference BTS cannot provide enough conditions to handle video streaming in a specific quality and there's a great possibility that this might happen when "*hole phenomenon*" occurs (theoretically), it has to exist another adjacent BTS that is able to compensate the lack of signal conditions from the previous one and maintain an acceptable QoS.

A full paper named "Cellular networks capacity to support video broadcasting in UAVs communications environments" has been submitted to IEEE VNC 2017 conference relying on the thesis developments.

#### 1.5. Dissertation Structure

This section presents the dissertation structure, which is divided into 5 chapters:

- Chapter 1 presents the overview, motivation, the objectives for this dissertation and respective contributions.
- Chapter 2 describes the general concepts about 2G, 3G and 4G technologies used in current cellular network infrastructures, the related events that might occur during the mobile station use and the frequency bands for each in technology in

Portugal. Besides that, it also studies the physical equipment like the drone in use and its definition and also the available spectrum analyzers by comparing them and define which one is the most reliable for measurements in unique conditions.

- Chapter 3 presents the characteristics of the most used propagation models for outdoor scenarios in current cellular networks and studies whether any of the available ones is able to support the characteristics of a drone or if it requires an extension of the previous models or the development of a new one model.
- Chapter 4 reveals the measurement results for three different locations by using 2D and 3D graphs to study the “*hole* phenomenon” relying on several parameters provided by the spectrum analyzer.
- Chapter 5 shows the main conclusions of all the work done in this thesis and shares some proposals to take into account for a future project.



# **CHAPTER 2**

## **CONCEPTS**

This chapter provides crucial concepts that are (in)directly related to this dissertation's main objectives, such as UMTS, LTE technologies and *handover* phenomenon. UAV and equipment requisites for measurement campaigns are also considered.

## 2.1 Cellular Networks

The cellular network infrastructure bases on cells/sectors, which distribution is according to land areas served by at least one base station. Considering this, it is possible to provide network coverage to the cell that require voice and data traffic used in various applications. To avoid interference and maintain an acceptable QoS, each cell uses a different set of frequencies.

Considering that only base station will not provide enough radio coverage for a wide geographic area, it is necessary to join various cells from different base stations, in order to communicate between a large number of users in different locations using the same network. The fact that users might be moving from cell to cell (e.g., walk/car travel) is contemplated and it is called *handover* phenomenon.

There are several recognizable aspects in cellular networks:

- Capacity: capable to have more capacity considering the fact that uses more than a single transmitter, since the same frequency might be enable for multiple links as long as they are in different cells;
- Power: with the large quantity of base stations that exist, it is possible to conclude that the distance between these and the user is not as big as if only single large transmitter is used. Considering this, it is possible to achieve that mobile devices use less power because they are closer to the cell towers due to their quantity;
- Coverage: when compared to a single terrestrial transmitter, this parameter can be improved anytime since additional cell towers can be added indefinitely and are not limited by the horizon.

Mobile phone service carriers (e.g., Vodafone, MEO) provide these networks and each one has their own carriers. The user might pick up a cell signal provided by one of the mentioned carriers, but the signal's strength might be different in distinct locations since it depends on the carriers' licenses that define the technology in use on each cell. In

Portugal, 3G and 4G are dominant in metropolitan areas. In less populated areas, the signal might assume worst rates (e.g., GSM, EDGE) or, in the worst case, no coverage.

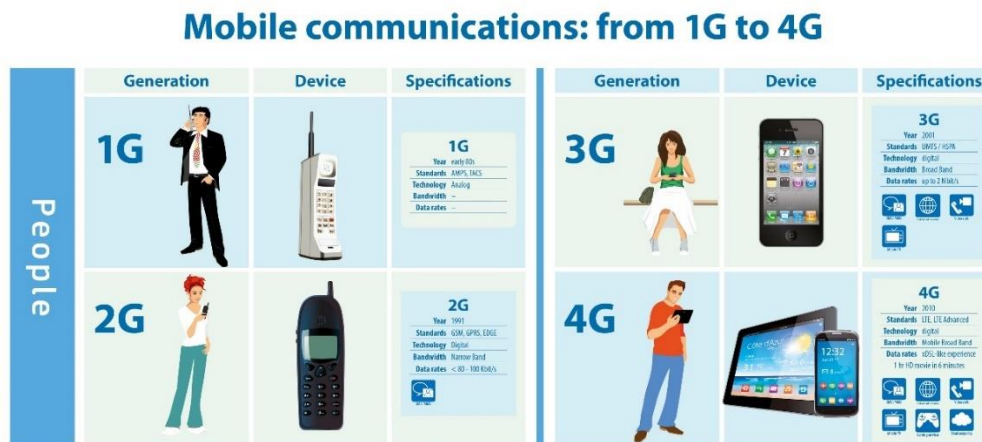


Figure 2- 1. Cellular Networks technologies evolution, Source: [4]

Nowadays, almost everyone owns a smartphone and there is an extreme necessity to send and receive large amounts of data in a short period, which relate to the content traded between users. Assuming that most of the content requires big data rates for photos, videos and streaming applications, this can only be provided when using the most advanced technologies, and that is the main reason why is so important to analyze people's tendencies and the respective evolution of cellular networks throughout the time.

### 2.1.1 GSM

Global System for Mobile Communications or GSM has become the dominant 2G radio access standard since its introduction, in the early 1990s. However, it still is widely used all over the world and there were about 3 million subscribers in 2010. Its growth has taken place with the large experienced expansion of access to the Internet, multimedia services. In addition, improvement in transmission quality, system capacity, coverage and standardization.

Speech transmission prevails to be dominant when compared to 1G, but services like SMS or fax emerged with it, by accomplishing higher demands. Regular improvements in all areas of telecommunication technology and the resulting steady price reductions for both infrastructure equipment and mobile devices were fundamental parameters to achieve it. Despite its age and the evolution toward new technologies (e.g., UMTS and LTE), GSM continues to be developed and has been enhanced with many features in recent years in

order to introduce new functionality and decrease operational cost to the service providers.



Figure 2- 2. GSM Coverage Worldwide, Source: [5]

A network based in GSM technology uses three subsystems [6]:

- Base Station Subsystem or BSS is the *radio network* and it is responsible to provide wireless connection to mobile subscribers over the radio or *air* interface by using all given nodes and functionalities from this subsystem.
- Network Subsystem or NSS is the *core network*, it contains all nodes, and functionalities that are fundamental for services like call switching, subscriber and mobility management.
- Intelligent Network Subsystem or IN can trigger optional functionalities to the network. This subsystem allows subscribers to first fund an account with a certain amount of money, which can be used later in network services like SMS, phone calls, etc. As an example, an IN node is contacted and the network operator (e.g., NOS) will deduct from a prepaid subscriber account in real time if the subscribers uses a service.

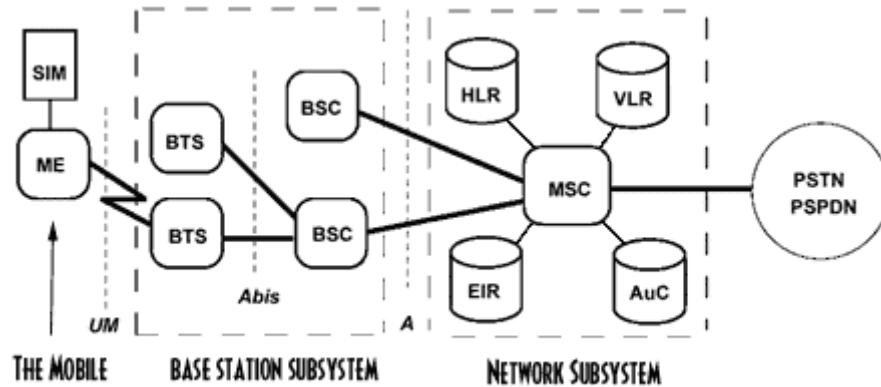


Figure 2- 3. GSM Architecture, Source: [6]

Some of the definitions from the previous illustration are available below:

- BTS – Base Transceiver Station – provides the communication between user equipment and the network. It is commonly composed by: transceiver, power amplifier, antenna, etc.
- BSC – Base Station Controller – establishment, release and maintenance of all connections of cells that are connected to a base station.
- MSC – Mobile Switching Center – connections between subscribers' management;
- VLR – Visitor Location Register – signaling reduction between the MSC and the HLR;
- HLR – Home Location Register – subscriber DB of a GSM network that stores information about the individually available services;
- AuC – Authentication Center – contains an individual key per subscriber which is a copy of the same key on the subscriber's SIM card. It is where the authentication process performs (e.g., establishment of a call and guarantees that the subscriber's id is not misused).

However, GSM was not able to meet the users' demands for better and faster data communications, which makes network and service evolution necessary in order to accomplish end users demands throughout time. EDGE (pre-3G) emerged in order to accomplish higher data rates and was able to accomplish several tasks like reduced latency, increased peak bit rate up to 1 Mbit/s by using DL DC and higher order modulations (16 and 32-QAM). Nonetheless, the 2G technologies were unable to meet the growing demand for more network capacity and 3G emerge to overtake this barrier.

### 2.1.2 UMTS

Universal Mobile Telecommunications System or UMTS is part of the third generation (3G) family, where mobile systems had the possibility to evolve and define new services like e-mail, mobile internet browsing, high speed data transfer, audio streaming (e.g., Spotify), multimedia, etc. When analyzing the previous examples, it is noticeable that UMTS network relates to data services that require newer QoS requirements, different traffic characteristics and updated bandwidth when compared to older technologies [7].

Several challenges were taking into account to develop this technology:

- Redesign the existing cellular technology to maximize the spectrum efficiency for voice and data services because GSM mainly goal was to provide high-quality voice services;
- Provide global roaming and interoperability of different mobile communications across diverse mobile environment.

Its architecture is composed in three domains: radio access network or UTRAN (Universal Terrestrial Radio Access), a core network (CN) based on the GSM Phase 2+ and the UE (e.g., smartphones, laptops, etc.).

UTRAN functionalities relate to resource management, admission control functionality and sets up the bearers enabling the user equipment to communicate with the core network.

CN manages telecommunication services for each UMTS subscriber. These services might relate to mechanisms for UE authentication, users' charging, etc.

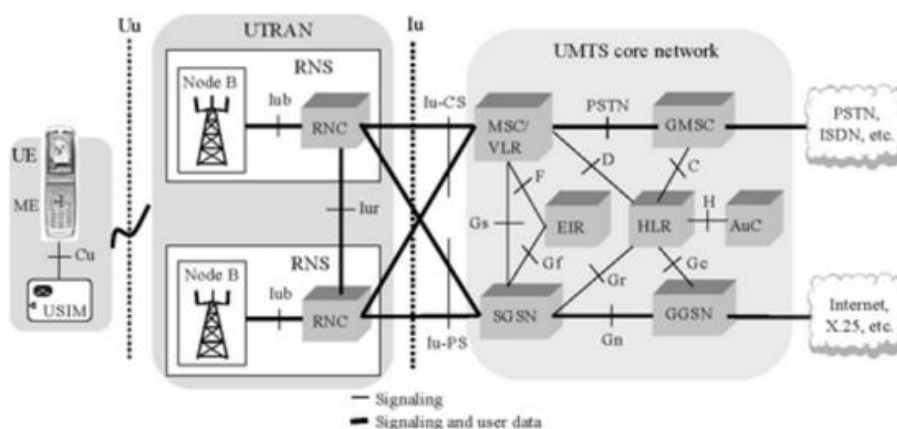


Figure 2- 4. UMTS Architecture, Source: [8]

In the same architecture, Uu and Iu stand for standardized interfaces that enable the communication between the three previous domains and also permit a UMTS operator to select different equipment suppliers for each domain.

The first release about UMTS was in March 2000 (Release 99), where it describes that two W-CDMA modes co-exist in UTRAN:

- FDD – Frequency Division Duplex – two different frequency bands are used for the uplink and downlink directions and the frequency separation between both might assume 190 MHz or 80 MHz;
- TDD – Time Division Duplex – Same frequency used for both the uplink and downlink allowing asymmetric traffic in both directions depending on the number of timeslots configured for each link.

Frequency division duplex (FDD)		Time division duplex (TDD)	
Region 1 (e.g. Europe and Africa)		Region 1 (e.g. Europe and Africa)	
1920-1980 MHz	Uplink	1900 – 1920 MHz	Uplink and
2110-2170 MHz	Downlink	2010 – 2025 MHz	Downlink
Region 2 (e.g. America)		Region 2 (e.g. America)	
1850-1910 MHz	Uplink	1850 – 1910 MHz	Uplink and
1930-1990 MHz	Downlink	1930 – 1990 MHz	Downlink
		1910 – 1930 MHz	

Table 2- 1. Frequency of the carrier according to region, Source: [9]

Besides WCDMA, 3GPP developed other technologies in 3G era. HSPA and HSPA+ are already considered as 3.5G and were the latest before 4G emerge, being able to reach a downlink data speed of 7.2 Mbit/s and 21.6 Mbit/s, respectively, against the 384 kbit/s provided by WCDMA [10]. These values are theoretical and defined by the available network service providers (e.g., NOS).

Considering the previous information, UMTS includes W-CDMA scheme using paired or unpaired 5 MHz wide channels and able to use two modes: TDD and FDD. However, downlink speed might be a limitation when comparing to HSPA and HSPA+ that are able to give greater bit rates and improves packet-switched applications [9].

### 2.1.3 LTE

Long Term Evolution emerges with the need to enhance and accomplish the following tasks [11]:

- Higher data rates at the cell edge;

- Higher capacity/spectral efficiency (e.g., end-users might be affected when capacity shortage occur);
- Cost reduction;
- Low complexity;
- Packet switch optimized system;
- Low delay;
- Frequency and bandwidth are not constant and might vary.

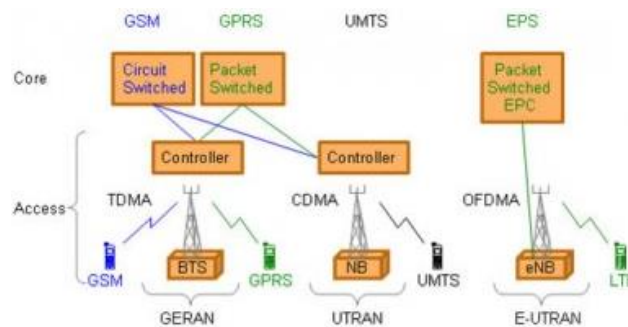


Figure 2- 5. Network infrastructure from GSM to LTE, Source: [11]

The LTE access network uses base stations denominated as eNodeB (eNB). This network uses a flat architecture where the intelligence distribution is amongst the base stations to ensure a higher speed set-up, fast communication and decisions between the eNB and the UE, and reduce delay for handover process. This process is essential when an end-user is using a real-time service that require high data peak rates (e.g., video streaming, online gaming, etc.).

LTE uses OFDMA for the downlink and SC-FDMA for the uplink, in order to achieve high radio spectral efficiency and enable efficient scheduling and frequency domain.

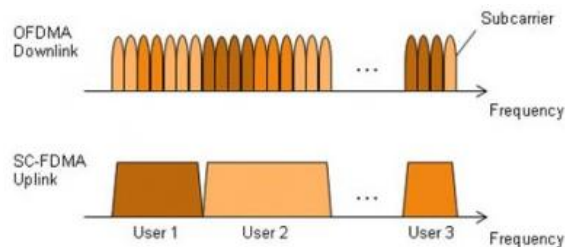


Figure 2- 6. OFDMA (DL) and SC-FDMA (UL), Source: [11]

OFDMA and SC-FDMA are modulation techniques. OFDM or Orthogonal Frequency Division Multiplexing encodes digital data in subcarriers from the available bandwidth. Orthogonal Frequency Division Multiple Access or OFDMA use these subcarriers and



share them between multiple users leading to high peak to average power ratio (PAPR) that increases the power consumption for the sender caused by power amplifiers.

SC-FDMA is the second modulation technique and creates a signal with single carrier characteristics, but the power consumption is lower when compared with OFDMA.

In order to support as many requirements as possible, LTE uses:

- E-UTRA operating bands from 700 MHz to 2.7 GHz;
- Channel bandwidths: 1.4, 3, 5, 10, 15, or 20 MHz
- Support two sub-modes: TDD and FDD
- In Release 8 from 3GPP, 8 bands specified for TDD mode were available;
- In Release 9 from 3GPP, 19 bands specified for FDD mode were available.

Feature \ System	UMTS	LTE
Duplex mode	FDD	
Multiple Access	WCDMA	OFDMA (DL) / SC-FDMA (UL)
Frequency [MHz]	[1920, 1980] for UL; [2110, 2170] for DL	Bands around 800, 900, 1800, 2100 and 2600
Switching map	Circuit and Packet Switched	Packet Switched IP-based
Scheduling	Time Domain	Time and Frequency Domains
Mobility [km/h]	Up to 250	Up to 350
Channel Bandwidth [MHz]	5	1.4, 3, 5, 10, 15, 20
Minimum frame size [ms]	2	1
Modulation	QPSK, 16QAM, 64QAM (DL); QPSK, 16QAM (UL)	QPSK, 16QAM, 64QAM (DL); QPSK, 16QAM, 64 QAM (UL)
DL Theoretical Peak Data Rate [Mbps]	42 (MIMO 2x2, 64QAM)	326 (20 MHz, MIMO 4x4, 64QAM)
UL Theoretical Peak Data Rate [Mbps]	11.5 (SISO, 16QAM)	86 (20 MHz, MIMO 2x2, 64QAM)

*Table 2- 2. Major differences between UMTS and LTE (theoretical), Source: [12]*

Analyzing the previous table, the differences between UMTS and LTE over similar parameters are notorious. LTE network is clearly superior when considering high data rate services, which makes it capable to accomplish end-users demands and achieve new established QoS requirements (theoretically).

### 2.1.3 Handover

Handover is the most important process because it provides mobility in cellular architectures and can accomplish user preferences. It enables continuity of mobile services to an end-user when in an ongoing communication and crossing the cell edge. Per example, when the end-user is at the cell edge, the signal strength provided from the

current cell might drop below a defined threshold value, making it worse when compared to another cell that can provide more favorable radio resources. Every time this situation occurs, there is a need for handover in order to maintain a good QoS.

The whole process of disconnecting from the current cell and establish a new connection in the proper cell is the *handover* process and it is equally important in voice services and data services.

There is more than one type of handover and this process might differ from technology to technology. In W-CDMA, there are three types of handover: hard, soft and softer handover.

- *Hard handover* uses the same process used for 2G networks where the radio links are broken and then re-established. In this process, user might notice a break in the connection and it might fail when re-establishing the link between the user and the new NodeB.

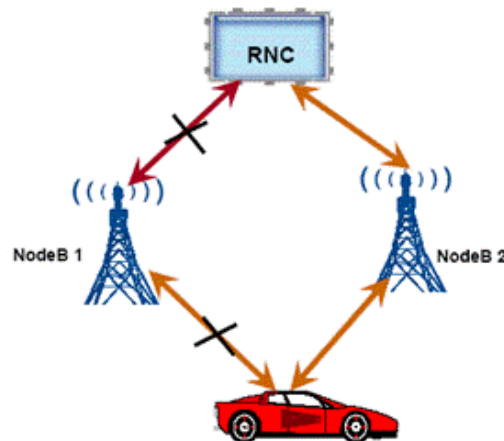


Figure 2- 7. *Hard Handover*, Source: [13]

RNC stands for Radio Network Controller (figure 2-7) and its main responsibility is to control the NodeBs connected to it, being also able to manage radio resources and mobility functions.

- *Soft handover* occurs when the UE is in the overlapping coverage area of two cells. The cell phone or UE is able to establish links with more than one base station simultaneously but these BSs have to be operating on the same frequency or channel. Having this, it will provide a more reliable way to perform handover.

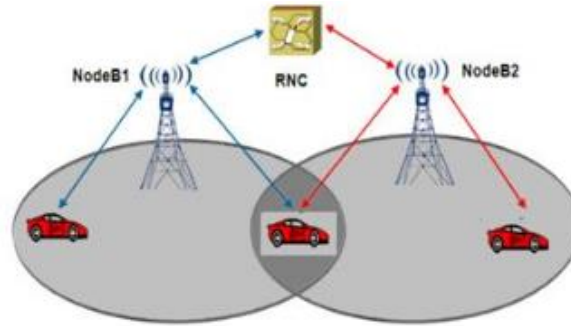


Figure 2- 8. Soft Handover, Source: [13]

- *Softer handover* is similar to soft handover, but in this case, UE establishes new radio links served from the same base station or NodeB.

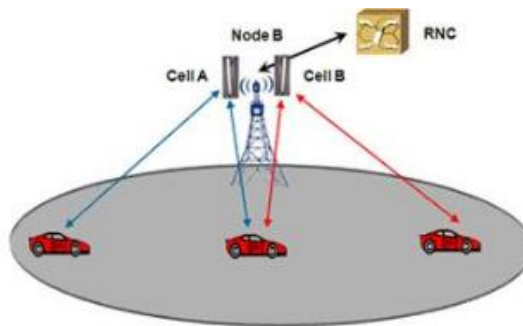


Figure 2- 9. Softer Handover, Source: [13]

Briefly, UMTS handover methodology evaluates information about the signals received by UE and the base station, considering parameters like RSCP and RSSI. When these parameters decrease significantly, assume values below a defined threshold and there is another available radio channel, which is able to improve radio resources, it triggers handover process [14].

There are also three types of handover in LTE network: Intra-LTE Handover, Inter-LTE Handover and Inter-RAT.

- Inter-LTE/Inter-RAT handover - the UE leaves an eNodeB sector to a sector controlled by an adjacent or neighbor eNodeB.

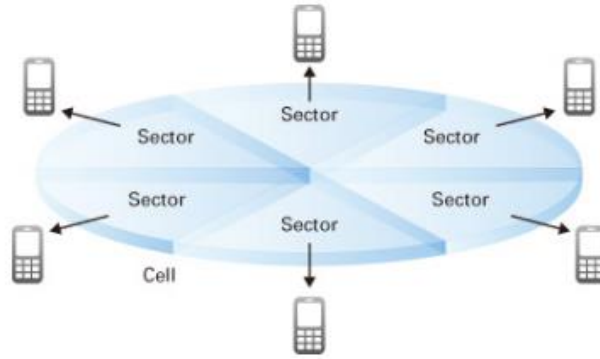


Figure 2- 10. Inter-LTE/RAT Handover, Source: [15]

- Intra-LTE handover - UE moves from one sector to another sector and both sectors belong to the same eNodeB.

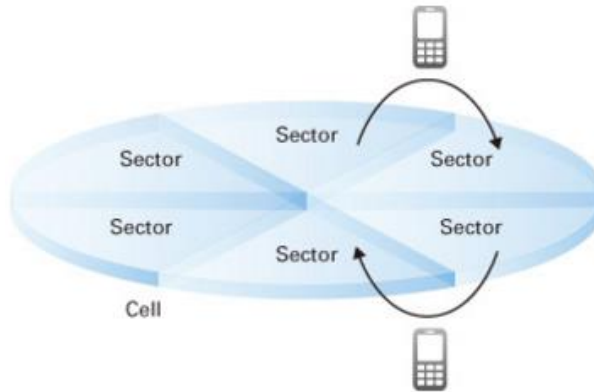


Figure 2- 11. Intra-LTE Handover, Source: [15]

## 2.2. Drone

Drones can fly autonomously using onboard computers, but also under remote control by a human operator where RC is the most common type of communication established between the controller and the vehicle, but it is not efficient when there is no line of sight. Cellular networks might be effective in both cases mentioned above, because the distance between the intervenient could be larger and the user controlling it could see what the drone is filming by using video streaming application supported by these networks. Considering this, it is crucial to verify the reliability and capacity of the actual infrastructure by using a real-life drone to simulate several flight routes attaching the spectrum analyzer to the UAV that will receive essential parameters based on UMTS and LTE technologies and will lead us to answer whether video streaming is possible and in what conditions.



*Figure 2- 12. Octocopter (drone) with TSMA attached (under it)*

In this case, only an UAV that lifts the spectrum analyzer's weight (~2.5 kg) is able to do measurement campaign. However, in order to simulate a real-life scenario, the octocopter represented in the figure 2-12 is used.

### 2.3. Spectrum Analyzer

The analysis of the possible spectrum analyzers is required before concluding which one would accomplish this dissertation's challenges/requisites in measurement campaigns:

- 1) Spectran HF-60100 is a measurement device that uses a frequency dependent measurement approach, the so-called spectrum analysis. It determines the signal strength for every individual signal in a certain frequency range defined by the user. However, the battery does not last long (~20 minutes), the memory size is limited in autonomous mode and the output parameters are not enough to obtain a sustainable conclusion.



*Figure 2- 13. Spectran HF-60100, Source: [16]*

- 2) R&S TSME is a scanner that measures up to eight different technologies simultaneously in the 350 MHz to 4.4 GHz. It is compact, lightweight, low power consumption and it has an internal GPS. Besides that, it also provides information related to base station ID, signal strength/quality, SINR and several codes (MCC

and MNC) that will permit to identify the service providers. The only defect is that needs a full-time connection to a host PC [17].



Figure 2- 14. R&S TSME scanner connected to a PC, Source: [18]

- 3) R&S TSMA is similar to TSME but the main difference between the two is that TSMA is battery powered with rechargeable batteries and charging function, ensuring that is always ready to operate. It delivers all measurement results required for optimizing LTE networks. These include power and quality measurements (RSRP, RSRQ, SINR) on reference signals for all eNodeBs transmission ports. Having this, it'll be possible to analyze and detect radio dead zones (e.g., “hole phenomenon”) or locations with too much interference. TSMA already comes with ROMES software, where it is possible to analyze the signal's behavior while the instrument is capturing it from several base stations that use different technologies (e.g., GSM, UMTS, and LTE) and/or save it in measurement files for posterior analysis [19].

The only requirement to access Windows OS in TSMA is a monitor or a tablet/smartphone/laptop connected to it using WLAN or Bluetooth to provide a user interface for previous configuration before starting the measurement campaign and for posterior analysis when access to measurement files is required. In this case, the only defect is the weight (~ 2.5 kg) but it is possible to overcome this problem by using a medium/heavy weight drone (e.g., octocopter).



Figure 2- 15. R&S TSMA scanner and TSMA-BP (battery pack), Source: [20]

After evaluating these three analyzers, it is clear that R&S TSMA Scanner together with a battery pack is the first choice because it accomplishes the most important challenges when compared to the others: battery autonomy and independency.

## 2.4. Frequency bands

This section pretends to share the frequency bands in use in Portugal territory for GSM, UMTS and LTE networks. The well-known network service providers in Portugal: MEO, NOS and Vodafone, use most of the bellow frequency bands [21].

- GSM:
  - E-GSM (900 MHz)
  - DCS (1800 MHz)
- UMTS:
  - B1 (2100 MHz)
  - B8 (900 MHz)
- LTE:
  - B3 (1800 +)
  - B7 (2600 MHz)
  - B20 (800 DD)

# **CHAPTER 3**

# **PROPAGATION MODELS AND PROPOSED MODEL**

This chapter describes the most used propagation models in actual cellular networks and proposes a new model or support empirically to an already existent one.



### 3.1. Overview

Propagation models are able to provide an attenuation estimation based on the transmitted signal that previews its behavior for different types of scenario. Nonetheless, there are three types of propagations models: empirical, theoretical and hybrid [22]. The characteristics for each different model are below:

- Empirical model:
  - Considers measurement data;
  - Simple relation between attenuation and distance
  - Ponder all the factors that affect the signal's propagation;
  - Consider a specific scenario to study this model.
- Theoretical model:
  - Uses topographic databases;
  - Counts some factors that might affect the signal's propagation but not all;
  - The scenario is irrelevant.

At last, hybrid models conjugate both empirical and theoretical models and it is able to reduce the error percentage by considering the relation between the estimated and the measured signal, which makes it more accurate.

This project bases on measurement campaigns, which coincides with the empirical model characteristics. Considering this, it is important to evaluate the already existing propagation models in order to reduce the number of possibilities and verify which adapts to the thesis requirements (e.g., scenarios, UAVs characteristics, technologies, etc.).

### 3.2. Propagation models

This section provides information about the existent propagation models for outdoor environments and it synthesizes the characteristics of each.

#### 3.2.1. Okumura Model

Okumura model is one of the most known models in use for signal prediction and its impact area is mainly in cities. However, its structure bases in three modes: urban, suburban and open areas [23].

This model's mathematical formulation is:

$$L \text{ [dB]} = L_0 \text{ [dB]} + A_{MU} \text{ [dB]} - G(h_t) - G(h_r) - G_{area} \quad (3.1)$$

The equation (3.1) depends on several parameters, which explanation is as it follows:

- $L \text{ [dB]}$  – median value of propagation path loss;
- $L_0 \text{ [dB]}$  – free space propagation loss, which comes from FSPL formula calculation;
- $A_{MU}(f,d) \text{ [dB]}$  – median attenuation related to free space;
- $G(h_t)$  - BS antenna height gain factor (transmitter);
- $G(h_r)$  - mobile antenna height gain factor (receiver);
- $G_{area}$  – gain depending on the type of environment/terrain.

In order to get a result from the previous formula, it is important to calculate FSPL in decibels (dB):

$$FSPL_{linear} = \left( \frac{4\pi df}{c} \right)^2 \quad (3.2)$$

$$FSPL_{[dB]} \text{ or } L_{0[dB]} = 20\log_{10}(d) + 20\log_{10}(f) + K \quad (3.3)$$

Based on the two preceding formulas,  $c$  stands for speed of light in vacuum ( $\sim 3 \times 10^8 \text{ [m/s]}$ ),  $d$  is the distance between the transmitter and receiver,  $f$  is the signal frequency and  $K$  is a constant that can assume more than one value since it depends on the previous parameters units and the following table is able to explain it:

K value	Distance units	Frequency units
92.45	Kilometers [km]	Gigahertz [GHz]
-87.55	Meters [m]	Kilohertz [KHz]
-27.55	Meters [m]	Megahertz [MHz]
32.45	Kilometers [km]	Megahertz [MHz]

Table 3- 1. K value according to d and f units

$A_{mu}(f,d)$  result is also required but it depends on the reference height of the base station and mobile antennas, which are 200 m and 3 m, respectively. If the real heights from the transmitter and receiver antennas or if the propagation type differ from the reference results, corrections implementation are mandatory. However, the following illustration

shows the results for the reference heights in an urban environment over a quasi-smooth terrain.

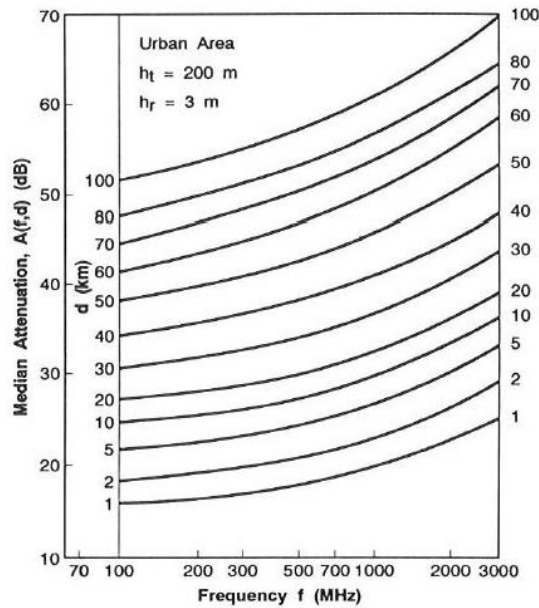


Figure 3- 1 - Median attenuation related to free space (Okumura model), Source: [23]

The gains from the transmitter ( $G_{ht}$ ) and receiver ( $G_{hr}$ ) antennas are also mandatory:

$$G(h_t) = 20 \log \left( \frac{h_t}{200} \right) \quad 30 \text{ m} < h_t < 1000 \text{ m} \quad (3.4)$$

The value “200” present in the only fraction from the previous formula stands for the base station antennas reference height. However, this formula is only useful if the transmitter antennas do assume heights between 30 and 1000 m. The following figure illustrates the gain’s behavior considering that interval.

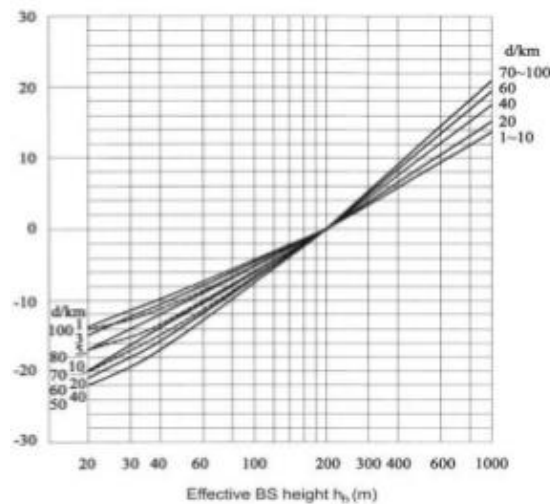


Figure 3- 2. BS Effective Height gain, Source: [23]

Unlike the previous situation,  $G_{hr}$  depends on the mobile's height and uses two formulas. However, the results might vary according to the operating frequency, which is more noticeable when the mobile is closer to upper limit height ( $\sim 10$  meters).

$$G(h_r) = 10 \log\left(\frac{h_r}{3}\right), \quad h_r \leq 3 \text{ m} \quad (3.5)$$

$$G(h_r) = 20 \log\left(\frac{h_r}{3}\right), \quad 3 \text{ m} < h_r < 10 \text{ m} \quad (3.6)$$

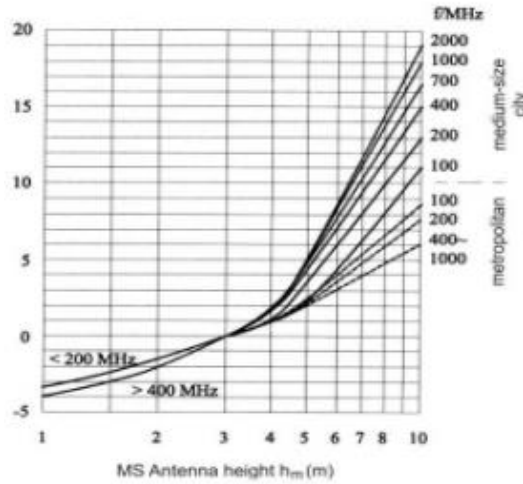


Figure 3- 3. Mobile height gain factor, Source: [23]

It is possible to conclude that mobile antennas that assume heights below 3 meters cause loss of referent signal level. When at 3 meters height, the gain is null. However, from 3 to 10 meters height, the antennas introduce gain that tend to increase while increasing the altitude, until it reaches its maximum gain at 10 meters height, which is the maximum limit for this model.

At last,  $G_{area}$  is the only parameter missing to calculate the median value of propagation path loss, which stands for correction factor and varies according to the type of environment, as it is possible to realize from the following illustration:

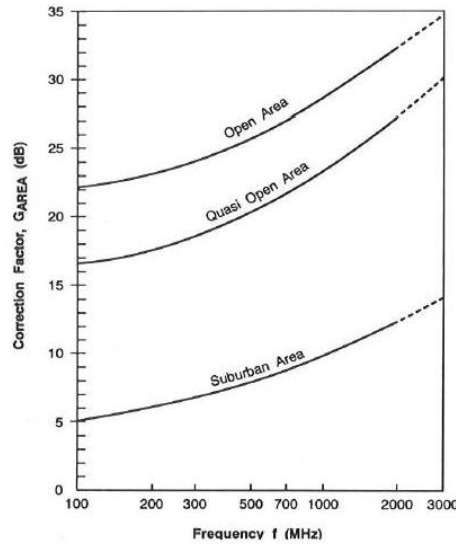


Figure 3- 4. Correction factor for different types of terrain, Source: [23]

In this case, different types of terrain assume distinct gain values that also vary according to the operating frequency. Open area environment is the only one that coincides with the proposed scenarios in this dissertation.

In the end, it is possible to summarize this propagation model considering the following characteristics:

- Frequency  $f$ : (150-1920) [MHz] but can extrapolate up to 3000 MHz
- Distance  $d$ : (1 – 100) [Km]
- BS antenna height ( $h_e$ ): (30 – 1000) [m]
- UE antenna height ( $h_r$ ): (1 – 10) [m]

The main technique to determine the path loss follows three steps:

1. Determine free space path loss between the transmitter and the receiver;
2. Read the value  $A_{mu}(f,d)$  from the curves in the graphic represented in figure 12 and also consider correction factors related to the type of terrain;
3. The remaining graphics are able to provide the gain values:  $G_t$ ,  $G_r$  and  $G_{area}$ ;

This propagation model does not fit in the scenarios considered in this dissertation measurement campaigns because the UE height maximum limit in this model is not high enough when comparing to the heights that UAV might assume (~ 60 meters).

### 3.2.2. Hata Model

Hata or Okumura-Hata model interprets graphical information from Okumura model, but it considers effects like diffraction, reflection, and scattering caused by cities structures (e.g., buildings, streets, etc.). Besides that, it also improves urban, suburban and rural scenarios with the corresponding corrections. However, characteristics as frequency interval, base station height, link distances and the corresponding formula are different.

Hata model considers the following characteristics:

- Frequency  $f$ : (150-1500) [MHz]
- Distance  $d$ : (1 – 10) [km]
- BS antenna height ( $h_e$ ): (30 – 200) [m]
- UE antenna height ( $h_r$ ): (1 – 10) [m]

Each scenario has a specific set of equations, but considering the place where the measurement campaigns take place, it is important to give most attention to rural. This environment is comparable to an open area where there are no obstacles to affect the signal transmission.

$$L_O[\text{dB}] = L_U[\text{dB}] - 4.78(\log_{10}(f [\text{MHz}]))^2 + 18.33 \log_{10}(f [\text{MHz}]) - 40.94 \quad (3.7)$$

- $L_O$  [dB] – Path loss considering an open area
- $L_U$  [dB] – Path loss result for small city considering urban environment equation
- $f$  [MHz] – Frequency of signal transmission

In order to get a result for path loss in an open area, it is crucial to calculate  $L_u$  first:

$$L_u(\text{dB}) = 69.55 + 26.16 \log_{10}(f) - 13.82 \log_{10}(h_B) - C_H + [44.9 - 6.55 \log_{10}(h_B)] \times \log_{10}(d) \quad (3.8)$$

- $L_u$  (dB) – Path loss in small cities (urban environment)
- $f$  [MHz] – Frequency of signal transmission
- $h_B$  [m] – Height of BS antenna
- $C_H$  – Antenna height correction factor;
- $d$  [km] – Distance between the transmitter (BS) and the receiver (e.g., UE, mobile station)

It is possible to verify that this model is not apt to support the drone's characteristics for two reasons:

1. The interval of frequencies is not as large as in Okumura model case, which makes it impossible to support UMTS frequencies since it is only able to reach a maximum of 1500 MHz
2. Mobile station maximum height still the same (10 meters) as in Okumura that makes it an issue.

### 3.2.3. Cost 231-Hata Model

This model is an extension of Hata model able to provide until 2 GHz frequencies and it is one of the most used in cellular networks [26]. Cost-Hata assume the following characteristics:

- Frequency  $f$ : (1500-2000) [MHz]
- Link distance  $d$ : (1-20) [km]
- BS antenna height: (30-200) [m]
- MS antenna height: (1-10) [m]

Like the previous models, Cost-Hata also assumes its own formulation to acquire the result of the median path loss:

$$L_{[dB]} = 46.3 + 33.9 \log(f) - 13.82 \log(h_B) - a(h_R, f) + [44.9 - 6.55 \log \log(h_B)] \log(d) \quad (3.9)$$

The parameter  $C$  assume different values according to the type of environment:

$C = 0$  dB, suburban areas and medium cities;

$C = 3$  dB, metropolitan areas (e.g. big cities).

In order to get a result from the last formula, it is necessary to calculate  $a(h_R)$  that assumes the following formulation for suburban and rural areas.

$$a(h_R, f) = (1.1 \times \log(f) - 0.7) \times h_R - (1.56 \times \log(f) - 0.8) \quad (3.10)$$

- $L$  [dB] – Median path loss;
- $f$  [MHz] – Frequency for signal transmission;
- $h_R$  [m] – UE antenna effective height;

- $h_B$  [m] – BS antenna effective height;
- $a(h_R)$  – UE antenna height correction factor as described in the Hata Model for urban areas;
- $d$  [km] – Distance between the transmitter and receiver (communication link distance)

When comparing the Cost-Hata model to the Okumura and Hata models, it is possible to verify that the UE antenna effective height is the same (~10 meters), which is still not acceptable when considering the heights that UAV can assume. Besides that, the frequency extends to 2 GHz but it is still not enough to complete the frequency spectrum in use in this dissertation.

### 3.2.4. COST 231 – Walfish-Ikegami Model

Walfish-Ikegami model considers reflection and scattering above and between structures like buildings in a specific environment (urban). Besides that, it also takes into account the line of sight (LoS), non-line of sight (NLoS) scenarios and it is more appropriate for micro cells and small macro cells [27].

Line of sight (LoS) situation assumes the following formulation:

$$L_{LOS} = 42.6 + 26 \log(d[\text{km}]) + 20 \log(f[\text{MHz}]) \text{ for } d \geq 20 \text{ m} \quad (3.11)$$

Non-line of sight (NLoS) formula has its own characteristics by considering scattering and diffraction properties caused by the adjacent buildings:

$$L_{NLOS} = L_0 + \max\{0, L_{rts} + L_{msd}\} \quad (3.11)$$

Where,

- $L_0$  [dB] – free space path loss already considered in Okumura model;
- $L_{rts}$  – correction factor related to diffraction and scattering from rooftop to street
- $L_{msd}$  – multiscreen diffraction related to urban rows of buildings

$L_{rts}$  and  $L_{msd}$  fluctuate according to several parameters related to urban structures (e.g., street width, building height, average building separation).

Its main characteristics are:



- Frequency interval: (800 – 2000) [MHz]
- BS antenna height: (4-50) [m]
- UE antenna height: (1-3) [m]
- Cell Range: (0.2-5) [km]

Based on the previous information, it is possible to realize that this model is especially convenient for urban scenarios since its main concern is to predict signal's attenuation in urban corridors, which strictly relates to medium cities and metropolitan centers.

### 3.2.5. Erceg Model (or basic SUI model)

Erceg model uses the following mathematical formulation to obtain a median estimate for path loss [27].

$$L [\text{dB}] = L_0[\text{dB}] + 10\gamma \log\left(\frac{d}{d_0}\right) + s \text{ for } d \geq d_0, f \leq 2000 \text{ MHz} \quad (3.12)$$

Where,

- $L_0$  – free space attenuation (FSPL), which is described by:

$$L_0[\text{dB}] = 20 \log\left(\frac{4\pi d_0}{\lambda}\right), d < d_0 \quad (3.13)$$

- $d_0 = 100$  meters
- $h_B$  [m] – BS antenna height
- $\gamma = \left(a - bh_B + \frac{c}{h_B}\right) + \chi\sigma_\gamma$
- $s = \gamma_0$
- $\sigma = \mu_0 + z\sigma_\sigma$
- $x, y, z$  stands for Gaussian random variables  $N(0,1)$

Some of the posterior parameters assume different depending exclusively on the terrain category:

Parameter	Terrain Category		
	A (Hilly / moderate to heavy tree density)	B (Hilly / light tree density or flat / moderate to heavy tree density)	C (Flat / light tree density)
$a$	4.6	4.0	3.6
$b(\text{m}^{-1})$	0.0075	0.0065	0.0050
$c$ (m)	12.6	17.1	20.0
$\sigma_\gamma$	0.57	0.75	0.59
$\mu_\sigma$	10.6	9.6	8.2
$\sigma_\sigma$	2.3	3.0	1.6

Table 3- 2. Parameter values for different types of terrain, Source: [27]

The basic SUI model assumes the following characteristics without correction factors:

- Frequency  $f$ : (800-2000) [MHz]
- BS antenna height: (10-80) [m]
- UE antenna height:  $\leq 2$  [m]
- Cell Range: (0.1-8) [km]

SUI model is an extension to Hata, which is able to use frequencies above 2000 MHz and under 11000 MHz by adding correction factors associated to frequency and receiver antenna height to the Erceg's model formula [28]:

$$L [dB] = L_0[dB] + 10\gamma \log\left(\frac{d}{d_0}\right) + s + \Delta L_{b,f} + \Delta L_{bh}, d \geq d_0, 2\text{GHz} < f < 11\text{GHz} \quad (3.14)$$

Frequency correction factor( $\Delta L_{b,f}$ ):

$$\Delta L_{b,f} = 6.0 \log\left(\frac{f}{2000}\right) \quad (3.15)$$

Receiver/terminal antenna height correction factor ( $\Delta L_{bh}$ ):

$$\Delta L_{bh} = -10.8 \log\left(\frac{h_t}{2}\right), \text{terrain type A} \quad (3.16)$$

$$\Delta L_{bh} = -20 \log\left(\frac{h_t}{2}\right), \text{terrain type C} \quad (3.17)$$

By using correction factors, it is possible to achieve the following values for frequency and mobile antenna height. The parameters remaining assume the same values as the basic SUI model.

- Frequency  $f$ : (2000-11000) [MHz]
- UE antenna height: (2-10) [m]

Despite the larger frequency interval that is able to sustain UMTS and LTE technologies, UE antenna maximum height only achieves a maximum of 10 meters, which is not high enough to support UAVs characteristics.

### 3.2.6. LUI Model

In the beginning, the LUI model [29] [30] main considerations were:

- Environments: outdoor, indoor or both
- Scenarios: urban, suburban and rural
- Vegetation influence
- Terminal station height: (0-10) [m]
- BS height: (0-200) [m]
- Frequency range: (2200-3500) [MHz]
- Operates in pico-cells (Wi-Fi), micro-cells (UMTS) and macro-cells (WiMAX)

Its mathematical formulation to calculate the median path loss is able to reflect every aspect referred previously:

$$PL(dB) = \left\{ \begin{array}{l} 20 \cdot \log_{10} \left( \frac{4\pi \cdot d_0}{\lambda} \right) + 10 \cdot \gamma_1 \cdot \log_{10} \left( \frac{d}{d_0} \right) \cdot u(d_{bp} - d) + \\ + ENV \cdot \left[ X_f + X_h + VEG \cdot A_m \cdot \left[ 1 - \exp \left( \frac{-d_{depth} \cdot \beta}{A_m} \right) \right] \right] + \\ + u[NE - 2] \cdot \left[ W_e + W_{GE} \cdot (1 - \sin \theta)^2 - G_f \right] \cdot u(d - d_{bp}) + \\ + (1 - ENV) \cdot \left[ \begin{array}{l} u[1 - NE] \cdot \left( 10 \cdot \gamma_1 \cdot \log_{10} \left( \frac{d_{bp}}{d_0} \right) + \frac{WAF_{bp}}{\sin \theta_H} + \right. \\ \left. + \frac{FAF_{bp}}{\sin \theta_V} + \sum_{floor=2}^{NF} \frac{FAF(floor)}{\log_{10}(10 \cdot floor)} \right) + \\ \left. + 10 \cdot \gamma_2 \cdot \log_{10} \left( \frac{d}{d_{bp}} \right) + \sum_{wall=2}^{NW} \frac{WAF(wall)}{\log_{10}(10 \cdot wall)} \right) \end{array} \right] \cdot u(d - d_{bp}) \end{array} \right\} \quad (3.18)$$

However, it is more accurate to consider only outdoor scenario since it fits in this dissertation's requirements, which uses a simpler formula:

$$PL [dB] = L_0 [dB] + 10\gamma \log \left( \frac{d}{d_0} \right) \times u(d_{bp} - d) + \Delta L_{b,f} + \Delta L_{bh} \quad (3.19)$$

Where:

- $L_0$  [dB] – Free space path loss
- $\gamma$  stands for path loss exponent, which assume different results according to the type of environment and the parameters a, b and c. These parameters assume the values from the table 3-2:

$$\gamma = \left( a - bh_B + \frac{c}{h_B} \right) \quad (3.20)$$

- $d_0$  - Reference distance that vary according to the technology in use
- $u(d_{bp} - d)$  – scalar function that depends on the distance and the breakpoint distance;
- $\Delta L_{bf}$  – Frequency correction factor, which is also similar to the one used in the previous model:

$$\Delta L_{bf} = 6.0 \log \left( \frac{f}{2000} \right) \quad (3.21)$$

- $\Delta L_{bh}$  - Correction factor for terminal antenna height.  $k_{TEC}$  is a constant that assumes a different value according to the size of the cell, which directly associates to the technology in use and it is shown in the table 3-3.

$$\Delta L_{bh} = -k_{TEC} \times \log \left( \frac{h_t}{2} \right) \quad (3.22)$$

Parameters	Wi-Fi	UMTS	WiMAX
f [Hz]	$2.4 \times 10^9$	$2.2 \times 10^9$	$3.5 \times 10^9$
$d_0$ [m]	1	25	100
$K_{TEC}$	24	10.8	20

Table 3- 3. LUI model parameters for three different technologies, Source: [30]

Considering the previous statements, the first phase of LUI model is not apt to calculate the median attenuation using LTE and it still assumes low terminal antenna heights. However, there is an extension based on LUI model considerations and equations [1], which is able to predict the signal attenuation using some new features:

- Environment: outdoor
- Frequency  $f$ : (800-2600) [MHz]
- Terminal station height: (0- $\infty$ ) (no limits)
- BS height: (0- $\infty$ ) (no limits)

In this case, the terminal station assumes a 3D coordination movement, which makes it more reliable considering the UAVs characteristics.

Part of the following equation is identical to the one used in the first phase of LUI model for outdoor environment, but distance parameter now considers three coordinates. Nonetheless, this extension also recognizes azimuth, elevation angle, tilt of the antenna and other angles as valuable aspects, which reflect on the addition of new correction factors.

$$L_{[dB]} = L_{0 [dB]} + 10 \times \gamma \times \log\left(\frac{d}{d_0}\right) \times u(d_{bp} - d) + \Delta L_{b,f} + u(h_{TS} - h_{BS}) \times X_{angles} + [u(h_{TS}) - u(h_{TS} - h_{BS})] \times \Delta L_{bh} \quad (3.23)$$

Where:

- $d$  [m] – distance using 3D coordination system (X, Y, Z):

$$d = \sqrt{(x_1 - x_2)^2 + (y_1 - y_2)^2 + (z_1 - z_2)^2} \quad (3.24)$$

- $d_0$  [m] – reference distance. It also varies according to the table 3-3 conditions. However, considering that experimental trials are close to the BS, it assumes picocell characteristics and  $d_0 = 1$  meter.
- $h_{TS}$  – terminal station or UE antenna effective height
- $h_{BS}$  – base station antenna effective height
- The correction factor associated to the BS effective height ( $\Delta L_{b,h}$ ) multiplies by a rectangular function ( $[u(h_{TS}) - u(h_{TS} - h_{BS})]$ ), which can result on 0 or 1 depending on the BS and the terminal height.

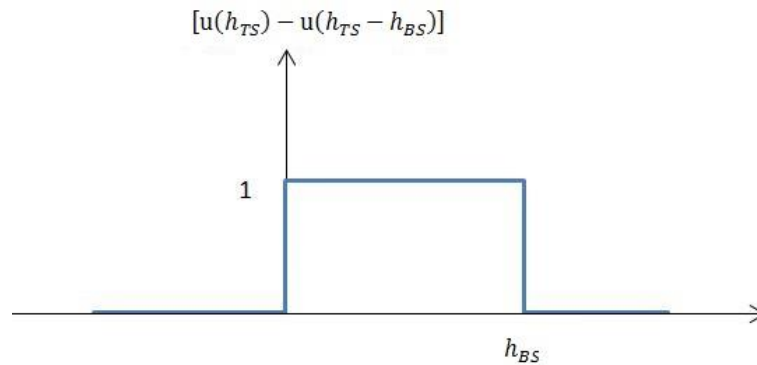


Figure 3-5. Rectangular function, Source: [1]

$$[u(h_{TS}) - u(h_{TS} - h_{BS})] = \begin{cases} 0, & 0 \leq h_{TS} \\ 1, & 0 < h_{TS} < h_{BS} \\ 0, & h_{TS} \geq h_{BS} \end{cases} \quad (3.25)$$

- $\gamma$  - Path loss exponent, which definition is the same as in the previous case. However, a modification in that equation by using a unit step function allows new

results for higher altitudes considering a specific interval since LUI model already works for lower altitudes.

$$\gamma_1 = \left[ a - b \times h_b + \left( \frac{c}{h_b} \right) \right] \times [u(h_{TS}) - u(h_{TS} - h_{BS})] + 2 \times u(h_{TS} - h_{BS}) \quad (3.26)$$

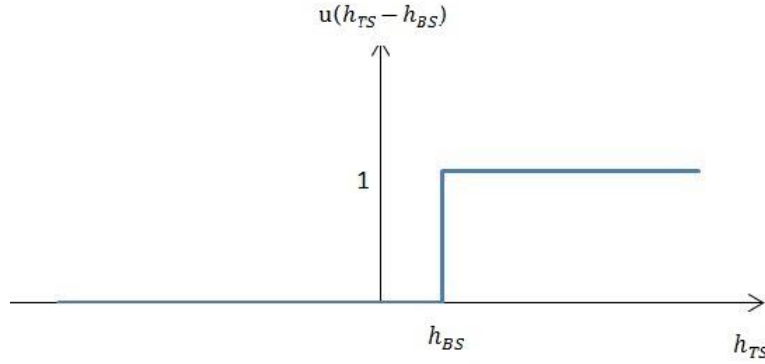


Figure 3-6. Unit step function, Source: [1]

Like in rectangular function, unit step function also bases in the same parameters, which only possible results are 0 or 1 according to the following condition:

$$u(h_{TS} - h_{BS}) \begin{cases} 0, & h_{TS} < h_{BS} \\ 1, & h_{TS} \geq h_{BS} \end{cases}$$

- $\chi_{angles}$  is another correction factor that use several parameters related to the antennas: azimuth, elevation angle, tilt of the antenna and the angle that determines where terminal station is located and respond to whether the antenna is sectorial or no. Besides that, it also multiplies by the unit step function to avoid higher attenuation below the BS.

$$\chi_{angles} = MIN(\chi_{\theta+\psi}, \chi_{\varphi+\beta}) \quad (3.27)$$

- $\theta$  – elevation angle;
- $\psi$  – tilt of the antenna - usually varies from 0 to 15 degrees;
- $\varphi$  – azimuth;
- $\beta$  – angle that determines in which sector the terminal station is located;
- $\chi_{\theta+\psi}$  – correction factor considering the elevation and the tilt of the antenna that uses the following formulation:

$$\chi_{\theta+\psi} = [1 - \delta(\theta + \Psi)] \times [0.0031 \times (\theta + \Psi)^2 - 0,6511 \times (\theta + \Psi) - 4.447] \quad (3.28)$$

$$\theta = \tan^{-1} \left( \frac{h_{TS} - h_{BS}}{d(x, y)} \right) \quad (3.29)$$

- $\chi_{\varphi+\beta}$  – correction factor that considers azimuth ( $\varphi$ ) and  $\beta$  that uses the next formula:

$$X_{\varphi+\beta} = [1 - \delta(\varphi + \beta)] \times (-0.0018) \times (\varphi + \beta)^2 - 0.0377 \times (\varphi + \beta) + 0.2115 \quad (3.29)$$

Both the previous correction factors use the inverse of the Dirac Delta Function (DDF), which are  $(1 - \delta(\theta + \Psi))$  and  $(1 - \delta(\varphi + \beta))$ . DDF can assume only two results: 0 or 1, depending on certain criteria:

$$\delta(\theta + \Psi) = \begin{cases} 1, & \text{if } \theta + \Psi = 0 \\ 0, & \text{if } \theta + \Psi \neq 0 \end{cases} \quad (3.30)$$

$$\delta(\theta + \beta) = \begin{cases} 1, & \text{if } \theta + \beta = 0 \\ 0, & \text{if } \theta + \beta \neq 0 \end{cases} \quad (3.31)$$

The following figures demonstrate the angles associated to the antennas in the BS and how they relate to each other:

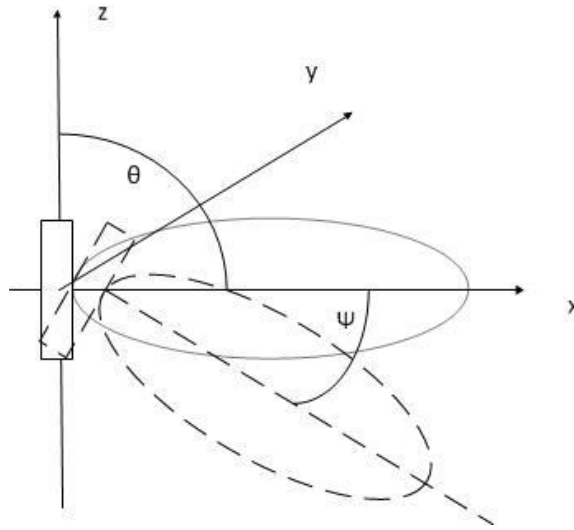


Figure 3-7. Angles associated to the antenna, Source: [1]

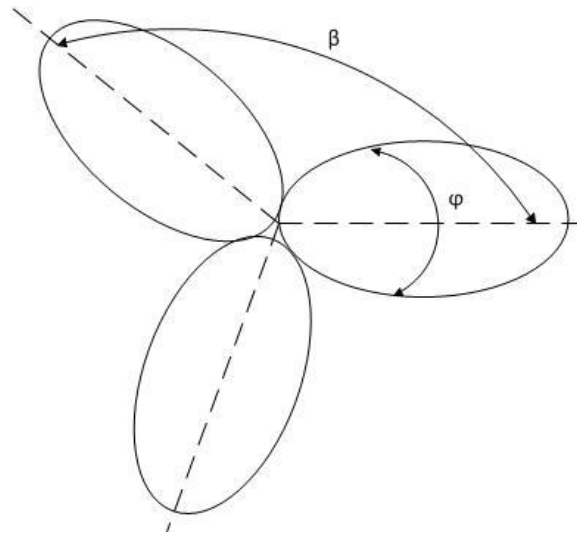
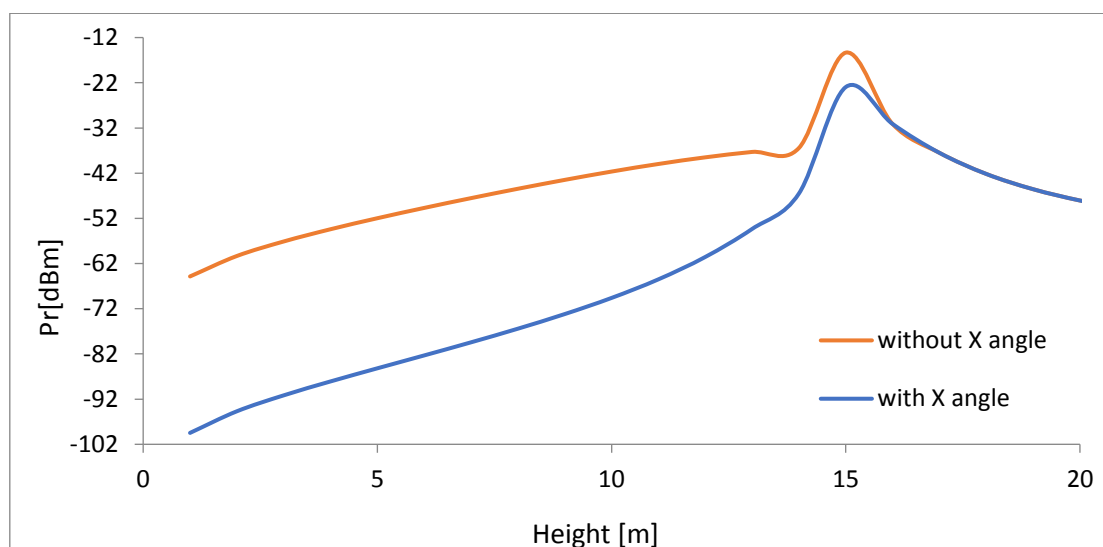


Figure 3-8. Sectorial choice and identification, Source: [1]

The extension of the LUI model brings new characteristics that are important regarding UAVs unique behavior when comparing to the typical user equipment. The frequency interval is now able to support UMTS and LTE frequency bands that are essential to provide higher data rates to maintain a reliable QoS for video streaming during the flight, which is one of the main concerns in this dissertation. Nonetheless, terminal station height is no longer a problem because this extension considers no limits for it.

Regarding the previous information, there is no need to propose a new model since LUI extended model analyzes every crucial aspect in UAVs domain. However, considering  $\chi_{angles}$  parameter results from a previous study, this model assumes two formulas that depend on the terminal and the BS heights.



Graphic 3 - 1. "Below BS antenna difference using  $\chi_{angles}$ ", Source: [1]



In graphic 3-1, it is possible to verify that the attenuation is greater when assuming the  $\chi_{angles}$  parameter below the BS height, which is the reason why it is not necessary to use it under those circumstances, resulting in two distinctive formulas that consider when the terminal station is below, or above and at the same level as the base station.

$$\left\{ \begin{array}{l} L_{[dB]} = L_{0 [dB]} + 10 \times \gamma \times \log\left(\frac{d}{d_0}\right) \times u(d_{bp} - d) + \Delta L_{b,f} + \\ \quad [u(h_{TS}) - u(h_{TS} - h_{BS})] \times \Delta L_{bh}, \mathbf{h}_{TS} < \mathbf{h}_{BS} \\ L_{[dB]} = L_{0 [dB]} + 10 \times \gamma \times \log\left(\frac{d}{d_0}\right) \times u(d_{bp} - d) + \Delta L_{b,f} + u(h_{TS} - h_{BS}) \times X_{angles} \\ \quad + [u(h_{TS}) - u(h_{TS} - h_{BS})] \times \Delta L_{bh}, \mathbf{h}_{TS} \geq \mathbf{h}_{BS} \end{array} \right. \quad (3.31)$$

# **CHAPTER 4**

## **MEASUREMENTS**

This chapter present several measurement campaigns results in three different locations that will allow a better analysis over signal's behavior during the UAV flight route

## 4.1. Overview

In order to obtain the results that lead to a conclusion over a specific scenario, several measurement campaigns are necessary, considering more than one location in the same environment (e.g. rural). The main goal in this chapter is to understand how signal behaves during the flight and conclude if there is any location where the producer/reference cell might not be able to provide sufficient throughput for a video streaming service considering more than one video quality option, since data rates vary according to quality demanded. If the producer cell is not able to provide the required strength and quality, the network might consider *handover* if the cellular infrastructure is prepared to support UAV's behavior (e.g., height, movement, etc.). The location where this scenario might happen is over the antennas where the “*hole* phenomenon” occurs according to the radiation pattern of most of the antennas and that is one of the reasons why it is necessary that the drone route considers those positions like illustrated in the following figure.

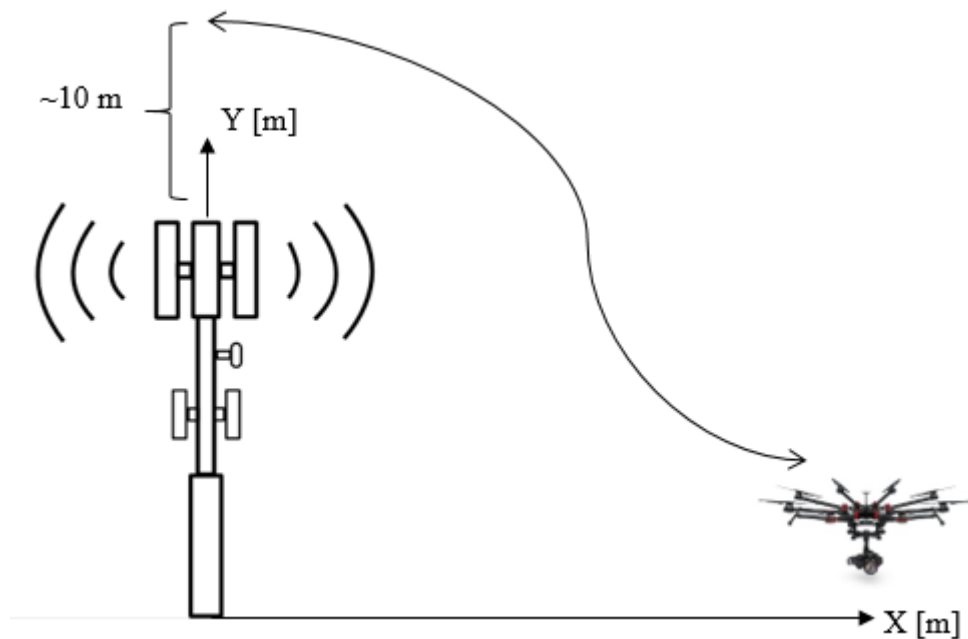


Figure 4- 1. Proposed flight plan: X(distance) and Y(altitude) axes

Nonetheless, the bit rate for a video streaming service is not as linear as it seems because it is mandatory to consider the device's specifications where the video stream is available, such as screen size, in order to determine the ideal bandwidth to encode a certain video. Per example, a video might look poor quality due to low resolution for such a big screen

and it might be adequate on a smartphone since its screen size admits lower resolution with good video quality that will directly affect the diminishing of the data rate.

There are a few types of scenes that require higher bandwidth to minimize certain errors (e.g., visual artifacts) and avoid loss of definition like detailed, high and chaotic (e.g., flames, waves) motion scenes.

It's also important to look at variable bit rate (VBR) possibility even if it's not considered in the following table. VBR allows higher encoding rate that is used in short sections of high complexity and/or motion resulting in a higher overall quality [31].

In order to achieve a more consistent video quality, it is also crucial to refer multiple qualities encoding since it allows the user to select manually the desired quality taking into account their device, desired quality and data plan. There's also the automatic option based in software (e.g., twitch.tv), which adjusts the streaming quality based on RF conditions by trying to keep a good QoE and QoS to the user.

Video Quality Level	Video (kbps)	Total (kbps)	Comments
VQ1	200	296	Smartphone
VQ2	400	496	Tablet / Smartphone
VQ3	800	896	Tablet / Smartphone
VQ4	1400	1496	SD 480P TV screen through games console and STBs, Connected TVs, PCs and Tablets
VQ5	3150	3246	HD 72P TV screen through games console and STBs, Connected TVs, PCs and tablets
VQ6	7100	7196	Full HD 1080P, TV screen through games console and STB, Connected TVs, PCs with General Processor Units.

*Table 4-1. Recommended bit rates for video streaming, Source: [31]*

Since throughput is a crucial parameter to answer if the received signal is good enough to maintain a video streaming service, the table 4-1 presents the standard thresholds considering more than one type of quality. The quality varies from 296 kbps (VQ1) to 7196 kbps, lowest to highest quality, respectively. In this case, the highest quality is VQ5 since only PCs and tablets assume to support the streaming service, so the minimum requirement for higher quality is 3246 kbps according to table 4-1.

## 4.2. Measurement campaign requirements

Accomplishing crucial requisites before starting the measurement campaign is extremely necessary. Most of these requisites are material and software related.

Besides the spectrum analyzer chosen for this measurement campaign (R&S TSMA) and the additional accessories that are in the figure below, it is also necessary a laptop and a drone that is able to lift at least 2.5 kg, since this is the necessary equipment's total weight. To attach the spectrum analyzer below the drone, velcro tape is indispensable.



Figure 4-2. R&S TSMA accessories, Source: [32]

The list of accessories presented in figure above is:

1. SCAN Link interconnection cable
2. 12 V DC power supply cable with a cigarette light connector
3. Wide range RF paddle antenna [700 MHz to 2600 MHz]
4. U-blox GPS – determines the 3D coordinates: Latitude, Longitude and Altitude
5. Two stub antennas for WLAN/Bluetooth

The second accessory in the previous list is not necessary because TSMA-BP is the module responsible for it. However, all the remaining accessories connect to the respective ports in the rear panel of the instrument, in order to have a correct measurement setup.



Figure 4-3. R&S TSMA - Rear Panel, Source: [32]

Only some of the ports in the rear panel are in use during the measurement. Assuming the image identification numbers, the ones in use are:

- <14, 15> - Two stub antennas;
- <13> - GPS;
- <5, 4> - SCAN link interconnection cable;
- <12> - RF antenna;
- <11> - DC IN Connector (in use when TSMA-BP is connected).

Considering that an autonomous equipment is required, it is also necessary the battery pack unit (TSMA-BP) to provide the necessary energy by using an interconnection cable (DC cable) that connects to R&S TSMA during its use.



*Figure 4-4. R&S TSMA and TSMA-BP with some accessories connected, Source: [32]*

It is necessary to attach the equipment to the drone using velcro tape, assuming that all the connections are done and correct.



*Figure 4-5. Equipment attached below the drone with velcro tape*

After accomplishing these requisites, it is fundamental to access the TSMA's user interface (based on Windows OS) by using WLAN and Remote Desktop Connection to establish a connection between the laptop and the equipment. When this connection is successful, it is possible to access ROMES Software, where configurations take place. Spectrum analysis during flight is also available if WLAN connection keeps stable. Nonetheless, it also requires a professional with a controller to handle the drone's movement during the flight.

### 4.3. Locations and flight routes

Measurements take place in three different locations and close to two base stations that belong to different network service providers [33].

- Base Station A (coordinates):
  - Latitude: 39° 2'23.93"N
  - Longitude: 9°22'30.41"W
  - Service provider: MEO (MCC: 268; MNC: 06) [41]
  - BTS Height: 50 meters



*Figure 4-6. Base Station A (MEO)*



*Figure 4-7. Scenario A (BS A) and respective flight route*



*Figure 4-8. Scenario B (BS A) and respective flight route*

Blue dots represent GPS data samples captured during the flight. The intention is to approach the drone to the antenna by decreasing the distance between them and increasing the drone's height until it reaches 10 meters above the base station. In this case, it corresponds to about 60 meters height. When drone reaches the exact position above the base station center, it stands there for a while to make sure that analyzer captures many samples, in order to provide a reliable statistic measurement for “hole phenomenon” analysis. After that, it returns immediately to its landing zone (represented by C) in scenario A. In scenario B, it goes further until it reaches position B and only then, it returns to its landing location represented by C.

Waypoints A and C assume different coordinates in scenarios A and B [Lat; Long]:



- Scenario A:
  - Waypoint A: [39° 2'24.36"N; 9°22'30.94"W]
  - Waypoint C: [39° 2'24.22"N; 9°22'30.88"W]
- Scenario B:
  - Waypoint A: [39° 2'22.77"N; 9°22'31.58"W]
  - Waypoint B: [39° 2'24.30"N; 9°22'30.31"W]
  - Waypoint C: [39° 2'22.79"N; 9°22'31.63"W]

Besides the previous scenarios, a posterior measurement is necessary considering the following characteristics:

- Base Station B (coordinates):
  - Latitude: 39° 2'15.98"N
  - Longitude: 9°22'38.56"W
  - Service Provider: Vodafone (MCC: 268, MNC: 01) [41]
  - BTS Height: 40 meters







*Figure 4-9. Base Station B (Vodafone)*



*Figure 4-10. Scenario C and respective flight route*

In figure above, it is possible to examine four waypoints:

-  – Departure location [ $39^{\circ} 2'15.10''\text{N}$ ;  $9^{\circ}22'38.33''\text{W}$ ]
-  – Furthest location from point A [ $39^{\circ} 2'16.74''\text{N}$ ;  $9^{\circ}22'38.76''\text{W}$ ]
-  – Landing location [ $39^{\circ} 2'15.54''\text{N}$ ;  $9^{\circ}22'38.53''\text{W}$ ]
-  – Base station location

Scenario C has the same characteristics as the scenario B. The main difference between both is the distance between the departure and landing location, which accentuates in this scenario. However, this disparity does not affect the results.

#### **4.4. Measurement results**

This sub-chapter base on the previous one, since it utilizes all the scenarios presented on it. Besides that, the results consider LTE and UMTS technologies.

In order to accomplish a better understanding, reference to 2D and 3D graphics are necessary. These graphics contemplate parameters that are able to understand the signal behavior in different positions and timings.

The general measurement results permit to conclude that both base stations assume a three-sectorial system since each BS associates with three different cells, where each one is represented by a hexagon according to the cellular network representation. So, in this case, sectors and cells have the same meaning [40].

3D graphics rely on the relation between signal strength and the way it varies when related with distance to base station and drone's height. Signal strength relates to RSRP or RSSI,

depending on the technology. Height can vary from 0 to 50 or 60 meters, depending on the base station where measurements take place.

2D graphics essentially bases on throughput/capacity and how this relates to time since the beginning until the end of the measurement and the signal strength. Shannon's theorem is fundamental to acquire throughput results for 3G and 4G technologies [38] [39] since bandwidth and SINR/SNR values are available for each acquired sample. These graphics contemplate the following relations:

- Throughput vs Time:
  - Cells from reference base station;
  - Provider/producer cell from reference base station and cells from adjacent base stations;
  - Logarithmic average for every cell in reference base station.
- Throughput vs Signal Strength:
  - Cells from reference base station and/or adjacent BS.
  - Provider/producer cell from reference base station.

Considering the limit of pages for a thesis, the graphics are available in Annex C and analyze the normal probability distribution function (PDF) and cumulative distribution function (CDF) for the same BSs and relates them with parameters like throughput and signal strength, which can vary between RSRP and RSSI according to the technology in use:

- CDF of Throughput
- PDF of Throughput
- CDF of (RSRP or RSSI)
- PDF of (RSRP or RSSI)

Before sharing the results, it is necessary to understand the previously mentioned parameters like RSRP, RSSI, SINR and SNR. There is also an approach to Shannon's theorem to be able to understand how to obtain the throughput values.

- RSRP [dBm] – stands for reference signal received power. According to definition TS 36.214: “is defined as the linear average over the power contributions (in [W]) of the resource elements that carry cell-specific reference signals within the considered

measurement frequency bandwidth” [34]. It represents signal strength and it prevails in LTE measurements.

RSRP Interval [dBm]	RF Conditions
$\geq -80$	Excellent signal
[-80 to -90]	Good signal
[-90 to -100]	Mid Cell (Low signal)
$\leq -100$	Cell Edge (Poor signal)

Table 4- 2. RSRP limits for LTE, Source: [35]

- RSSI [dBm] – Received Signal Strength Indicator is mainly seen in UMTS captures. According to definition TS 36.214: “comprise the linear average of the total received power (in [W]) observed only in OFDM symbols containing reference symbols for antenna port 0, in the measurement bandwidth, over N number of resource blocks by the UE from all sources, including co-channel serving and non-serving cells, adjacent channel interference, thermal noise etc.”. This parameter is similar to the previous one, but it assumes signal strength value in UMTS technology. RSSI relies on other parameters in order to obtain results according to the following formula:

$$RSSI \text{ [dBm]} = RSCP \text{ [dBm]} - \frac{Ec}{I0} \text{ [dB]} \quad (4.1)$$

RSSI Interval [dBm]	RF Conditions
[-50 to -75]	High signal
[-76 to -90]	Medium signal
[-91 to -100]	Low signal
[-101 to -120]	Poor signal

Table 4-3. RSSI limits for GSM/3G(UMTS)/HSPA, Source: [35]

The table 4-3 is able to demonstrate the limits of RSSI for several technologies like UMTS and HSPA, which will help to define the received signal by the spectrum analyzer.

- SINR [dB] (or S/N) – Signal-to-Interference-plus-Noise Ratio defines the quality of the channel and it is useful to obtain the throughput values because Shannon’s theorem considers it after converting to linear.
- SNR [dB] (or S/N) – Signal to Noise and Interference ratio. It is also need in Shannon’s theorem formula, but first, conversion to linear is mandatory.

- SC – Scrambling Code – using this parameter, NodeB (UMTS) is able to separate signals coming simultaneously from different UEs, and UE can also separate signal coming from various base stations (NodeBs).

All these parameters are essential to understand if there is a handover need.

Shannon's theorem is able to tell the channel capacity  $C$  in bps, requiring bandwidth and SINR or SNR to calculate it. The theorem formula is:

$$C = B \times \log_2 \left( 1 + \frac{S}{N} \right) \quad (4.2)$$

In equation 4.2,  $B$  corresponds to bandwidth that might assume different values depending on the capture results. In this case, UMTS only considers 5 MHz bandwidth channels but LTE assume 10 MHz and 20 MHz bandwidth channels as represented in figure below.

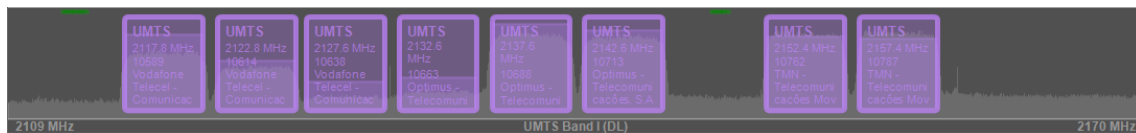


Figure 4-11. 5 MHz channels UMTS Band I (DL)



Figure 4-12. 10 MHz channels LTE Band 20

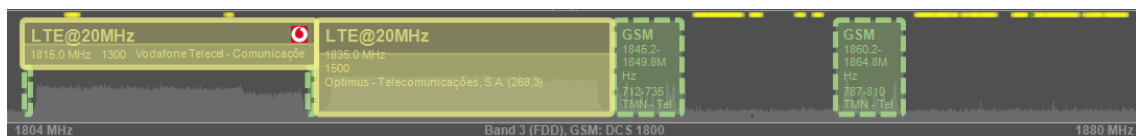


Figure 4-13. 20 MHz channels LTE Band 3

S/N is similar to SNR and SINR. These two parameters correspond to the quality of the channel in UMTS and LTE technologies, respectively. However, it is mandatory to convert them from dB to linear scale like described below:

$$\frac{S}{N} = 10^{\frac{S}{N}[dB]} \quad (4.3)$$

LTE and UMTS assume different names to describe certain matter. The divergences between both are in the following table:

Technology	Cell Identifier	Name	Channel Quality	Signal Strength (Level)
UMTS	SC	Node B	SNR	RSSI
LTE	PCI	eNodeB	SINR	RSRP

*Table 4-4. Parameter differences between UMTS and LTE*

It is now easier to identify the cell that provides the best results according to our position in each analyzed scenario and name it as the provider/producer cell.

#### 4.4.1. Scenario A

According to section 4.3 and table 4-4, it is possible to nominate the reference and adjacent base stations based on the data provided by the spectrum analyzer, depending on certain parameters like quality, strength and their respective results. The 2D and 3D graphics related to this scenario are available in section B.1 and B.2 from the Annex B.

##### LTE

- eNodeB: 1675
- PCI: 177, 178 and 179
  - Adjacent sectors: 177 and 178
  - Reference sector: 179
- Channel bandwidth: 10 MHz
- YouTube URL is available at the “References” section [43]

In this scenario, adjacent base stations from the same service provider (e.g. MEO) are not available considering spectrum analyzer results.

The graphic B-1 considers the relation between data rate and time. By using Shannon’s theorem, data rate (or throughput) is calculated. UTC (in seconds) parameter present in .csv files from the spectrum analyzer is also used to calculate the instant of time for each sample considering the full-time interval. In this case, this interval varies from 0 to 250 seconds, which corresponds to the flight time from the UAV’s moment of the departure, till the moment it lands.

Considering all the previous statements and looking to the graphic content, the cell that stands most from the others identifies as “PCI\_179”, represented by gray dots and assumes itself as the provider/producer cell. It is able to reach peak data rates close to 70 Mbps between 100 and 150 seconds and maintains a high average rate throughout the

flight. It is now possible to assume that measurements take place in the sector identified by PCI\_179, because it is where higher rates are achievable based on spectrum analyzer results.

It is possible to conclude that reference sector guarantees the poorest quality throughout the entire flight. However, it is not able to grant the highest quality between 50 and 100 seconds, but the following graphic will show what happens in that situation and if the others cells from the same eNodeB are able to compensate this failure or not.

Graphic B-2 shows the behavior of all the cells aggregated to the same eNodeB in a situation where the reference cell is not able to provide the sufficient data rate to grant a high-quality video streaming. Before 80 seconds and between 90 and 100 seconds, the reference cell rate is below the threshold for VQ5. In this case, the adjacent sectors (PCI\_177 and PCI\_178) compensate the failure from the reference sector, by assuming higher data rates in those intervals. This compensation is similar to the softer handover process, since it is able to maintain the QoS by using cells from the same base station.

The graphic B-3 is able to show how signal strength (RSRP) behaves when related to throughput. It is possible to conclude that both parameters are directly proportional based on the order 2 polynomial trend line represented on graphic B-3. It means that when RSRP increases, throughput assume the same tendency.

Nonetheless, it is also meaningful a comparison between the trend lines associated to the adjacent cells from the same base station, in order to verify the tendencies of each one.

The graphic B-4 represents the tendencies for every sector from the reference base station. PCI\_179, which represent the producer cell, stands out considering the acquired samples reaching about 60 Mbps when close to -30 dBm. PCI\_177 reaches his maximum when close to -80 dBm, acquiring data rates close to 20 Mbps. At last, PCI\_178 identifies its peak between -70 dBm and -60 dBm with rates close to 15 Mbps.

The following table reveals the number of samples captured for each sector, which is useful because it allows to calculate the percentage of samples that are above, under and between the two defined quality thresholds:

Channel Frequency: 796 MHz			
PCI	179	178	177
Nr. Samples/sector	107	91	89
< VQ1	0 (0%)	5 (5.5%)	16 (18%)
> VQ 5	101 (94.4%)	59 (64.8%)	41 (46.1%)
> VQ 1 & < VQ5	6 (5.6%)	27 (29.7%)	32 (35.9%)

Table 4-5. Nr. of samples and respective percentage for the defined thresholds

Considering table 4-5, it is possible to conclude that the cell identified by 179, which is the producer cell, is the one achieving the best results since the number of samples below the minimum threshold is inexistent. In cell 178 and 177, this percentage tends to increase from 0 to 5.5% and 18%, respectively.

Scenario A also considers 3D graphics to relate signal strength with simultaneous changes in distance and altitude parameters. It also assumes the same sectors and number of samples considered in the previous three graphics. The following graphics will deliver 3 coordinates and they correspond to distance to BTS, UAV's height and signal strength. For a more intuitive interaction between the reader and the graphics in order to analyze a specific location, it assumes (d, h, s\_strength).

In graphic B-5, it is possible to spectate the lowest values for signal strength when drone assumes distance to BTS interval of 13 to 18 meters and its height is between 0 and 20 meters. The absolute minimum occurs in these intervals and it is close to -80 dBm when (d, h, s\_strength) = (16.2 m, 0 m, -79.25 dBm).

Still considering the same distance interval and assuming that height's interval is now between 20 and 60 meters, signal strength increases significantly, reaching its absolute maximum peak in (12.8 m, 58.1 m, -50.93 dBm). After that, drone starts to decrease its distance to the base station by also increasing its altitude until it reaches the base station center, where the signal strength will decrease but not significantly, since it assumes a minimum of -63.72 dBm in (d, h) = (0 m, 59.5 m). After this, drone begins its return path until it reaches the landing position, where it will assume a similar flight route but in a different direction.

Graphic B-6 presents a similar behavior to the previous one in the same intervals. The absolute minimum occurs in (16.2 m, 0.8 m, -79.95 dBm), while maximum absolute stands in (13.7 m, 42.5 m, -50.03 dBm). When drone reaches the top and center of the reference base station, it assumes the following results: (0 m, 59.5 m, -60.63 dBm).



Graphic B-7 shows the signal behavior from the reference cell from eNodeB: 1675, which corresponds to the reference base station. In this case, when distance from BTS assumes an interval of 12 to 16 meters, and the drone's height between 0 and 30 meters, it is where signal strength parameter assumes lower values. However, in those intervals it is able to reach a maximum of -50 dBm, approximately. The absolute minimum is also possible to observe when considering the full measurement interval, by assuming the following characteristics: (15.7 m, 8 m, - 69.69 dBm).

When drone's position assumes the same distance interval as the one in the previous paragraph (12-16 meters), but its height is now between 40 and 50 meters, the maximum peak signal strength occurs in (13.7 m, 42.5 m, -31.68 dBm).

After that, drone decreases its distance to BTS until it reaches the center of the base station where this parameter assumes a null value. While null, its height assumes its peak when reaching close to 60 meters. Concluding, when drone assumes null distance and 60 meters height, the signal strength drops dramatically, reaching about -65.8 dBm in  $(d, h) = (0 \text{ m}, 59.5 \text{ m})$ , which is very similar to the two adjacent sectors.

Considering the return path, it is very similar to the previous one because it assumes the same flight route, but using different directions.

In order to synthesize this information, table with the main parameters is available below. These parameters refer to  $(d \text{ [m]}, h \text{ [m]}, s\_strength \text{ [dBm]})$ , the maximum and minimum peak for signal strength, and the center position above the reference base station.

PCI	Max. Peak	Min. Peak	Above BS
177	(12.8, 58.1, -50.93)	(16.2, 0, -79.25)	(0, 59.5, -63.75)
178	(13.7, 42.5, -50.03)	(16.2, 0.8, -79.95)	(0, 59.5, -60.63)
179	(13.7, 42.5, -31.68)	(15.7, 8, -69.69)	(0, 59.5, -65.8)

*Table 4-6. Main parameters for all sectors in reference BS*

Nonetheless, it is possible to conclude through this table that maximum and minimum peaks occur in different cells but almost in the same position. It is possible to verify that for maximum peak results in cell 178 and 179. In addition, minimum peak column presents almost the same position in cell 177 and 178, and the only divergence between them is a difference of 0.8 m in height, which is not substantial.

## UMTS

- LAC: 8290

- Channel Frequencies: 2152.4 MHz and 2157.4 MHz
- Cell IDs from reference base station:
  - CI: 31462, 34163, 34164 (2152.4 MHz)
  - CI: 49162, 49163, 49164 (2157.4 MHz)
  - SC plan: 406, 414, 422 (in both channels)
- Cell IDs from adjacent base station:
  - CI: N/A
  - SC: 213
- Channel Bandwidth: 5 MHz

It is correct to affirm that the reference NodeB allocates two channels with two different frequencies (2152.4 MHz and 2157.4 MHz) since both use the same scrambling codes plan. However, when considering disparate NodeBs it is necessary to use a different one, which helps to reduce the quantity of work and reduces the system complexity.

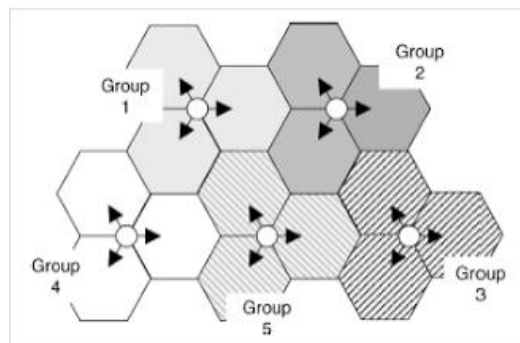


*Figure 4-14. Different SC associated to each NodeB plan [36]*

The previous illustration demonstrates a different SC per group differentiating it by different color pattern and groups. In this case, one group represents one NodeB.

It is possible to identify the same channel frequency (2152.4 MHz) in two different base stations. This channel is available in all the cells from the reference base station (31462, 34163 and 34164) and in a sector of an adjacent base station. In case there is a need for soft or hard handover, this adjacent sector from a neighbor base station does not provide enough samples (7 samples) and signal strength to ensure the required QoS considering this route. It also does not fulfill the video streaming minimum quality requirements.

According to graphic B-8, there is not a single sample able to accomplish the highest quality requirement during this capture. Cell or sector 34164 is the only one who is able to reach close to 3 Mbps, which is the maximum peak rate comparing to all the others

cells. Also considering its signal behavior during the capture, it assumes the reference cell standards. Although it seems to fulfill most of the requirements during the measurement process, there are times when it is not able to reach the minimum threshold.

The graphic B-9 represent the time intervals where most of the samples are below this limit and compares them to the samples from adjacent sectors. It is possible to analyze that the reference sector is not able to guarantee the minimum requisites between 210 and 230 seconds. However, sector 34162 grants it since it captures higher capacity as seen in the previous graphic. In this case, it exists a softer handover phenomenon, where the streaming service is capable of maintaining the minimum quality by using a different sector from the same base station to support it.

Graphic B-10 evaluates the relation between throughput and signal strength (RSSI). It is possible to see that there is an increasing tendency according to the order 2 polynomial trendline, which means that, in this case, throughput and RSSI are directly proportional.

Considering the graphic B-11, it is possible to state that cell 34164 is the one that stands out comparing to the other cells. This cell is able to reach a maximum peak rate of 2.5 Mbps, while the cells 34162 and 34163 only ensure close to 1.5 Mbps and 0.5 Mbps, respectively. The minimum rate peak is similar to the previous logic since cell 34164 assume the highest rate when comparing to the others.

In order to follow the previous section pattern, the following table demonstrates the number of samples and the percentage of them that are under, above and between the high and the low thresholds referent to video quality considering the 2152.4 MHz frequency channel.

<b>Channel Frequency: 2152.4 MHz</b>			
<b>PCI</b>	34162	34163	34164
<b>Nr. Samples/sector</b>	114	100	117
< VQ1	36 (31.6%)	61 (61%)	6 (5.1%)
>VQ 5	0 (0%)	0 (0%)	0 (0%)
> VQ1 & < VQ5	78 (68.4%)	39 (39%)	111 (94.9%)

*Table 4-7. Nr. of samples and respective percentage for the defined thresholds*

None of the cells is able to guarantee the highest quality video streaming service. However, every cell guarantees the lowest quality requisite but not every sector is equally reliable. In this case, the most efficient cell during the measurement interval is the 34164,

since only 5.1% of the samples are below the minimum limit, while the adjacent cells assume values between 30% and 65%.

When frequency channel assumes 2157.4 MHz, it is possible to verify some similarities with the previous graphics, since the emitted signal belongs to the same NodeB. However, the following graphics are able to demonstrate that.

Unlike the previous case (2152.4 MHz channel frequency), this channel is able to provide higher data rates in a specific cell (cell 49164), which makes it able to ensure the best quality (VQ5) in some moments of time, considering the graphic B-12 results. However, a few samples are below the minimum limit and the graphic B-13 will focus on time interval where these occur. Cell 49164 assumes the reference cell role since is able to reach higher rates throughout the full-time interval.

The last graphic proves the signal's behavior similarities between the two different channels. In this case, the adjacent sectors corresponding to the same NodeB are also able to compensate the lack of channel capacity. The following intervals: [90 s – 100 s] and [110 – 120 s] prove this statement. The first interval shows that both adjacent cells (49162 and 49163) compensate the low-quality signal from the reference cell. In the second interval, only cell 49162 is able to do it, since cell 49163 is also below the minimum threshold.

Once again and based on graphic B-14, this channel proves to have a similar behavior when comparing to the adjacent channel (2152.4 MHz), since both assume that reference sector allows higher data rates with a positive tendency, while the other cells assume the opposite trend. Besides that, the throughput results are also approximate.

Channel Frequency	2157.4 MHz			2152.4 MHz		
PCI	49162	49163	49164	34162	34163	34164
N. Samples	113	102	117	114	100	117
< VQ1	29 (25.7%)	50 (49%)	12 (10.3%)	36 (31.6%)	61 (61%)	6 (5.1%)
> VQ 5	0 (0%)	0 (0%)	4 (3.4%)	0 (0%)	0 (0%)	0 (0%)
>VQ1 & <VQ5	84 (74.3%)	52 (51%)	101 (86.3%)	78 (68.4%)	39 (39%)	111 (94.9%)

Table 4-8. Nr. of samples and respective percentage for the defined thresholds

The table 4-8 shows the percentages of samples below, between and above the defined thresholds for each channel from the same network service provider.

Below the minimum quality limit, the results for both channels are a bit different since channel 2152.4 MHz assumes a higher percentage of samples that are below the minimum threshold. Besides that, only 2157.4 MHz frequency channel is able to reach such high rates but it is not constant neither reliable, since not more than 3.4% of the samples represent it.

It is possible to conclude that in this situation UMTS is able to guarantee the lowest quality video streaming using softer handover whenever necessary since the reference cell does not provide full coverage during the entire drone's route. When there is a higher demand for quality, this third-generation technology is not the solution.

Since both adjacent channels have approximate results, the 3D graphics analysis only evaluates the cells from 2152.4 MHz channel. These graphics are similar to the ones given in LTE section, but now considers UMTS technology, which relies on RSSI and not RSRP for signal strength parameter.

The signal's characteristics from the graphic B-15 are similar to the LTE graphic for reference sector, where it is possible to verify a signal strength accentuated increase close to 40 meters height where it reaches the highest value:  $(d, h, s\_strength) = (12.2, 40.6, -12.87)$ . Considering the video streaming record, it is possible to verify a few antennas around 40 meters height on the base station structure, which lead to the conclusion that these might be the antennas providing these signals. Besides that, -12.87 dBm is almost impossible to reach in a normal scenario because it is too high when compared with the normal standards, which are available in the table 4-3.

Unlike the reference sector, the adjacent sectors from the same NodeB (34162 and 34163) are not able to reach such a high peak data rate based on the graphics B-16 and B-17. However, the maximum peak data rate from both those sectors continues to be high comparing to the intervals from table 4-3. Maximum and minimum peaks are available in the table 4-9.

Channel Frequency	PCI	Max. Peak	Min. Peak	Above BS
2152.4 MHz	34162	(12.4, 43.4, -19.63)	(17.1, 5.6, -65.04)	(0.3, 59.6, -40.61)
	34163	(13.7, 40.2, -21.86)	(17.1, 5.6, -64.33)	(0.3, 59.6, -35.47)
	34164	(12.2, 40.6, -12.87)	(17.1, 5.6, -64.55)	(0.3, 59.6, -35.28)

Table 4-9. Main parameters for all sectors in reference BS

Signal's strength reaches its minimum peak in the same position for every cell in the reference Node B and the results do not vary much from cell to cell. When the drone is above the base station, the signal strength is higher in cells 34164 and 34163 but only by a difference close to -5 dBm. The discrepancy is more noticeable when comparing the maximum peak rate results where the difference between the results from the reference cell and adjacent cells can go to -7 dBm. However, all the signals captured are high enough to support various services but might not be sufficient for streaming applications since these need higher data rates and UMTS is not the ideal unless low quality is an option, in order to guarantee the minimum requisites.

#### 4.4.2. Scenario B

This scenario maintains the base station from the previous case but the measurement starts in a different location, which corresponds to a different sector from the same eNodeB or NodeB, depending on the technology in use.

- YouTube URL is available at the "References" section [44]

#### LTE

Unlike the previous case and considering our position according to the base station, the graphic B-18 demonstrates that a new sector/cell is able to provide superior throughput results. Considering that a sector is associated to an antenna, the reference sector is not the same as the one from scenario A.

As expected, cell 178 assumes the reference cell role since it is the only one who is able to provide the higher rates throughout the entire measurement when comparing to the adjacent cells throughput results. It is also clear that the signal's behavior from the reference sector is coincident with "hole phenomenon" theory since, between the two maximum peaks, the signal's quality drop drastically and in some cases, is not able to provide the highest quality (VQ5) for video streaming.

Like the previous scenario, it is necessary to zoom in the correct time interval from the last graphic, in order to understand what happens when the reference sector is not able to support the minimum requisites. These requisites for LTE are to maintain a high-quality transmission to be able to support platforms like tablets, PC, etc.

The time interval defined in graphic B-19 is able to show that reference cell is not able to provide enough quality in some moments of time but the adjacent cells from the same eNodeB are capable to compensate this, by keep providing enough rate to support the highest quality video streaming. One more time, like in the scenario A, there's a necessity for softer handover in order to fulfill these requirements since there are no other adjacent base stations in the current network to support other types of handover.

Basing this analysis on the trendlines from the graphic B-20, the reference cell assumes a clear positive tendency and it is able to reach rates close to 75 Mbps when RSRP is close to -25 dBm. Once again, RSRP and throughput are directly proportional. However, in the adjacent sectors, this statement is not so clear since the same higher RSRP does not mean higher throughput results. This aspect relates to SINR since this is fundamental to calculate throughput, which states that it is possible to capture great signal strength but if there are much noise and interference, the signal's quality drops greatly.

The number of samples is useful because it allows calculating the percentage of samples that are above, under and between the two defined quality thresholds:

<b>Channel Frequency: 796 MHz (MEO)</b>			
<b>PCI</b>	<b>179</b>	<b>178</b>	<b>177</b>
<b>Nr. Samples/sector</b>	80	91	88
< VQ1	10 (12.5%)	0 (0%)	9 (10.2%)
> VQ 5	24 (30%)	86 (94.5%)	34 (38.6%)
>VQ1 & <VQ5	46 (57.5%)	5 (5.5%)	45 (51.2%)

*Table 4-10. Nr. of samples and respective percentage for the defined thresholds*

Considering the previous table, it is noticeable that the reference sector is capable to assure minimum quality requirements throughout the drone flight. However, five samples show that in some moments of time, it is not able to provide enough data rate to guarantee the highest quality but the adjacent cells compensate the lack of strength considering the graphic 4-20.

When analyzing the 3D graphics below, the expectation is that these might be similar to the ones from scenario A, since the base station, the antennas and the flight goals are the same. The only difference between them is the reference sector, which relates to the location where measurement took place. The distance between the departure position and the base station is also larger and that might reflect on the signal's behavior.

Graphic B-21 shows that signal strength assumes lower values when the distance to the base station is larger (from 50 to 40 meters) and the height not more than 20 meters. From 20 to 40 meters height, strength increases and reaches close to -45 dBm when closer to the base station (~14 meters) and 40 meters height. Although these values might look promising, between 40 and 50 meters height and from 14 to 11 meters from the BS, the analyzer is not able to capture any signal from this sector and that is the main reason for the presence of a hole in the graphic above. It is possible to conclude that this sector is not able to guarantee a full coverage during the whole drone path but it is able to compensate in some moments of time when the reference sector can't.

The signal represented on graphic B-22 assumes a similar behavior to the one present on graphic B-21 but there is a main difference between them, which in this case is the inexistence of a hole between 40 and 0 meters height. In this interval, this sector is able to provide good signal strength and that is where the relative maximum peak is located.

The signal's tendency is clearer in this case (graphic B-23) due to the number of captured samples from this sector. The initial pattern is similar from the two previous graphics and the main differences are more noticeable between 40 and 50 meters height and when the drone is above the base station, where it assumes a null distance, which is the center position above the BS where the height parameter reaches about 60 meters.

The following table shows the position where signal strength reaches its maximum and minimum peaks. Besides that, it also takes into account the signal's behavior above the base station. It follows the same rule as in the previous scenario: (d, h, s\_strength)

Ch. Freq.	PCI	Max. Peak	Min. Peak	Above BS
796 MHz (MEO)	177	(8.8, 53.5, -46.47)	(32.3, 11.9, -76.99)	(1.5, 60.9, -56.61)
	178	(15.2, 43.6, -25.71)	(11.5, 60.3, -67.7)	(1.5, 60.9, -60.9)
	179	(14.3, 36.3, -49.88)	(37.8, 10.9, -78.2)	(1.5, 60.9, -62.91)

Table 4- 11. Main parameters for all sectors in reference BS



The maximum peak rate is considerably higher in the reference cell by a difference of about -20 to -25 dBm when comparing to the adjacent cells results. Theoretically, the highest peak rate is reachable when closer to the BS and in the same direction as the antenna in order to capture the main lobe, which is able to provide better results. Outside the main lobe, there are secondary lobes that are also able to provide coverage but the results are not as good as in the main lobe.

Above the base station, all the cells are able to get good results and even cell 177, which is an adjacent cell, is able to get a better signal strength than the reference cell in the exact same position.

### UMTS

The characteristics of this scenario are identical to the ones from the scenario A. This scenario considers only the 2152.4 MHz channel frequency and the analyzer does not identify any adjacent base stations from the same network service provider that are capable to provide a good quality signal using the same technology.

Like in LTE technology from the present scenario, the reference sector is no longer the same and now cell 34163 assumes this role, which it is possible to conclude by analyzing this cell throughput results in graphic B-24, being able to reach the highest average rates throughout the entire measurement. However, there are a few moments of time where this sector is not able to provide enough rate to support the poorest video streaming quality. In the graphic B-25 it is analysed that situation considering the available adjacent cells.

Between 80 and 110 seconds approximately, the reference sector does not provide enough throughput to support the lowest quality video streaming. However, in that same interval, the adjacent cells are able to compensate the lack of rate and maintain the QoS.

Channel Frequency: 2152,4 MHZ (MEO)			
PCI	34162	34163	34164
<b>Nr. Samples/sector</b>	80	93	89
< VQ1	55 (68.75%)	11 (11.8%)	44 (49.4%)
> VQ 5	0 (0%)	1 (1.1%)	0 (0%)
> VQ1 & < VQ5	25 (31.25%)	81 (87.1%)	45 (50.6%)

Table 4-12. Nr. of samples and respective percentage for the defined thresholds

Only one sample from the reference cell reaches a throughput superior to the highest quality threshold, so it is not reliable to admit that UMTS is able to support high quality video streaming demands. However, admitting that it can guarantee the minimum

requisites is more reliable since it is capable to do so throughout the entire measurement, even if softer handover is an option.

Unlike the LTE 3D graphics, the spectrum analyzer is only capable to capture the first sample from this sector when the distance to the NodeB is below 20 meters as represented in graphic B-26. Once more, the signal strength results are lower when the distance parameter is between 15 and 20 meters while the drone height is between 0 and 20 meters.

When drone approaches the base station and increases its altitude, the signal strength also increases and reaches its maximum peak between 40 and 50 meters height and 12 to 14 meters distance from BS. From 50 to 60 meters height and while distance gets closer to null, the signal strength decreases but does not assume such lower values when comparing to the initial pattern.

The signal's behavior represented in graphic 4-27 is comparable to the previous one, where the main difference is that in this case, the spectrum analyzer is able to capture since 50 meters distance from the base station. However, from 50 to 20 meters distance, it also assumes the lowest results of the entire measurement. The remaining performance is quite similar to the remaining adjacent sector from graphic 27.

In the graphic B-28, the lowest results are present from 40 to 50 meters distance from the BS and between 0 to 10 meters height. From that location, the signal strength increases significantly until it reaches its maximum peak of -20 dBm close to 30 meters height and 18 meters distance from the BS. Between that location to 45 meters height and 10 meters distance, signal strength decreases until it reaches close to -40 dBm, which is a good result. While decreasing the distance to 8.5 m and increasing its altitude to 50 meters, the signal strength rises once again and reaches a relative maximum of -25 dBm. From that location to the top of the BS, the signal does not modify considerably its behavior since it assumes a -31 dBm value when above the BS.

<b>Channel Frequency</b>	<b>PCI</b>	<b>Max. Peak</b>	<b>Min. Peak</b>	<b>Above BS</b>
2152.4 MHz (MEO)	34162	(17.1, 40.5, -27.96)	(44.1, 6.6, -55.78)	(1.5, 60.9, -31.08)
	34163	(18, 30.6, -20.65)	(44.1, 6.6, -56.24)	(1.5, 60.9, -31.08)
	34164	(18, 30.6, -20.88)	(44, 1, 6.6, -56.2)	(2.2, 60.9, -32.99)

*Table 4- 13. Main parameters for all sectors in reference BS*

The table 4-13 demonstrates that all the sectors provide almost the same signal strength results for close positions and there is not reasonable discrepancy when comparing the reference cell to the others.

#### **4.4.3. Scenario C**

Unlike the previous scenarios, this sub section considers a new base station from a different network service provider (Vodafone). It also analyzes the signal's behavior in UMTS and LTE technologies.

- YouTube URL is available at the “References” section [45] (from 0 to 4:30)

#### **LTE**

In this scenario, the spectrum analyzer is able to capture signal's information from more than one base station considering the same channel frequency.

- eNodeB: 913, 5174
- PCI: 474, 475, 476 for eNodeB 913
- PCI: 360 for eNodeB 5174
- Channel bandwidth: 10 MHz
- Channel frequency: 806 MHz (Vodafone LTE)

The following graphics consider the signal provided by eNodeB 913 and its behavior according to measurement's time.

Graphic B-29 demonstrates that sector 475 is the only who is able to reach the highest rates throughout the measurement. However, from 120 to 200 seconds does not grant the necessary rate to support high quality video streaming.

The graphic B-30 shows that the sectors from the same eNodeB compensate each other in any moment of time. When the reference cell is below the highest quality limit, at least one of the adjacent cells are able to solve this problem by providing a superior throughput for maintaining the QoS. Per example, close to 180 seconds, when the reference cell assumes the lowest throughput comparing to the adjacent cells results, the cell 474 compensates it since it provides close to 30 Mbps rate.

According to graphic B-31, the reference cell assumes a positive tendency throughout the measurement as expected when comparing to the previous scenarios. The adjacent cells trendlines estimate a different behavior, which means that higher signal strength reflects

on higher interference (SINR) and the throughput results will not be as good as in the reference cell. The reference cell assumes higher signal strength but the corresponding SINR is lower, which leads to higher throughput values.

The next table displays the number of samples and the respective percentage that is below, between and above the defined thresholds.

<b>Channel Frequency: 806 MHz (Vodafone)</b>			
<b>Nr. Samples/sector</b>	125	126	107
<b>PCI (Cell ID)</b>	474	475	476
< VQ1	0 (0%)	2 (1.6%)	10 (9.3%)
> VQ5	94 (75.2%)	79 (62.7%)	77 (72%)
> VQ1 & < VQ5	31 (24.8%)	45 (35.7%)	20 (18.7%)

*Table 4- 14. Nr. of samples and respective percentage for the defined thresholds*

The cell that obtains the best results is cell 474, where 75.2% of the samples are above the highest quality threshold and there is not a moment of time where this sector does not concede enough throughput to guarantee the minimum requisites for video streaming. Although the cell 476 assumes worst results since it has the highest percentage of samples below the minimum requisites, it is also capable of obtaining high rates, allowing the highest quality video streaming in some moments of time.

The signal strength values from this cell do not vary much throughout the measurement based on graphic B-32. However, it is possible to verify that the minimum peak rate occurs when the drone is between 12 to 14 meters from the BS and close to the ground, where assumes close to -79 dBm. Increasing the height while maintaining the distance to the BS, makes the signal strength to increase but not considerably since it is only able to reach -65 dBm between 40 and 50 meters height. After that, while the drone flies to the top of the base station by diminishing the distance and increasing its height until approximately 55 meters, the strength decreases again and reaches close to -75 dBm, which is similar to the values when the drone was beginning the flight.

Graphic B-33 demonstrates that in the beginning of the measurement, from 20 to 17 meters distance from the BS and until the drone reaches 20 meters height, signal strength results are between -65 and -60 dBm. When drone increases its height to close to 30 meters and decreases its distance to 16 meters, the analyzer captures an absolute maximum strength value from this cell that corresponds to -35 dBm. From that location, maintaining its distance while increasing its height until it reaches close to 40 meters, analyzer captures several samples where obtains a relative maximum of -47 dBm,

approximately. While decreasing the distance and increasing its to height to be able to get at the top of the BS, the signal will drop significantly, assuming a value close to -73 dBm, which correspond to a difference of about 40 dBm when comparing to the absolute maximum.

Initially, considering the graphic B-34, the spectrum analyzer is not able to acquire the RSRP values for various positions from drone's flight route and that is the main reason why there are so many lines across the graph, which indicate the trace from a location to another lacking the correspondent signal strength. The absolute maximum takes place when the distance to the BS is close to 7 meters and drone's height is approximately 37 meters, reaching about -58 dBm. From that position, the signal assumes the same tendency as in the previous graphics, which is the significant drop of strength while drone gets closer to the base station and increasing its height until it reaches the top of the BS.

It is also important to assume the adjacent base station analysis if hard handover is an option.

The graphic B-35 shows that the cell 360 from the adjacent eNodeB 5174 is able to provide enough rate to ensure the minimum requisites for video streaming but only in some moments of time. This sector would be helpful if any of the adjacent sectors from the reference eNodeB could not supply enough rate to guarantee the minimum quality and hard handover would be considerable if that situation would occur. However, during the flight, there is no necessity to get resources from another base station because the sectors from the reference BS are able to compensate in case of necessity as seen in the graphics above.

Channel Frequency: 806 MHz (Vodafone)			
PCI	Max. Peak	Min. Peak	Above BS
474	(7.1, 36.7, -48.9)	(12.6, 0.1, -79.2)	(2.4, 52.8, -73.1)
475	(16.1, 26.7, -35.7)	(12.9, 51.8, -79.9)	(2.4, 52.8, -72.6)
476	(11.6, 26.6, -56.4)	(12.2, 0.7, -83.3)	(2.4, 52.8, -71.3)
360	(15, 5.6, -81.7)	(15.5, 12.3, -88.6)	(2.4, 52.8, -85.9)

Table 4- 15. Main parameters for all sectors in reference BS

## UMTS

- Channel Frequency: 2117.8 MHz
- Cell IDs from reference base station:
  - CI: 44894, 44895, 44896

- SC: 103, 111, 119
- Cell IDs from adjacent base station:
  - CI: N/A
  - SC: 213
- Channel Bandwidth: 5 MHz

The following graphics consider three cells associated with a single base station where it is possible to analyze the signal's throughput for all sectors during the measurement.

According to graphic B-36, the sector 44895 assumes the reference sector role since it is the only one providing a higher average rate during the whole measurement. However, it is possible to verify from 150 to 200 seconds that the produced throughput is not good enough to reach the minimum quality threshold.

The spectrum analyzer is able to capture information about sectors from the reference base station but it also acquires another sector's data associated to an adjacent base station, which is identifiable by using different scrambling code group (SC: 213). However, this sector's signal does not guarantee the minimum quality video streaming in any moment of time since it does not provide enough throughput considering the captured samples.

Based on graphic B-37, for every moment of time where the reference cell assumes throughput values below the minimum threshold, the adjacent cells from the same base station are able to compensate it and guarantee the minimum quality video streaming.

Once again, in graphic B-38, the reference sector (44895) assumes a positive throughput tendency from the minimum to the highest RSSI result, which means that interference and noise (SINR) do not affect significantly the signal.

The adjacent cell 44896 assumes a negative tendency since the beginning. This means that when signal assumes higher signal strength values, interference and noise are abundant, which will affect the throughput results by dropping dramatically. The other adjacent cell (44896) assumes a positive tendency in the beginning until it reaches close to -45 dBm but that tendency is reversible for higher RSSI outcome once the interference starts affecting the signal's behavior.

	Reference BS (2117.8 MHz)			Adj. BS (2117.8 MHz)
Nr. Samples/sector	113	137	123	24
PCI (Cell ID)	44894	44895	44896	475
< VQ1	41 (36.3%)	17 (12.4%)	66 (53.7%)	24 (100%)
> VQ 5	0 (0%)	10 (7.3%)	0 (0%)	0 (0%)
> VQ 1 & < VQ5	72 (63.7%)	110 (80.3%)	57 (46.3%)	0 (0%)

Table 4- 16. Nr. of samples and respective percentage for the defined thresholds

The table above demonstrates that all the captured samples from the sector that belongs to the adjacent base station are below the minimum threshold, which makes it possible to conclude that there is no hard handover possibility.

In the reference base station, the cell that acquires the best results is the reference cell since only 12.4 % of the samples are below the minimum limit while the others assume higher percentages between 35% and 55%, approximately. It is also unique since is the only one who is able to reach rates superior to the highest quality threshold, representing 7.3% of the samples captured on the reference cell.

The 3D graphics demonstrate the signal's strength behavior according to the changes that occur in distance and height parameters like studied in the previous scenarios.

The last two graphics, graphic B-39 and B-40, show similar aspects in close locations and that is the reason why both descriptions are not separate.

From 30 to 18 meters (furthest location) and from 15 to 12 meters (close to landing and departure locations) distance from BS and between 0 to 10 meters height, it is where the analyzer is able to capture the lowest strength values. However, these results change while increasing the height and decreasing the distance, where it reaches the strongest value from all the measurement, which is close to -26 dBm in  $(d, h) = (9.8, 29.6)$ . From that position to the top of the BS, the RSSI values tend to decrease but do not assume the same pattern as in the distance intervals previously referred. In  $(d, h) = (2.4, 52.8)$ , which corresponds to the closest location to the top of the BS, assumes about -45 dBm.

These graphics only assume an absolute maximum that correspond to  $(d, h, s\_strength) = (9.8, 29.6, -26)$ .

Unlike the two previous cases, the graphic B-41 demonstrates the existence of two absolute maximums considering almost the same height but in different distances from the BS. The main reason why this happens relates to the drone flying in front of the

antenna main lobe when going from location A to B, and from B to C like demonstrated in figure 24. The reference cell from every scenario show this behavior but sometimes the signal strength value for both locations is not as close as in this case. The two maximum peaks occur at  $(d, h, s\_strength) = (9.8, 29.6, -25.9)$  and  $(16.1, 26.7, -25.9)$ .

Ch. Freq.	PCI	Max. Peak	Min. Peak	Above BS
2117.8 MHz (Vodafone)	44894	(9.8, 29.6, -26.3)	(14.6, 1.5, -59.6)	(2.4, 52.8, -45.5)
	44895	(16.1, 26.7, -25.9)	(12.6, 0.1, -59.4)	(2.4, 52.8, -45.4)
		(9.8, 29.6, -25.9)		
44896	(9.8, 29.6, -25.8)	(14.6, 1.5, -59.7)	(2.4, 52.8, -45.4)	

*Table 4- 17. Main parameters for all the cells from reference BS*

According to table 4-3 and comparing its intervals with the results from the table above, it is possible to verify that even the minimum peak results for every cell assume a high signal behavior. However, the RSSI parameter is not the only that should be taking into account since the channel quality is also crucial. The quality relies on throughput parameter, which considers Shannon's theorem that use noise and interference ratio to get a result. This means that a high strength signal with high noise and interference values is not a good quality signal, the previous 2D graphics are able to demonstrate that comparing signals provided from more than one cell.

All the cells have similar results in the parameters considered in table 4-17 but only the reference cell gets two absolute maximums, while the adjacent cells are only able to get one for each.



# **CHAPTER 5**

---

# **CONCLUSIONS**

This chapter presents the main outcomes of developed work, based on experimental trials and theoretical research about the existent propagation models, technologies and current cellular networks architectures

## 5.1. Main conclusions

Regarding the results achieved from theoretical research, it is possible to point out the extended LUI model as the reference propagation model since its main considerations base on UAVs characteristics and its frequency spectrum is large enough to include UMTS and LTE technologies, which are extremely important to high data rates services like streaming. However, the experimental tests regarding this model were made for 2D coordinate system, by considering altitude and distance but not simultaneously, which means that only one of these parameters is constant while the remaining is varying. Besides that, the drone never assumed the position above the base station where the elevation angle value is  $90^\circ$  ( $\theta = 90^\circ$ ).

This dissertation proposed to predict those scenarios, which consequently affected the measurements criteria by considering a 3D coordinate system (latitude, longitude and altitude) where distance and altitude change simultaneously during the flight. Besides that, the drone assumes the top of the base station and respective antennas (~ 10 meters above it) where “*hole* phenomenon” analysis is theoretically achievable.

According to the previous statements and considering the graphics from chapter 4 available in Annex B, measurement begins when the drone takes off from terrain surface (altitude = 0 m) and a few meters distance away from the BS, varying between 15 to 30 meters, depending on the scenario (A, B or C). However, the main goal was to raise the drone while approaching the BS, until it reached only 10 meters above it due to windy conditions that could put in danger the high-cost instruments. When drone reaches the top, it maintains that position for a while to capture more samples in order to achieve a reliable statistic to analyze the “*hole* phenomenon”. After that, it goes back to the landing area, which is close to the departure area by assuming the same route but with the opposite direction.

Before reaching the top of the BS and according to the radiation pattern of a basic antenna, drone receives a higher signal strength when located in front of the main lobe as it is possible to verify at least a maximum peak on the reference sector related 3D graphics. Nonetheless, the secondary lobes are also able to provide signal but not as strong as in the main lobe, which is also reflected by lower signal strength results in the same graphics.

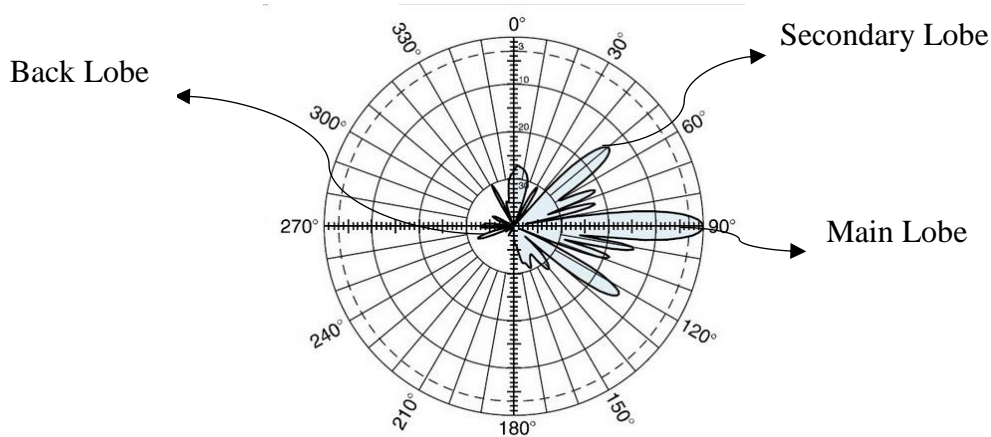


Figure 7- 1. Radiation pattern example vertical plane (Kathrein 742215), Source: [37]

The back lobe represents the rear part of the antenna and, in this case, it assumes lower values than secondary lobe. In the center of the radiation pattern, there is no signal strength and that's where the hole theoretically occurs, which is the most important location during the measurement to respond whether there's enough signal from the current antenna to maintain the QoS for the streaming service.

Considering the measurements done throughout the semester, it is possible to refer that the antenna supporting the reference sector is able to fulfill the minimum requisites when using LTE in any scenario since there are no samples below the minimum threshold, which corresponds to the minimum quality throughput (296 kbps). However, by using this technology, the demand must be greater to achieve the highest quality (3246 kbps), in order to support a higher resolution in more than one type of device. To be able to achieve such quality, it is not trustable to rely only on the reference sector due to the fact that it can't keep higher data rates during the entire flight but it is possible when considering softer handover where the adjacent cells from the same BS provide better quality signal when comparing to the reference cell in certain moments of time during the flight. This procedure occurs in every scenario where measurements took place.

As expected, UMTS is not able to achieve such higher rates when compared to LTE. However, the demand is not as high as in LTE and the main goal is to maintain or overcome the minimum requisites for video streaming during the entire flight, by providing a throughput equal or above 296 kbps using the reference sector or adjacent sectors. Based on this technology measurement results for the scenarios A, B and C, in the interval of time where the "hole phenomenon" takes place, the reference sector is not

able to achieve the minimum requisites but the adjacent sectors from the same BS are able to compensate it if softer handover is taken into account.

Summarizing the previous statements, the “*hole* phenomenon” occurs at the top of the base station/antennas in both technologies. However, if the main goal is to guarantee the minimum requisites for a video streaming service, the referenced sectors achieve it for LTE technology in every analyzed scenario. When considering UMTS, it is only possible to accomplish it from the beginning until the end of the flight by appealing to the adjacent sectors from the same base station. So, it is more reliable to use LTE under these circumstances.

One of the other main concerns during the measurement is the signal’s quality parameter. High signal quality does not mean high signal strength or vice-versa, since interference can disturb significantly the signal’s behavior and that’s clear in the “Signal Strength vs Throughput” graphs. Considering the three measurement locations results, the reference sector is constant providing a higher average signal strength and also high quality, which is explicit by the order 2 polynomial trendlines, while the adjacent sectors may provide similar and/or lower signal strength values, but the quality is not as high as in the reference sector, which is a consequence of the interference (SINR/SNR) effect.

## 5.2 Future Work

Several tests and experiments have been left for future work due to lack of time since measurement campaigns are usually time consuming and there was no opportunity to have the equipment for more time. Based on the previous statement, the following ideas could be interesting:

- It would be interesting to perform new measurement campaigns in all the possible environments (rural, suburban and urban), considering the maximum heights for drone according to the law. Portuguese legislation permits a limit of 120 meters in when drone is in user’s LoS [42], but in this dissertation, it was only able to reach about 60 meters due to windy conditions that could put in risk the expensive equipment;
- Analyze the relation between the various speeds that drone can assume during the flight and how this can affect *handover* event;
- Realize several measurements considering a flight plan where drone goes from a BS to another that belong to the same network service provider assuming the

highest possible altitude during the path to verify if the infrastructure is ready to maintain the QoS for a video streaming service or other.

# **ANNEX A**

## **ROMES SOFTWARE**

This annex demonstrates how to configure the software to be able to start a correct measurement campaign considering the most important aspects

Before adjusting the configurations on ROMES software, it is necessary to access the TSMA user interface, which is possible by opting for one of the following: Local operation and remote access.

Remote access is the best option considering the possibility to establish a connection between the spectrum analyzer and a laptop without physical links (e.g., cables). In order to make this possible, the TSMA generates a WLAN network during the boot process that makes it identifiable for other devices considering that all accessories including WiFi/Bluetooth antennas are properly connected in the rear panel of the TSMA. After that, on the laptop, it is necessary to access the remote desktop connection program assuming that a Windows OS is in use.

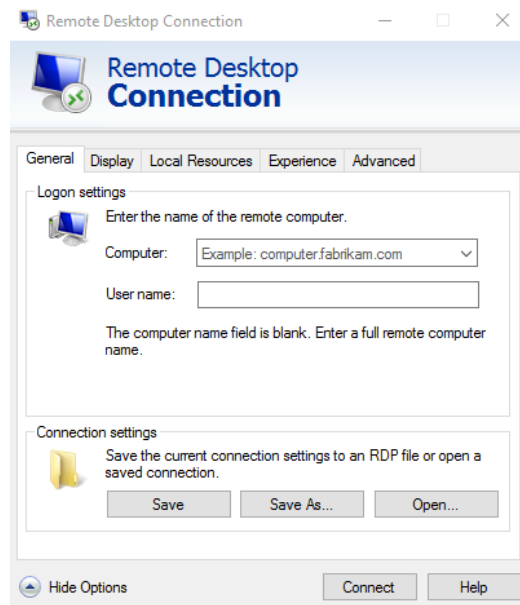


*Figure A- 1. Remote Desktop Connection to access TSMA UI*

The “Computer” and the “User name” fields assume *192.168.1.10* and *instrument*, respectively. After filling in these fields, click “Connect” and a new window pops up, asking for username and password. If the inserted credentials are correct, click “OK” and the remote desktop connection is finally established. From now on, the spectrum analyzer can be controlled as a standard PC.

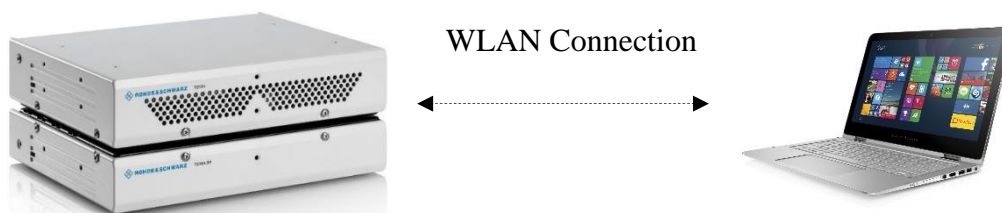


*Figure A- 2. WLAN connection between TSMA and laptop*

It is also necessary to certify that a valid dongle is connected to one of the USB ports in the rear panel of TSMA since it is the only way possible to have full access to ROMES software.

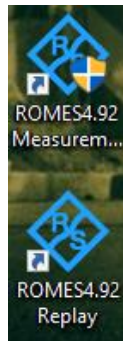


Figure A- 3. ROMES software icons

By double clicking the *ROMES4.92 Measurement* icon, the window in figure A-4 pops up if the dongle is still valid.

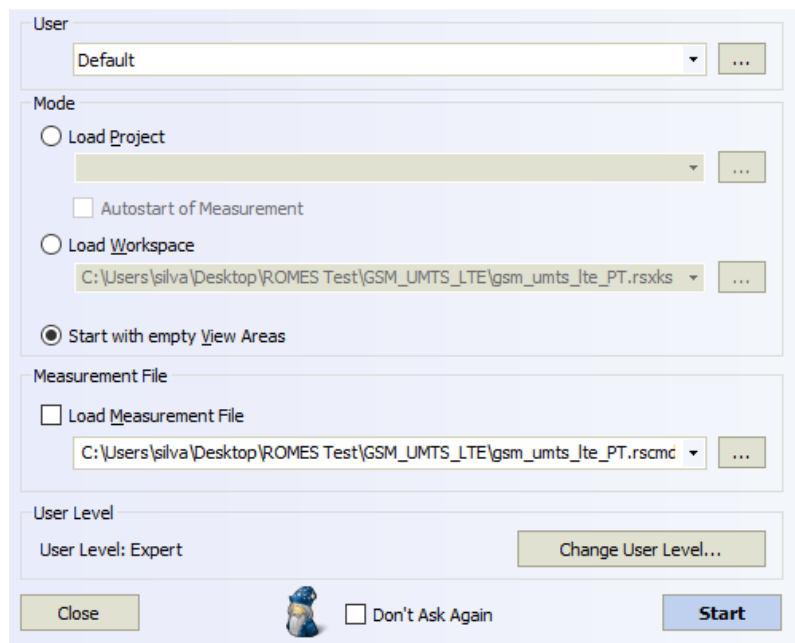


Figure A- 4. StartUp window of ROMES software

It is possible to change the user but in this case, it is not necessary and it maintains as *default*. The user level option (figure A-5) is extremely important in order to ensure that the user has full access to all the software functionalities, which is only possible by selecting *Expert*.



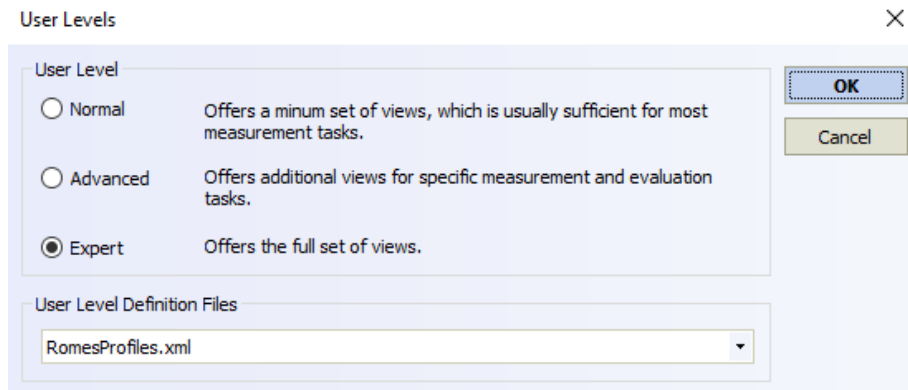


Figure A- 5. User levels

Considering the previous steps as successful, the user is able to press the *Start* button on *StartUp* (figure A-6).

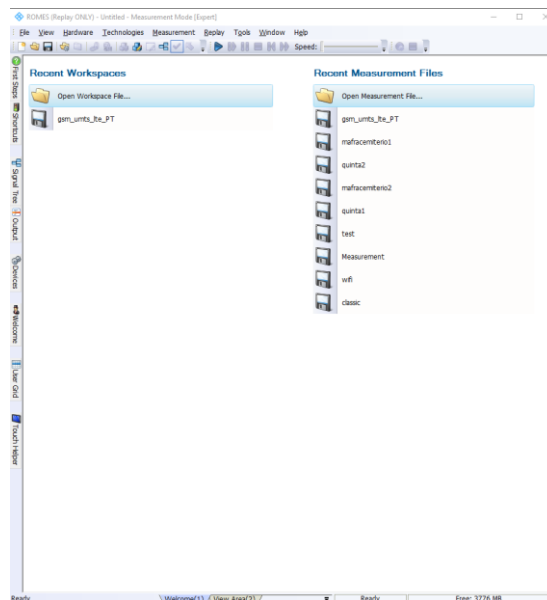


Figure A- 6. Empty workspace

A new empty workspace named “Untitled” is available to configure it from the scratch considering the project requirements.

It is now necessary to verify if the software has automatically detected the device (figure A-7). In this case, during the ROMES startup, the system scans for connected devices and updates the connected devices list if the software is already running.

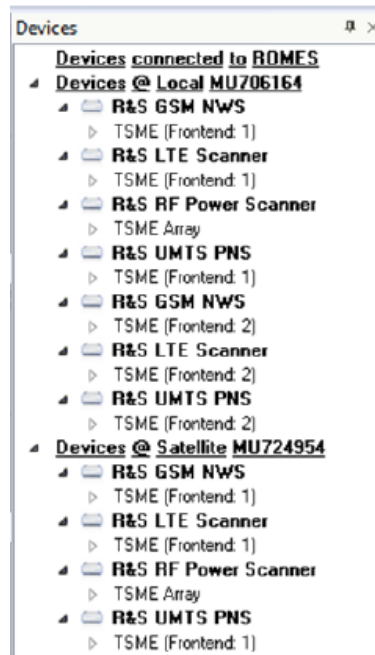


Figure A- 7. List of devices connected to TSMA connected to ROMES, Source: [34]

Figure A-7 shows the tab that presents all the devices connected to ROMES with their respective status. In this dissertation's case, it is supposed to reveal R&S TSMA but is not demonstrated here due to the lack of screenshots at the time of the measurement campaign. It is crucial to certify that the equipment is connected to the software and this tab is ideal to make it clear.

Once these devices are detected in ROMES software, the corresponding drivers are loaded and ready for further configurations.

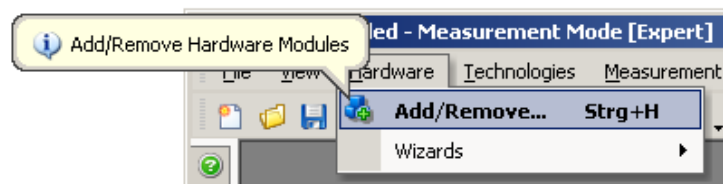


Figure A- 8. Add/Remove drivers, Source: [34]

The option described in figure A-8 is only clickable when the device is detected and connected to R&S ROMES. By selecting that option, several drivers are available but only a few are necessary for the proposed measurement campaign.

Driver Group	Driver
Navigation	uBlox GPS TSME GPS
Network Scanner TSME	TSME GSM TSME WCDMA (UMTS) TSME LTE TSME RF Power Scanner

Table A - 1. Drivers used in the measurement campaign

TSME drivers are compatible with TSMA equipment since they have similar characteristics like studied in section 2.3 and that's the main reason why most of the driver's name consider "TSME" and not "TSMA".

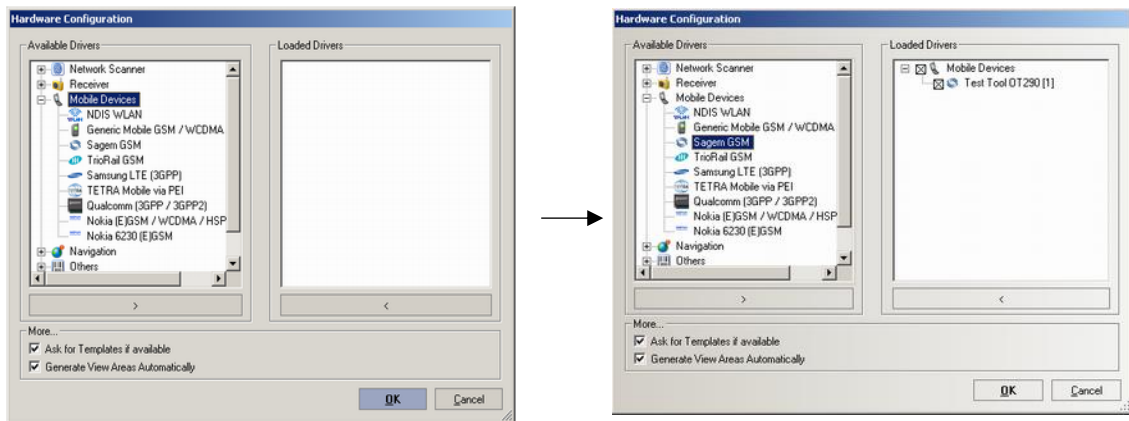


Figure A- 9. Available and loaded drivers (example), Source: [34]

In figure A-9, it is possible to verify the selection of a driver related to mobile devices even if it is not the same as the one in use in this dissertation. However, the main goal of this figure is to demonstrate the available drivers when the software detects a certain device and the way they can be loaded.

According to the dissertation's requirements, it is necessary to access the "Network Scanner TSME" section on the "Available Drivers" box as well as its related drivers that are present in its subsection. After selecting the necessary drivers, there's the possibility to generate the related view areas automatically, by selecting the respective combo box.

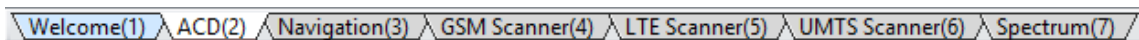


Figure A- 10. Generated view areas labels

- ACD – Automatic Channel Detection – its main function is to detect and locate all available channels in a defined frequency band for several technologies like

GSM, UMTS and LTE. In order to define the frequency bands of Portugal, the following steps accomplishment is indispensable:

- ACD command path: *Hardware > Wizards*
- Indicate the Radio Access Technologies, add GPS driver and press *Next* (figure A-11).

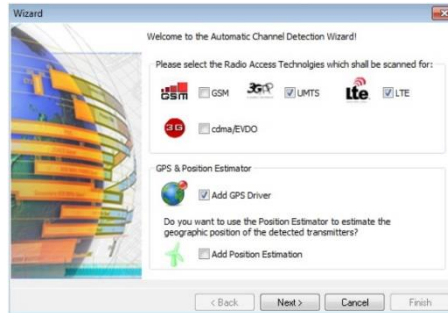


Figure A- 11. RAT selection, Source: [34]

- Specify the frequency range (750 to 2650 [MHz]) to be used in ACD > *Next* (figure A-12)

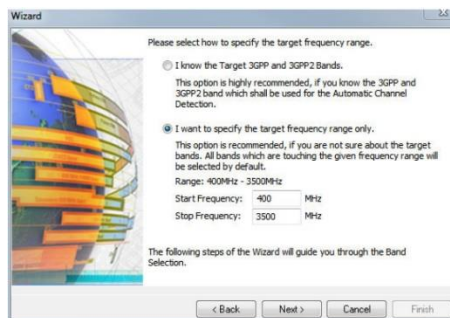


Figure A- 12. Frequency interval, Source: [34]

- Select the frequency bands according to the section 2.4 since these are between the previously defined frequency interval. After selecting the options, select *Next* (figure A-13).

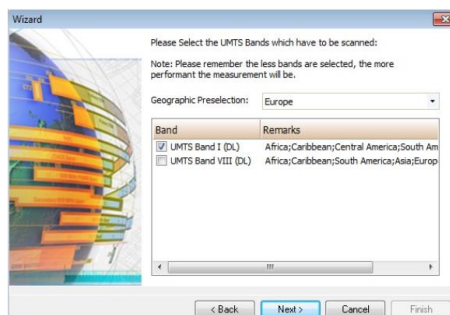


Figure A- 13. Frequency bands available, Source: [34]



- *Top N Chart* - a chart panel displaying 2D and 3D values of the signal selected for ranking, following the configuration represented in figure A-17.

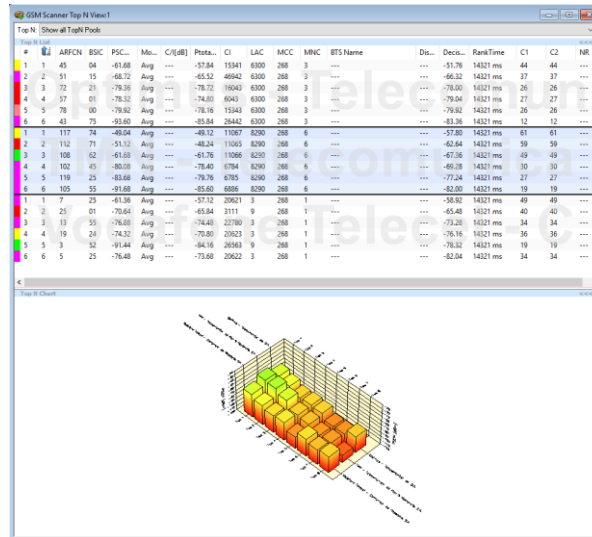


Figure A- 16. GSM Scanner Top N View during measurement

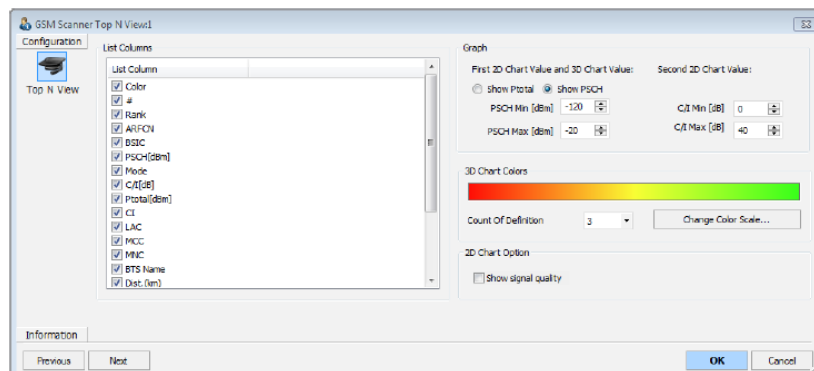


Figure A- 17. GSM Scanner Top N Configuration, Source: [34]

- *GSM Scanner BCH View* displays a list of all the “system information (SI) type decoded by the GSM BCH demodulator”, where the content of each SI respect the information described in standard 3GPP TS 44.018.

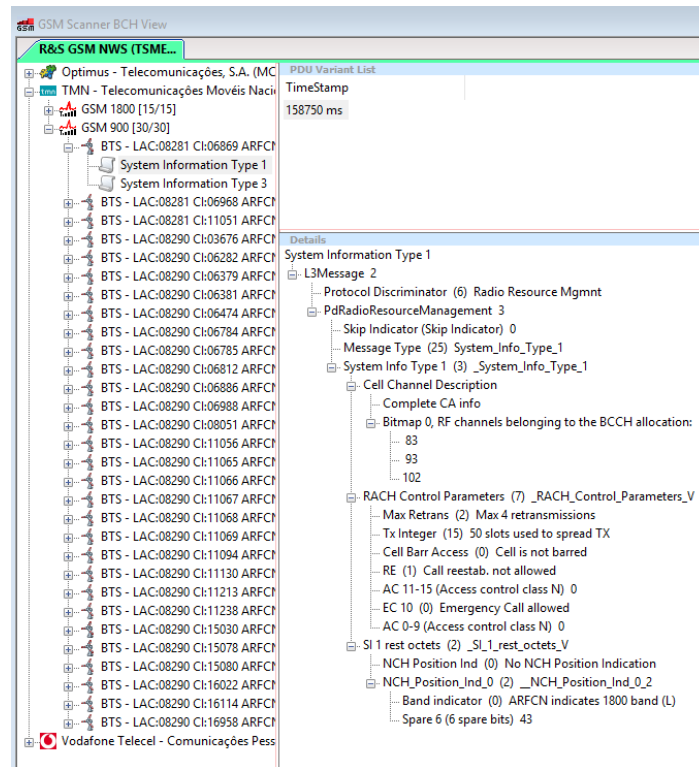


Figure A- 18. GSM Scanner BCH Tree View during measurement

UMTS and LTE Scanner view areas consider the same panels but with different names and support new parameters, which are characteristic to each technology:

- UMTS Scanner:
  - UMTS Scanner Top N View (Top N List/Chart)
  - UMTS Scanner BCH View
- LTE Scanner:
  - LTE Scanner Top N View (Top N List/Chart)
  - LTE Scanner BCH View
- *Spectrum* tab displays the *RF Power Spectrum View* [34], which splits into three different sections and each one represents a distinctive way to represent the spectrum:
  - *Power Spectrum Overview* is the top section of the view and represents an overview of the sweeps considering the driver configuration, which in this case rely on the defined frequency band.
  - *Spectrum View* is the middle section and displays the spectrum of the top section selected sweep.
  - *Spectrum History View* considers the spectrum related to a time dimension, where the power values are indicated using a color scale.

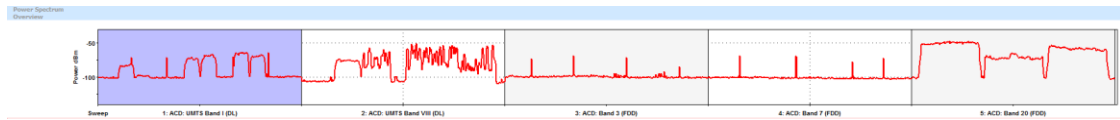


Figure A- 19. Power Spectrum Overview

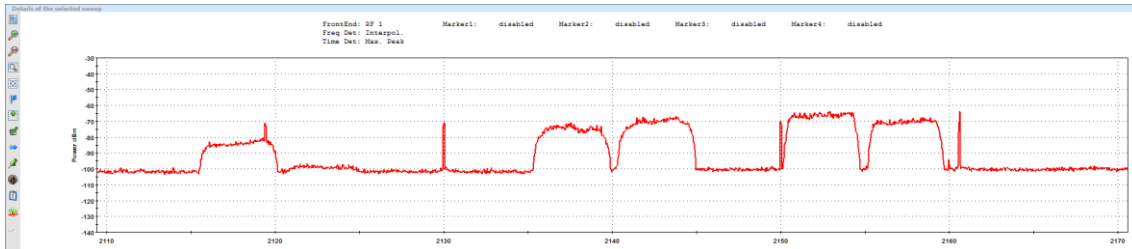


Figure A- 20. Details of the selected sweep

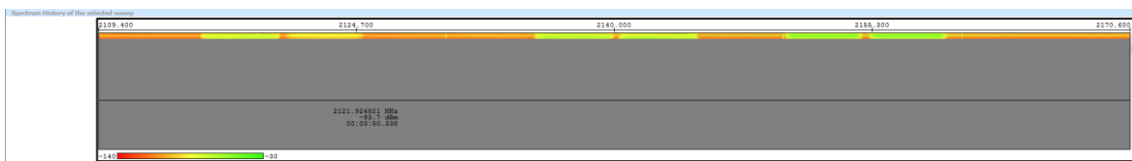


Figure A- 21. Spectrum History of the selected sweep

After defining the view areas with the correct settings, the available signals are displayed in a tree diagram:

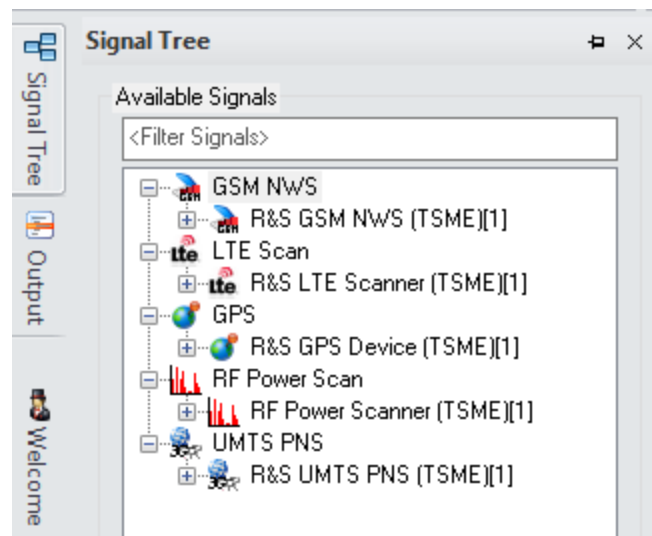


Figure A- 22. Available signals

Besides the previous steps, it is also fundamental to define the preferences before starting the measurement by accessing the *Tools* menu and clicking *Preferences* option.



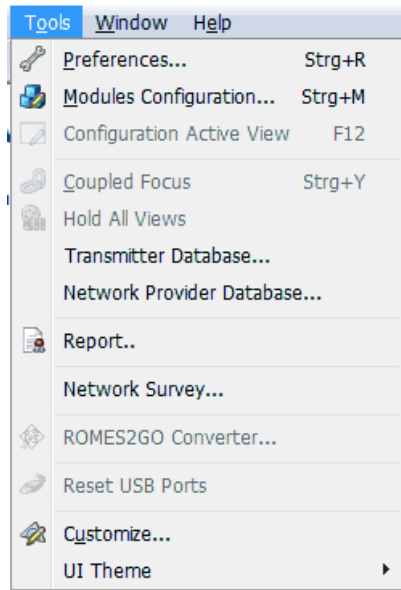


Figure A- 23. Tools menu

In *Preferences* menu, six tabs are available to make the necessary changes. However, only three are crucial:

1. *General* tab permit to define new default directories for measurement files, workspace files and exported data files.

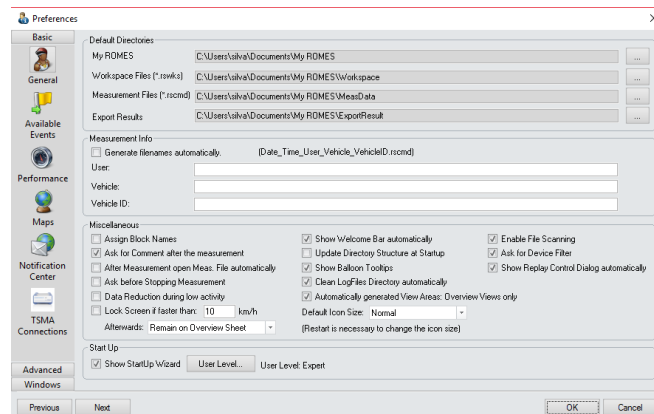


Figure A- 24. General settings

2. *Performance* tab improves the performance from the measurement software, as the update rate of the list (e.g., *Top N Views*). In this case, the option *Show all measurement results* is selected to update the lists for each changed measurement result.

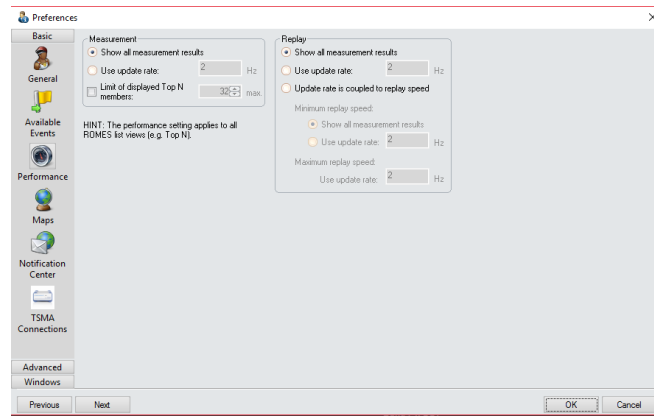


Figure A- 25. Performance tab settings

3. *TSMAs Connections* tab has the option to define the maximum number of TSMAs since the software is able to support up to four units. However, it is important to ensure that only one is selected and there's no need to search for others close to it.

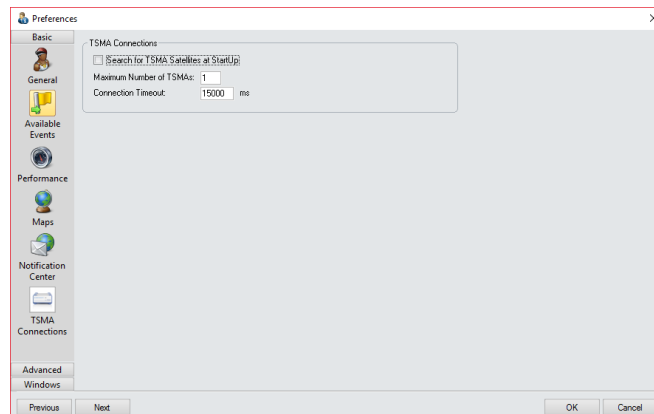


Figure A- 26. TSMAs connections settings

It is now time to save the workspace using the path: “File” > “Save Workspace As...”. This generates a workspace file (\*.rsxks) with all the desired settings, the view areas, and preferences in the default directory defined on the General tab for workspace files. In this case, the file name is: “gsm\_ums\_lte\_PT”.

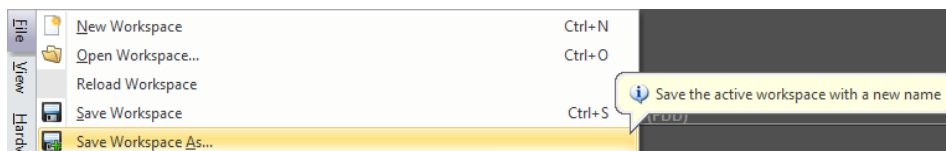


Figure A- 27. Save workspace file

Assuming that the workspace is loaded and the device is still available in the ROMES software, it is now possible to start the measurement and write the data to a measurement file to replay or export with a different extension to analyze the acquired results later.

After clicking the *Start recording button*, the system asks to define a name for the measurement file.



Figure A- 28. Start recording button, Source: [34]

Clicking on the stop button after finishing the measurement ensures that the measurement and the data recording stop. Besides that, it saves all the information captured by the spectrum analyzer in the file considered in the previous step. The file extension is \*. rscmd and it is available for replay, export to other extension or overwriting actions.



Figure A- 29. Stop button, Source: [34]

The statistical analysis is necessary and the MS Excel is the best option to deal with it. However, the actual \*. rscmd file can't be open in such software so, it has to be export to a different extension to make sure that the generated file is compatible with it.

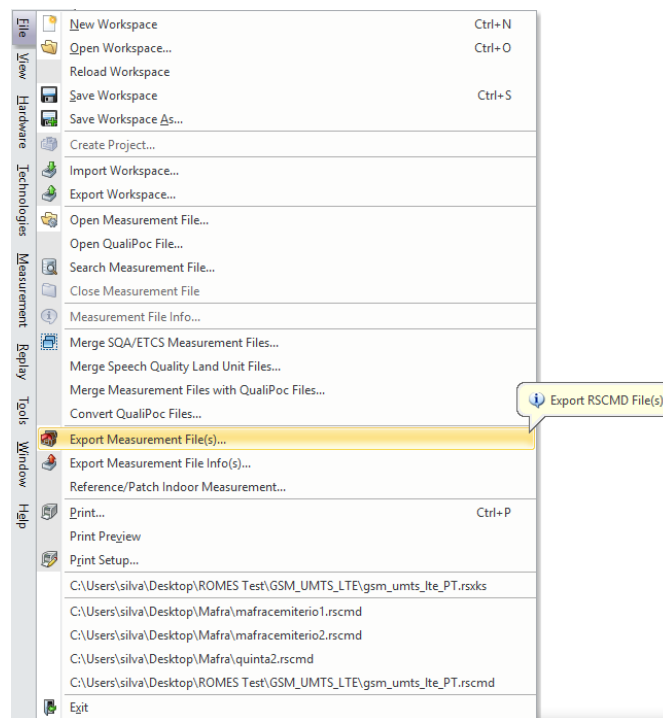


Figure A- 30. Export measurement file to another extension

*Scanner Data* export is the most reliable option since it is able to generate the equipment's track route via KML files besides the .csv files that contain all the information from the selected RATs. To generate these files, it is necessary to achieve the following steps:

1. Select export format > Click "OK" (figure A-29).

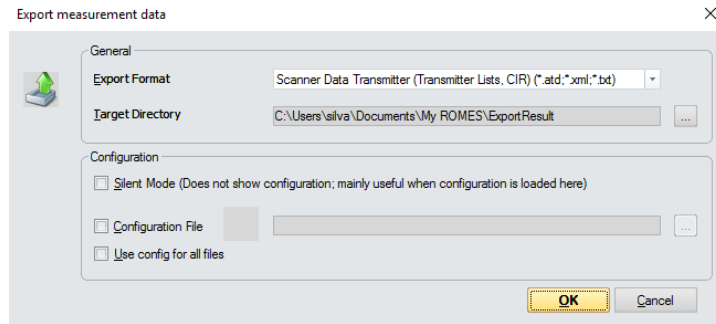


Figure A- 31. Export measurement data menu

2. Select the measurement file to export > Click “Open” (figure A-30).

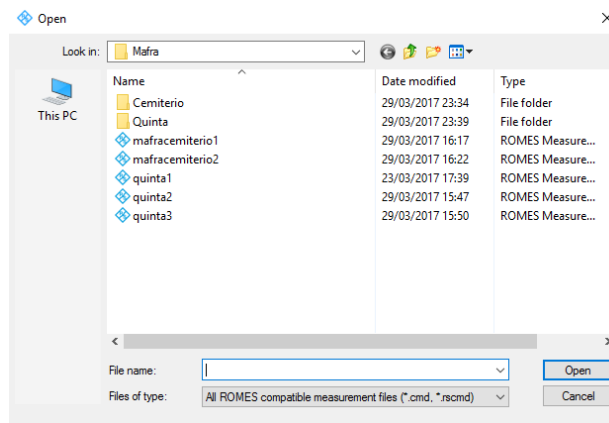


Figure A- 32. Measurement file to export

3. Confirm the available devices by clicking “OK” (figure A-31).

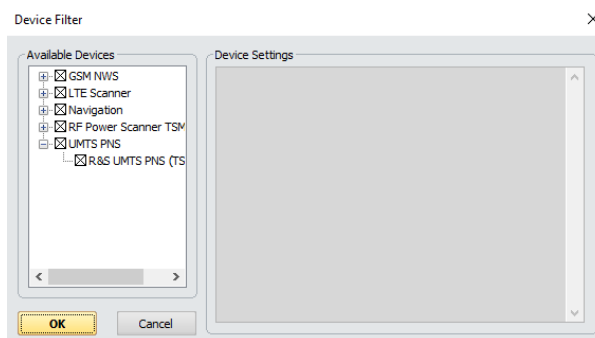


Figure A- 33. Available devices in selected measurement file

4. Use the following settings and click “OK” (figure A-32).

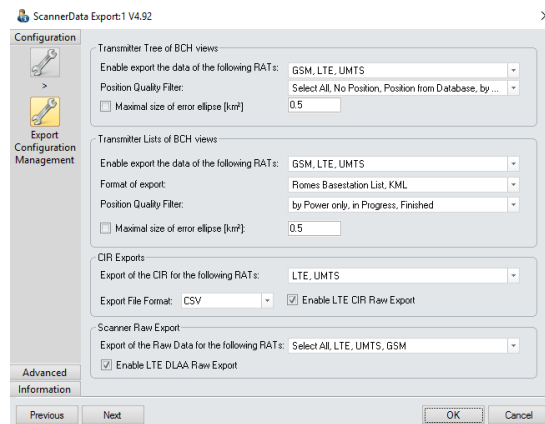


Figure A- 34. ScannerData Export settings

This method creates a KML file, which can be open in Google Earth to verify the route track of the equipment and it is important to achieve the flight routes that are present in section 4.3. Besides that, it creates a new folder with the same name as the measurement file that contains the .csv and other extensions files.

quinta2	29/03/2017 15:47	ROMES Measure...	20 147 KB
---------	------------------	------------------	-----------

Figure A- 35. Measurement file (\*.rscmd)

quinta2	17/04/2017 18:51	File folder	
quinta2	30/03/2017 16:43	KML	3 222 KB

Figure A- 36. Scanner data export result (folder and KML file)

GSM_R&S GSM NWS (TSME)_11_trans_its...	30/03/2017 16:21	ROMES BTS impor...	2 KB
GSM_R&S GSM NWS (TSME)_11_trans_its...	30/03/2017 16:21	KML	4 KB
GSM_R&S GSM NWS (TSME)_11_trans_its...	30/03/2017 16:21	Text Document	1 KB
GSM_R&S GSM NWS (TSME)_11_trans_tr...	30/03/2017 16:21	Text Document	1 KB
LTE_11_cir_15_19_42_30_03_2017	30/03/2017 16:21	Microsoft Excel C...	1 808 KB
LTE_11_peaks_15_19_42_30_03_2017	30/03/2017 16:21	Microsoft Excel C...	3 097 KB
LTE_11_RefSig_cir_15_19_42_30_03_2017	30/03/2017 16:21	Microsoft Excel C...	2 050 KB
LTE_11_RefSig_peaks_15_19_42_30_03_20...	30/03/2017 16:21	Microsoft Excel C...	1 779 KB
LTE_21_CIR_Raw_15_19_42_30_03_2017	30/03/2017 16:21	XML Document	722 714 KB
LTE_R&S LTE Scanner (TSME)_11_trans_li...	30/03/2017 16:21	ROMES BTS impor...	2 KB
LTE_R&S LTE Scanner (TSME)_11_trans_li...	30/03/2017 16:21	KML	4 KB
LTE_R&S LTE Scanner (TSME)_11_trans_li...	30/03/2017 16:21	Text Document	1 KB
LTE_R&S LTE Scanner (TSME)_11_trans_tr...	30/03/2017 16:21	Text Document	2 KB
mafra1_GSM_TecRaw_15_19_42_30_03_2017	30/03/2017 16:21	Microsoft Excel C...	13 KB
mafra1_LTE_TecRaw_15_19_42_30_03_2017	16/04/2017 01:35	Microsoft Excel C...	654 KB
mafra1_UMTS_TecRaw_15_19_42_30_03_2...	15/04/2017 15:34	Microsoft Excel C...	799 KB
quinta2_vodafone	17/04/2017 18:42	Microsoft Excel W...	113 KB
UMTS_11_cir_15_19_42_30_03_2017	30/03/2017 16:21	Microsoft Excel C...	646 KB
UMTS_11_peaks_15_19_42_30_03_2017	30/03/2017 16:21	Microsoft Excel C...	1 008 KB
UMTS_R&S UMTS PNS (TSME)_11_trans_...	30/03/2017 16:21	ROMES BTS impor...	2 KB
UMTS_R&S UMTS PNS (TSME)_11_trans_...	30/03/2017 16:21	KML	4 KB
UMTS_R&S UMTS PNS (TSME)_11_trans_...	30/03/2017 16:21	Text Document	1 KB
UMTS_R&S UMTS PNS (TSME)_11_trans_...	30/03/2017 16:21	Text Document	2 KB

Figure A- 37. Folder content

Considering the folder content in figure A-35, it is now possible to start the statistical analysis of each measurement using the indispensable data and avoiding the unnecessary information with filtering options in MS Excel. All graphics in section 4.4 were obtained

using this method, MATLAB software and a small JAVA program to organize the values into matrices of three columns to design the 3D graphics.

The process explained in this annex is viable to use with any measurement file.

# **ANNEX B**

## **MEASUREMENT**

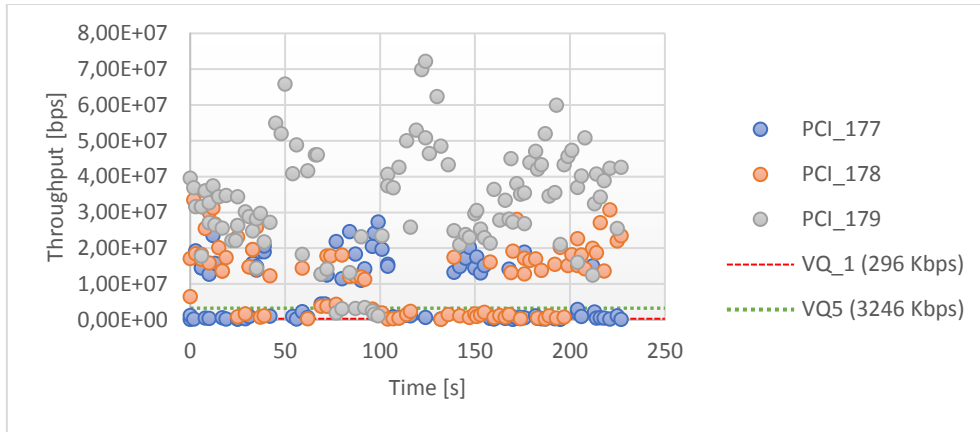
### **RESULTS**

This annex considers 2D and 3D graphics related to the measurement campaign taken place in this thesis and integrated in section 4.4

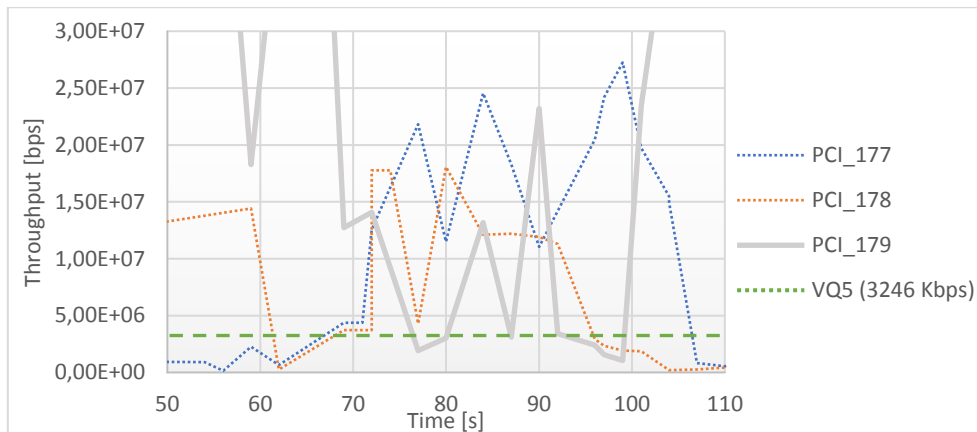
## B.1. Scenario A:

The results related to the scenario A from section 4.4.1. are presented here relating parameters like throughput, signal strength, time, distance and height considering the use of UMTS and LTE technologies from a specific service provider (MEO).

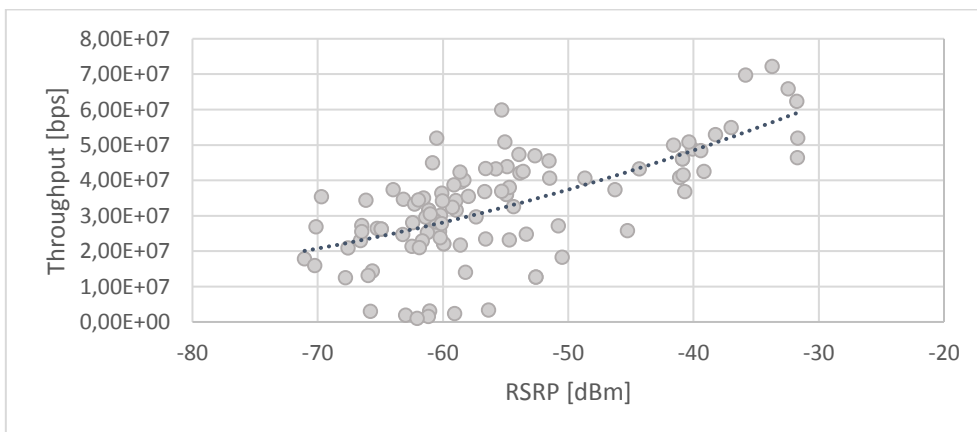
- **LTE (796 MHz Channel)**



*Graphic B - 1. All sectors/cells from reference BS (eNodeB: 1675)*

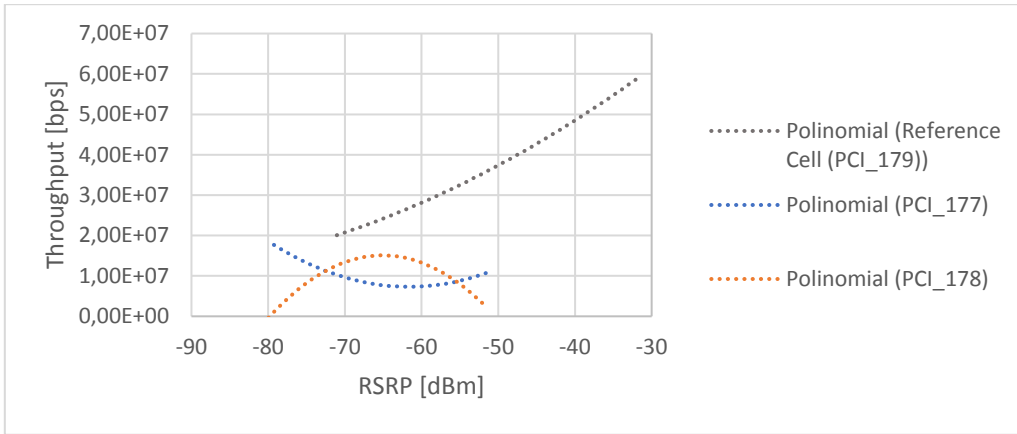


*Graphic B - 2. Reference sector below the highest quality threshold*

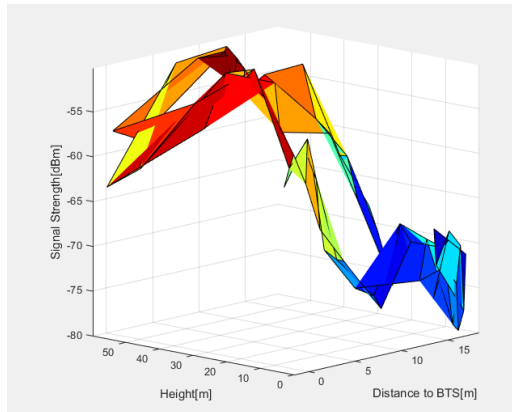


*Graphic B - 3. Throughput vs RSRP from the reference sector*

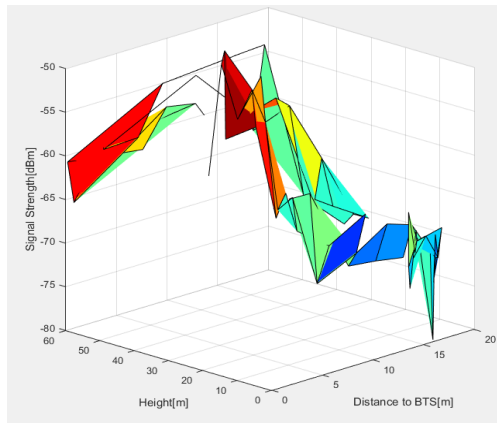




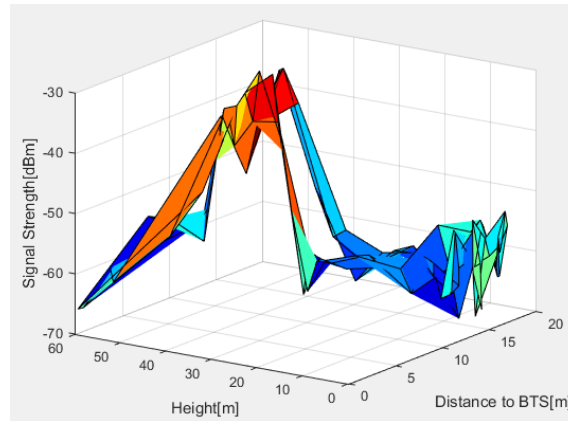
Graphic B - 4. Order 2 polynomial trendlines for every sector in reference BS



Graphic B - 5. RSRP vs Height vs Distance to BS (PCI\_177)

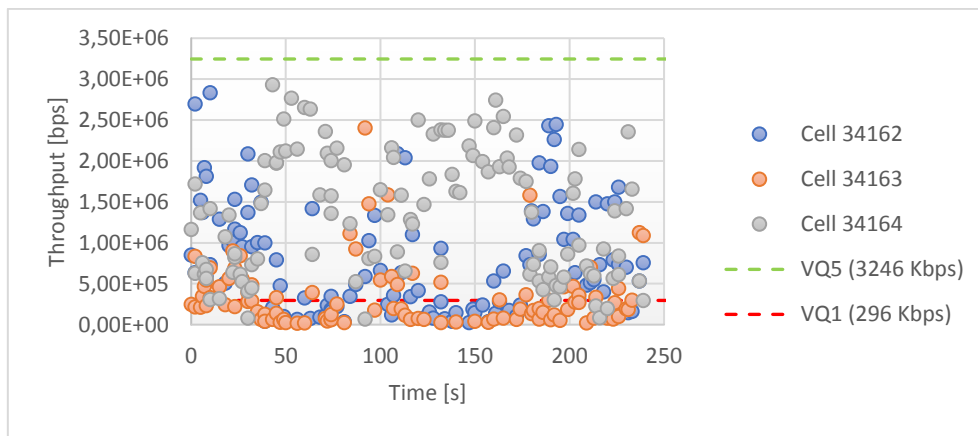


Graphic B - 6. RSRP vs Height vs Distance to BS (PCI\_178)

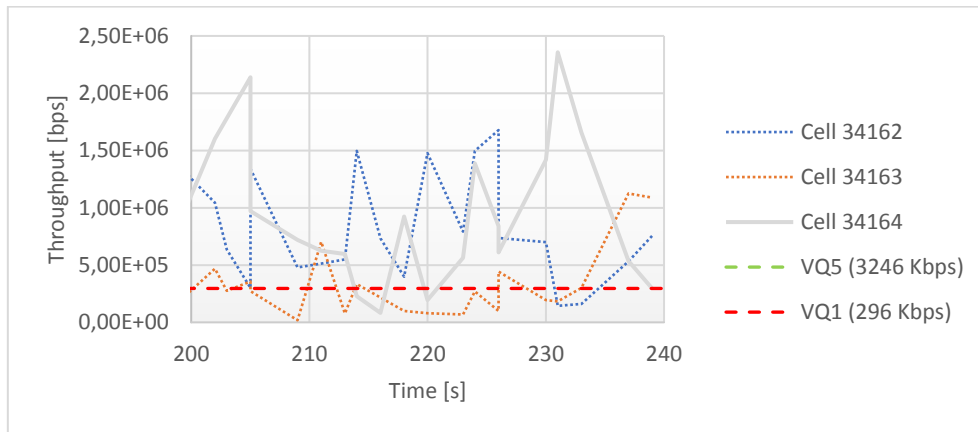


Graphic B - 7. RSRP vs Height vs Distance to BS (PCI\_179)

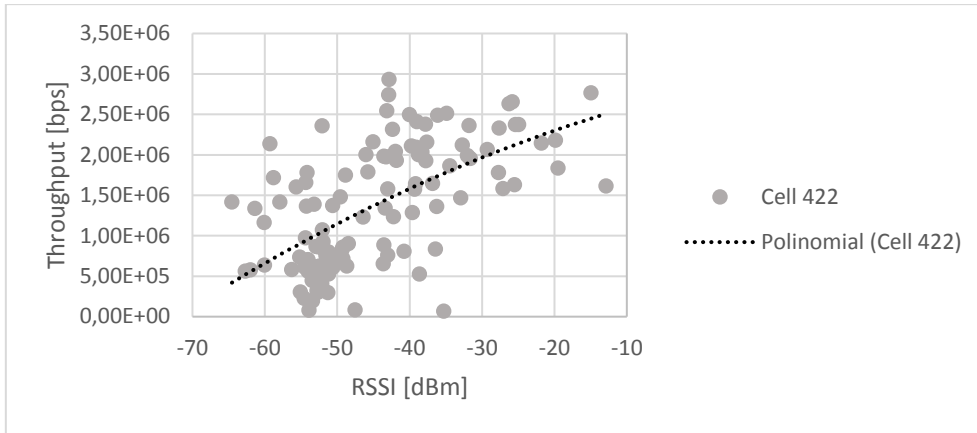
• UMTS (2152.4 MHz Channel):



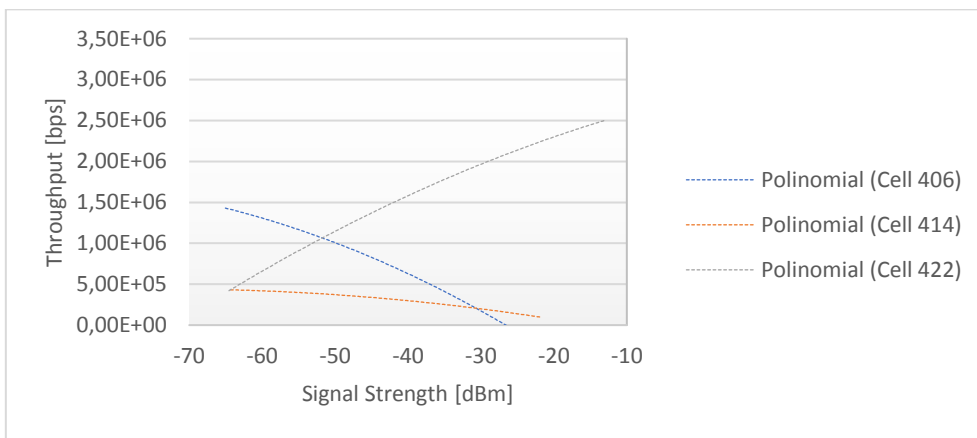
Graphic B - 8. Throughput vs Time [All sectors, reference BS]



Graphic B - 9. Reference sector throughput below minimum threshold

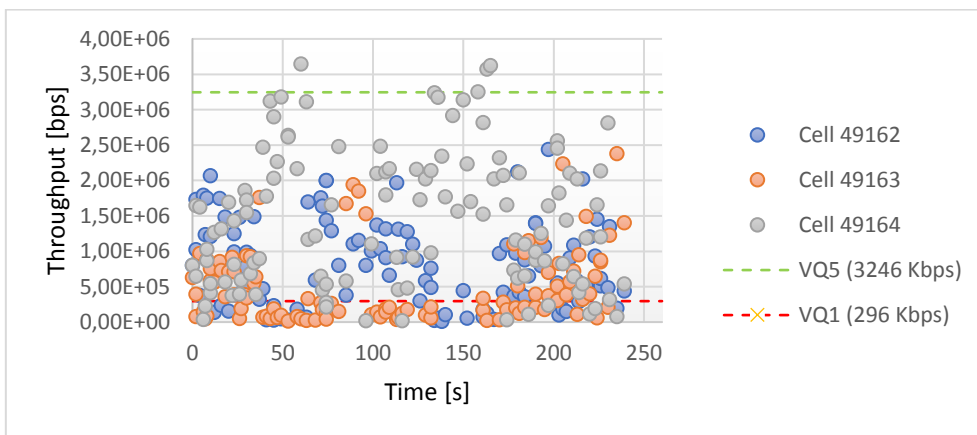


Graphic B - 10. Throughput vs RSSI [reference sector]

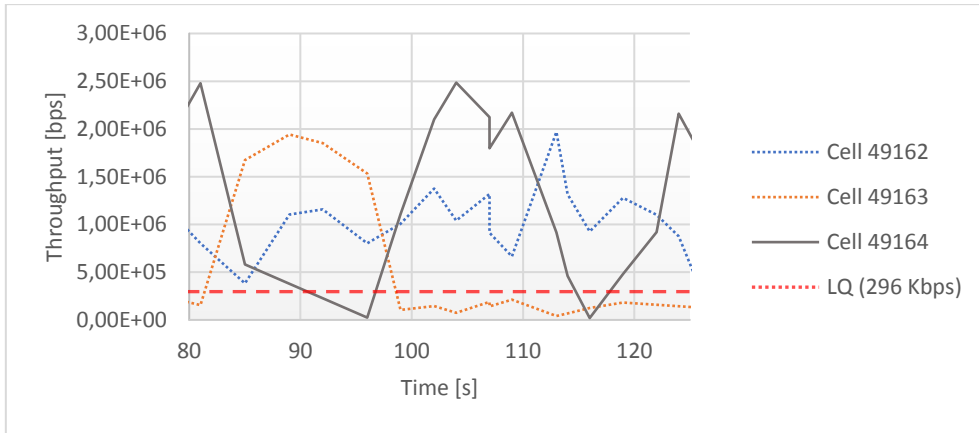


Graphic B - 11. Order 2 polynomial trendlines for every cell in reference BS

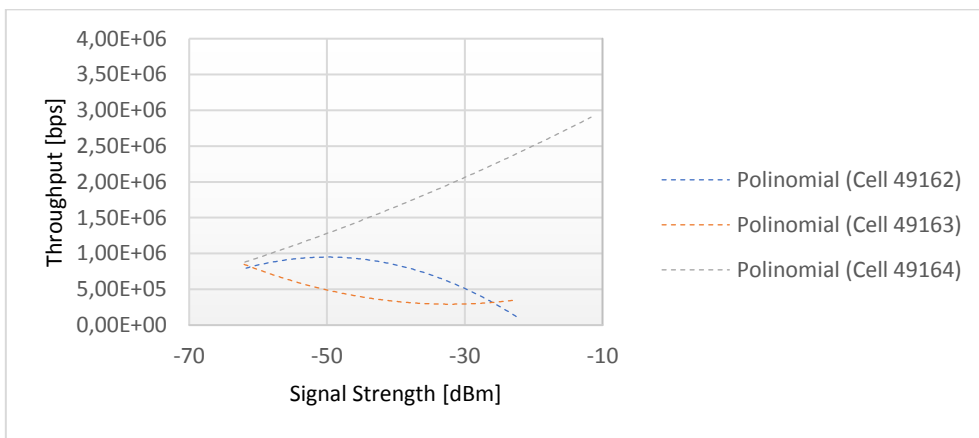
• UMTS (2157.4 MHz Channel):



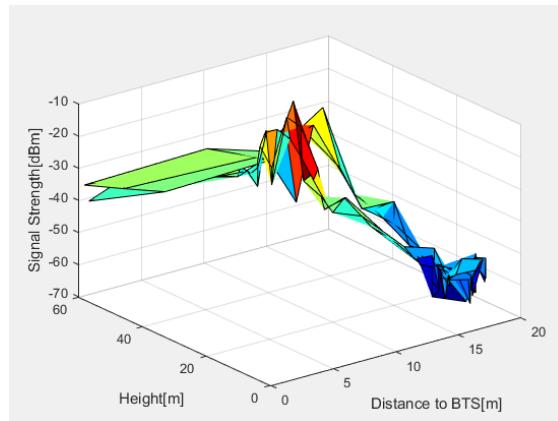
Graphic B - 12. Throughput vs Time [All sectors, reference BS]



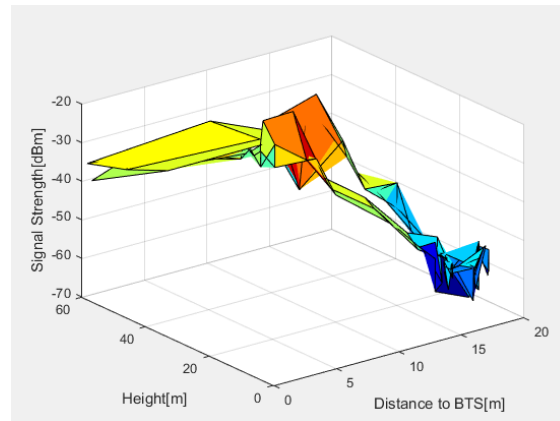
Graphic B - 13. Signal strength from reference sector below minimum threshold



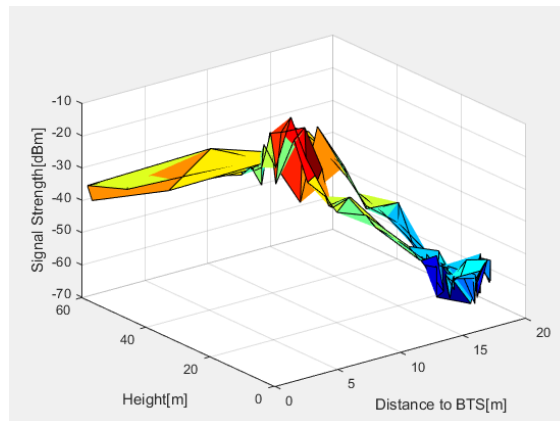
Graphic B - 14. Order 2 polynomial trendlines for every cell in reference BS



Graphic B - 15. RSSI vs Height vs Distance to BS (Reference cell: 34164)



Graphic B - 16. RSSI vs Height vs Distance to BS (Cell 34163)

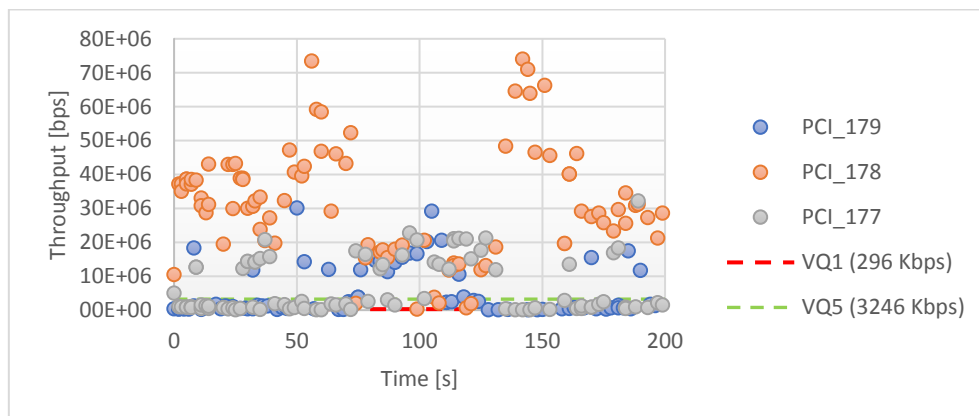


Graphic B - 17. RSSI vs Height vs Distance to BS (Cell 34162)

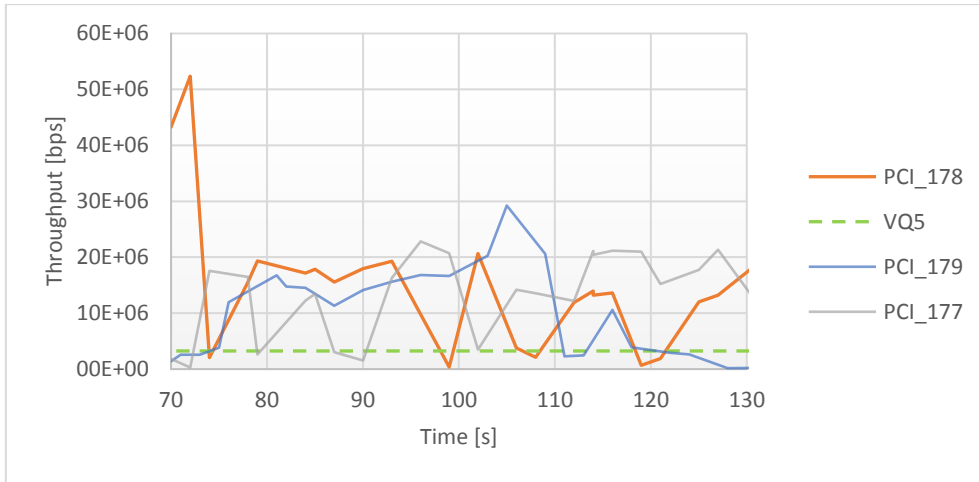
## B.2. Scenario B:

The results related to the scenario B from section 4.4.2. are presented here relating parameters like throughput, signal strength, time, distance and height considering the use of UMTS and LTE technologies from a specific service provider (MEO).

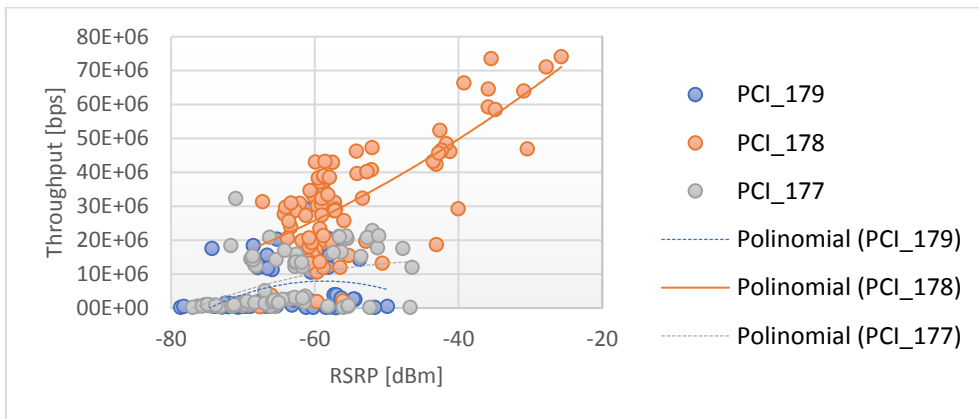
- **LTE (796 MHz Channel):**



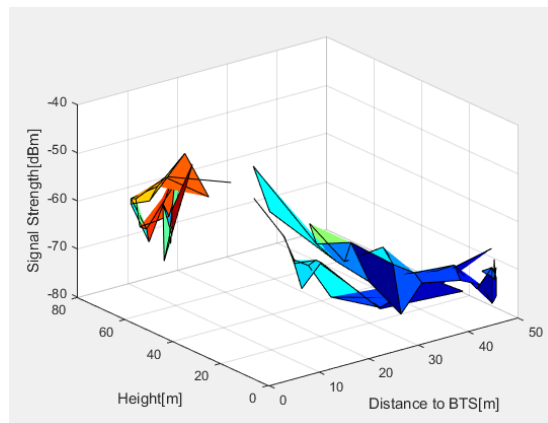
Graphic B - 18. Throughput vs Time considering all sectors from reference BS



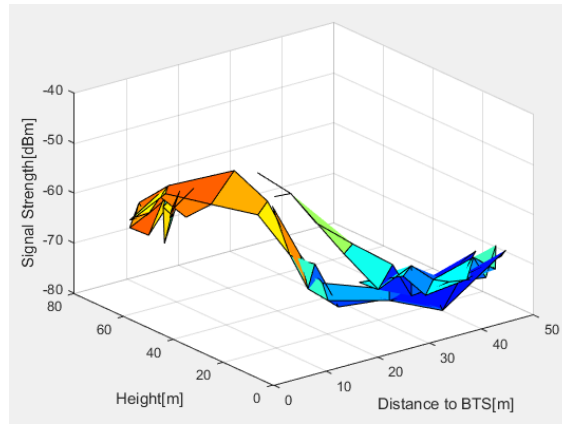
Graphic B - 19. Reference sector results below VQ5 threshold



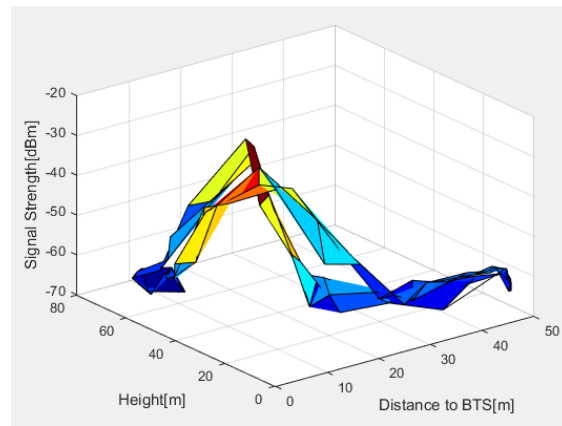
Graphic B - 20. Throughput vs RSRP for all sectors from reference BS



Graphic B - 21. RSRP vs Height vs Distance to BTS for sector 177 (adjacent)

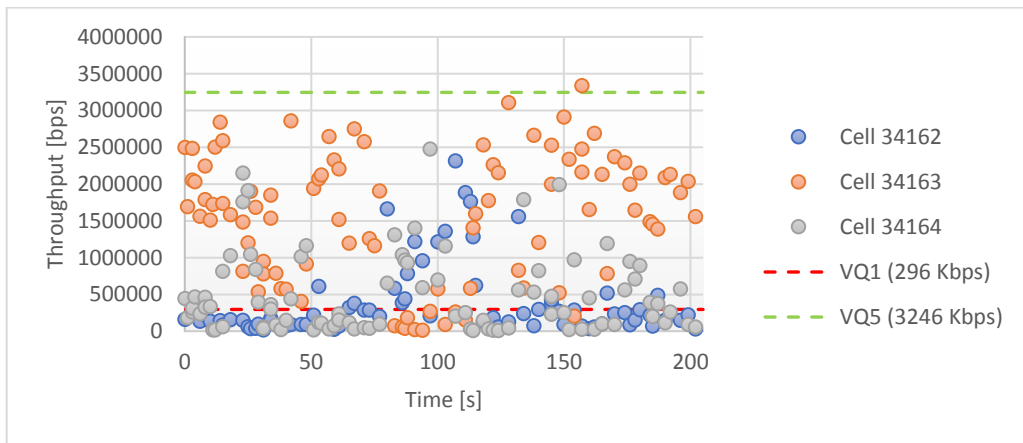


Graphic B - 22. RSRP vs Height vs Distance to BTS for sector 179 (adjacent)

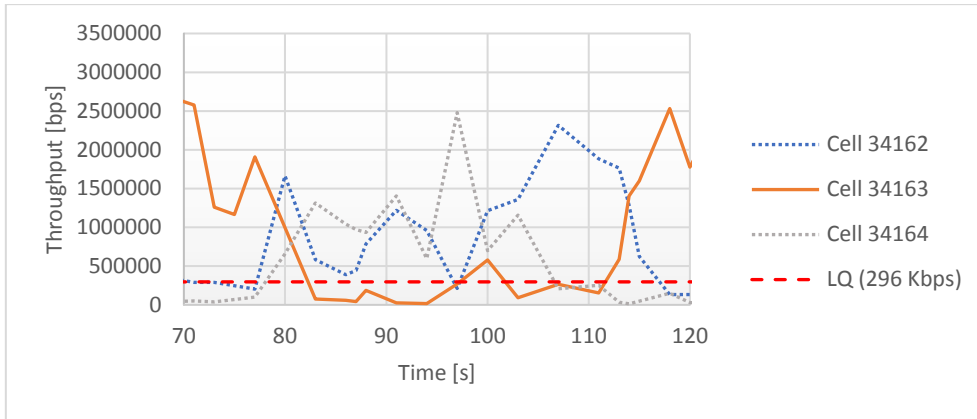


Graphic B - 23. RSRP vs Height vs Distance to BTS for sector 178 (reference)

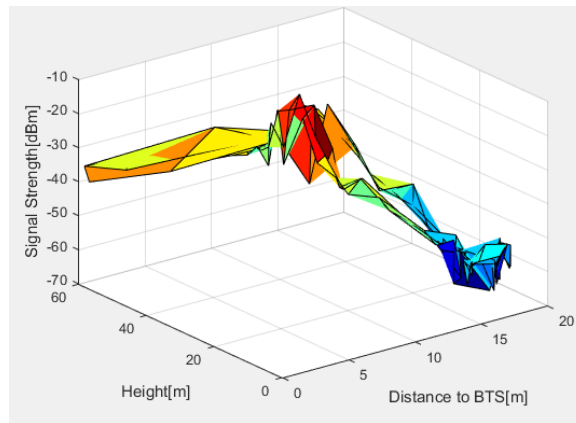
• UMTS (2152.4 MHz Channel):



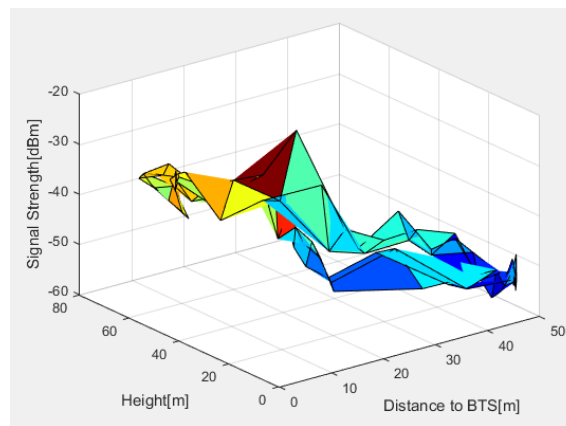
Graphic B - 24. Throughput vs Time for all sectors from the reference BS



Graphic B - 25. Reference sector throughput below poorest quality threshold

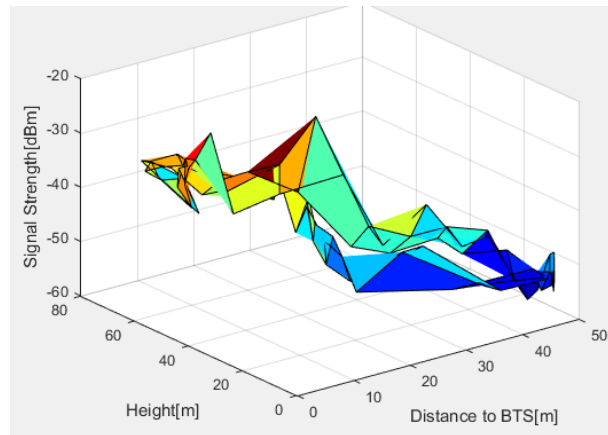


Graphic B - 26. RSRP vs Height vs Distance to BTS for sector 34162 (adjacent)



Graphic B - 27. RSRP vs Height vs Distance to BTS for sector 34164 (adjacent)



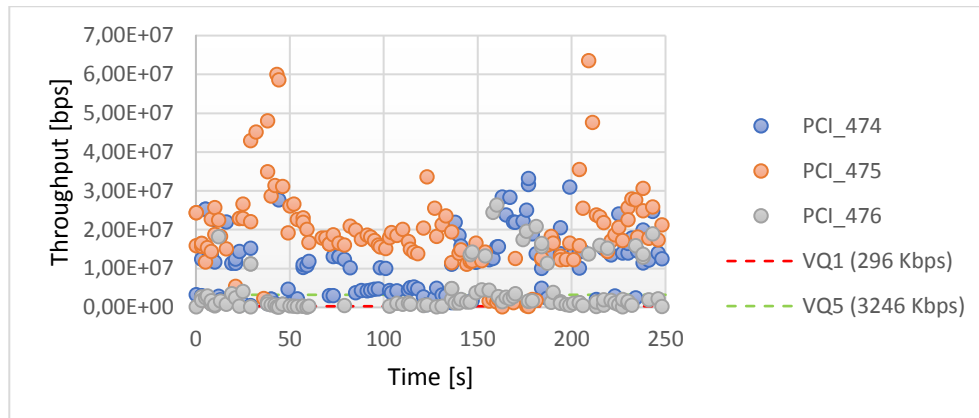


Graphic B - 28. RSRP vs Height vs Distance to BTS for sector 34162 (reference)

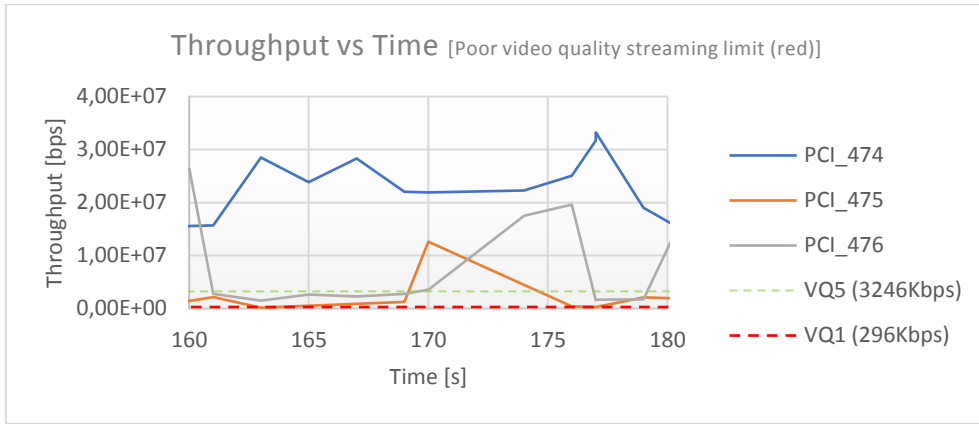
### B.3. Scenario C:

The results related to the scenario A from section 4.4.3. are presented here relating parameters like throughput, signal strength, time, distance and height considering the use of UMTS and LTE technologies. However, it considers a difference service provider (Vodafone) comparing to the previous scenarios A and B, being the main reason to consider channel frequencies.

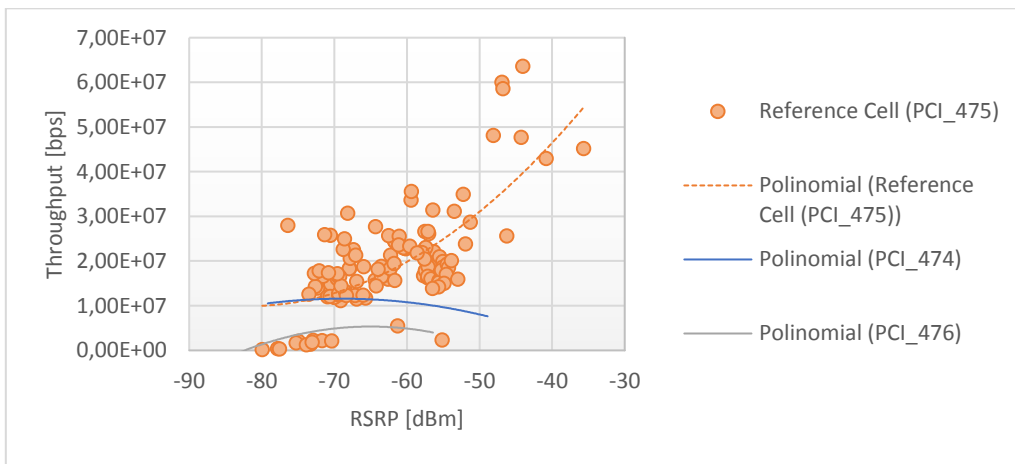
- **LTE (806 MHz Channel):**



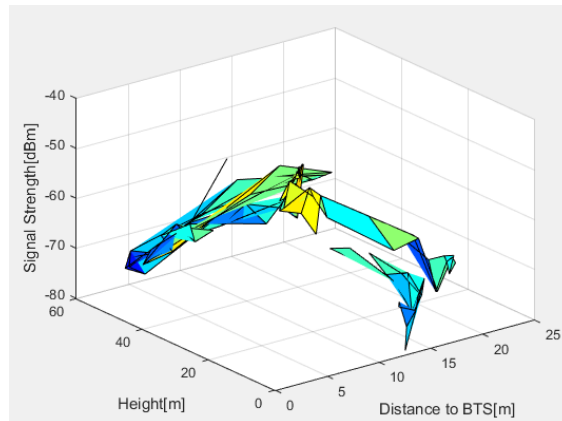
Graphic B - 29. Throughput vs Time considering all the cells from the reference BS



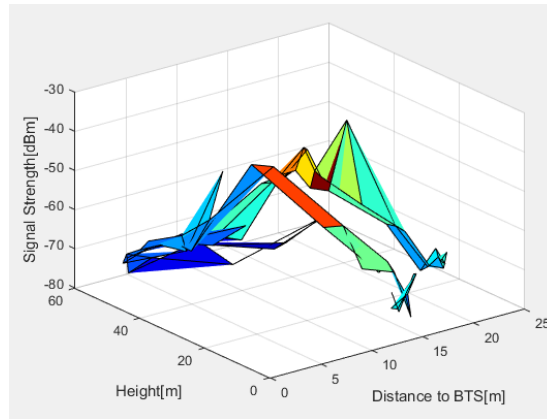
Graphic B - 30. Reference sector throughput below the HQ threshold



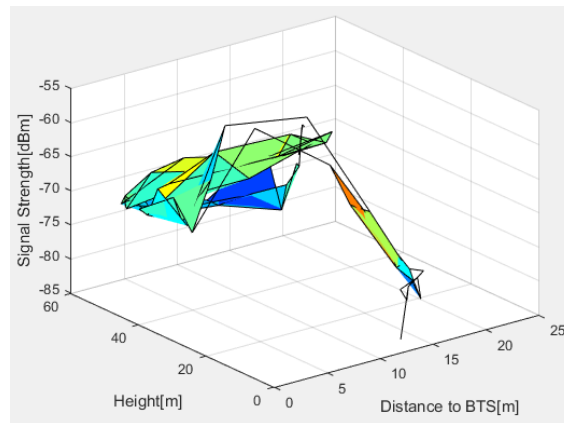
Graphic B - 31. Throughput vs RSRP for reference eNodeB/BS



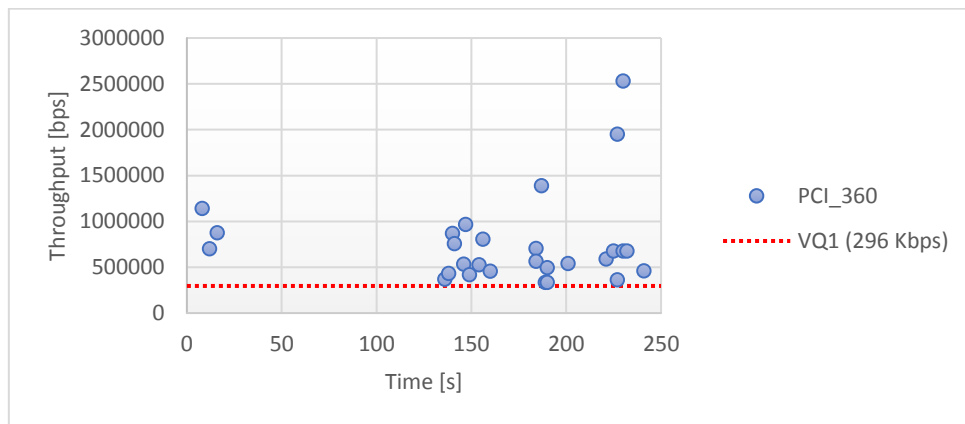
Graphic B - 32. RSRP vs Height vs Distance to BTS for sector 474 (adjacent)



Graphic B - 33. RSRP vs Height vs Distance to BTS for sector 475 (reference)

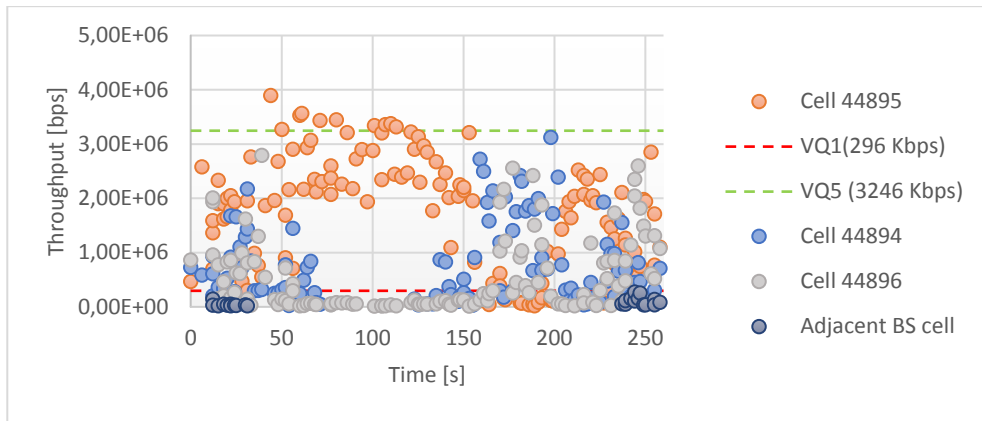


Graphic B - 34. RSRP vs Height vs Distance to BTS for sector 476 (adjacent)

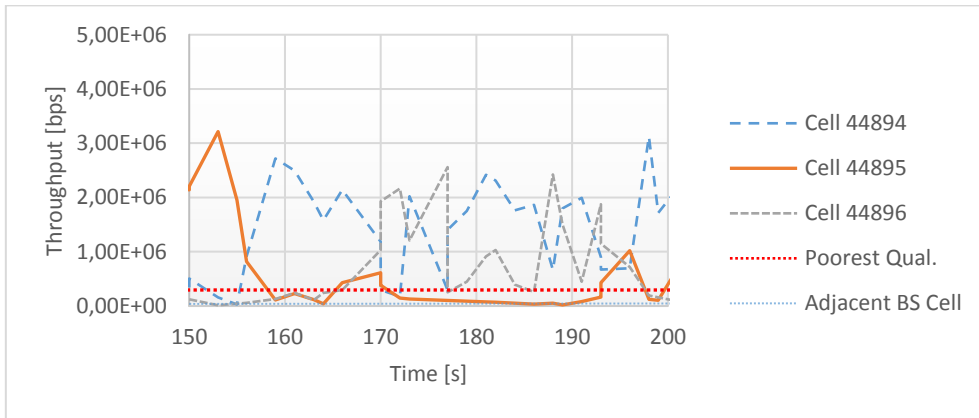


Graphic B - 35. Throughput vs Time considering sector from adjacent BS

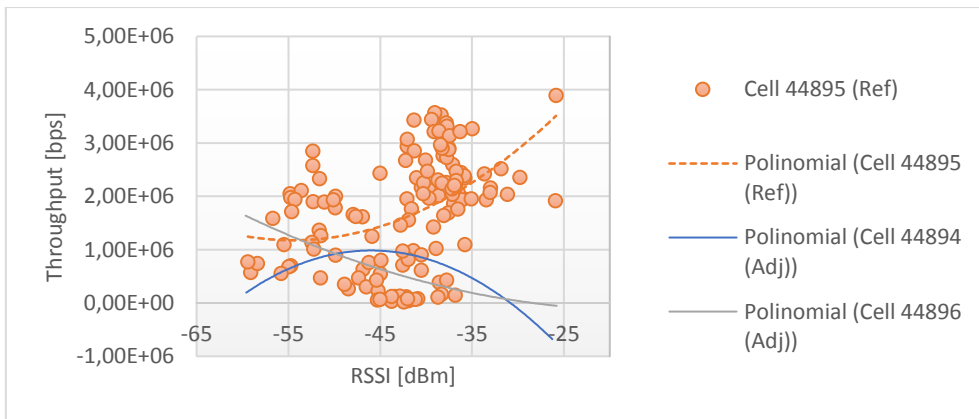
• **UMTS (2117.8 MHz Channel):**



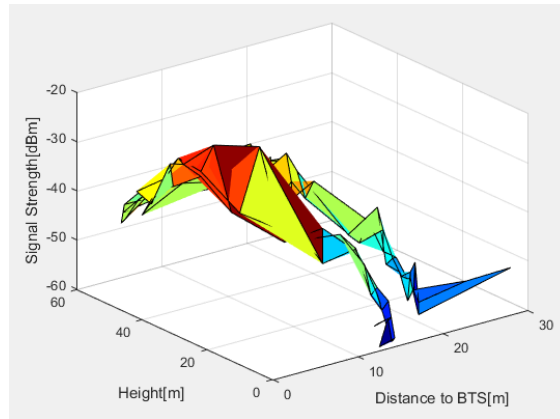
*Graphic B - 36. Throughput vs Time relation – sectors from ref. and adj. BS*



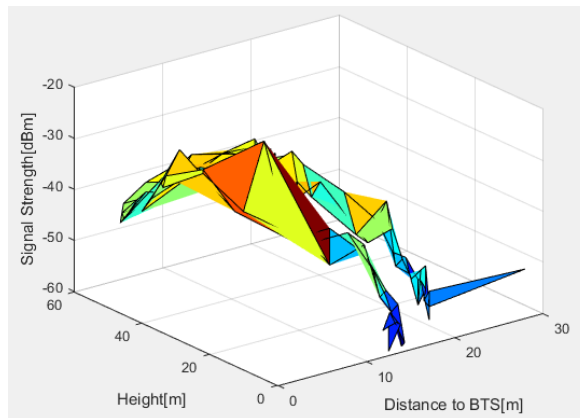
*Graphic B - 37. Reference sector below minimum VQ threshold*



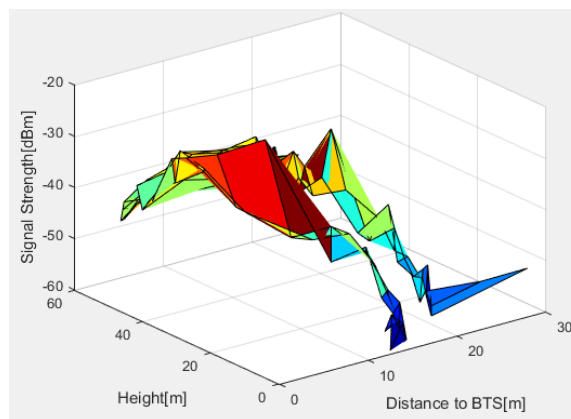
*Graphic B - 38. Throughput vs RSSI for every sector in reference BS*



*Graphic B - 39. RSRP vs Height vs Distance to BTS for sector 44894 (adjacent)*



*Graphic B - 40. RSRP vs Height vs Distance to BTS for sector 44896 (adjacent)*



*Graphic B - 41. RSRP vs Height vs Distance to BTS for sector 44895 (reference)*

# **ANNEX C**

# **ADDITIONAL**

# **STATISTIC**

This section demonstrates an accurate performance testing for cellular networks using normal probability density function and cumulative probability density function based on the scenarios A, B and C from chapter 4

## Overview

Before commenting on the graphics below, it is important to reveal the reasons why PDF and CDF are so used in performance testing related to wireless network infrastructures.

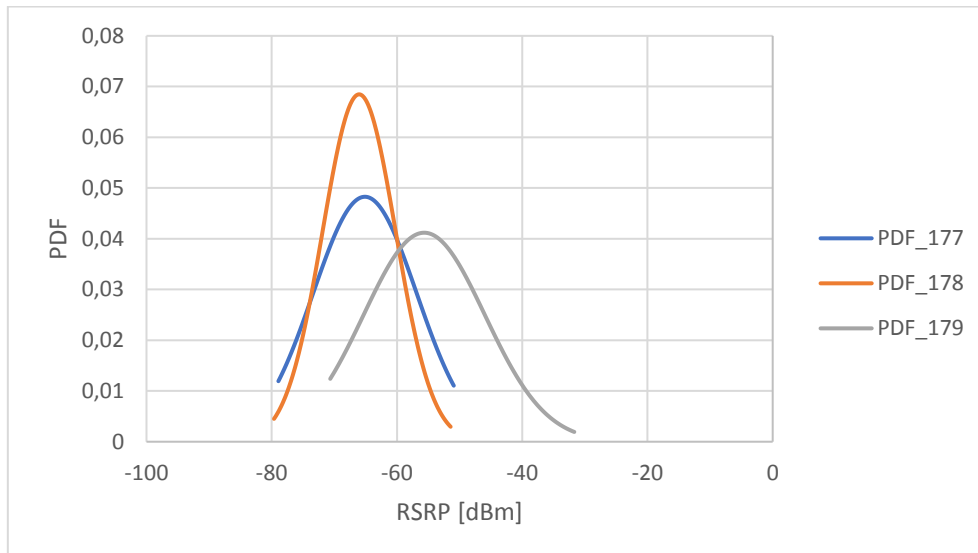
The normal probability density function (PDF) describes approximately any variable that tends to cluster around the mean and it is usually represented by a bell curve. Basically, it is capable of providing the relative probabilities to obtain different values by answering this question: “What is the chance to verify a certain value?”.

.Its main role is to answer a different question: “What is the chance to verify a result less than or greater than a particular value?”.

The graphics represented in the following sections demonstrate three curves with different behaviors, which relates to the fact that each available base station only has three antennas from the same network service provider, where each antenna covers a different sector. Briefly, each curve represents a distinct sector/cell.

### C.1. Scenario A

#### LTE



*Graphic C - 1. PDF of RSRP; LTE: 796 MHz; Sc: A*

Based on graphic C-1, the average for both adjacent sectors 177 and 178 stands close to -70 dBm in both cases, while in the reference sector (PCI\_179) stands close to -55 dBm and it has a low probability to reach signal strength values between -40 dBm and -30 dBm. This probability is calculated based on the area in between these two limits which, in this case, is really small and that's why it corresponds to a low probability.

The probability to reach between -60 dBm and -40 dBm is greater in the reference sector since the area considering this interval is bigger when comparing to the remaining sectors using the same interval.

To obtain the average of PDF could be used the equation (C.1):

$$\mu = \frac{\sum x}{K} \quad (C.1)$$

where:

$\mu$  –average;

$\sum x$  – Sum all the acquired samples;

$K$  – Total number of samples;

and the variance could be obtained by equation (C.2):

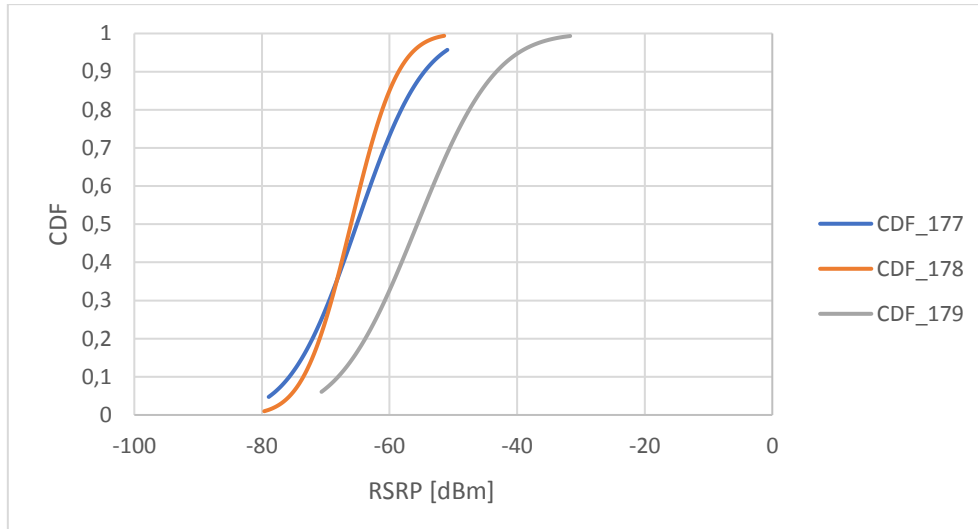
$$\sigma^2 = \frac{\sum(x - \mu)}{K} \quad (C.2)$$

Sector	177	178	179
Minimum [dBm]	-79,25	-79,95	-71,05
Maximum [dBm]	-50,93	-51,43	-31,68
Average [dBm]	-65,12	-66,04	-55,65
Variance [dBm]	8,26	5,83	9,68

Table C - 1. Main parameters to calculate CDF and PDF of RSRP; LTE; Sc: A

MS Excel has its own function to calculate CDF and PDF, which are essential to obtain the graphics present in this section and in the remaining two. The function is: NORM.DIST(x, mean, standard\_dev, cumulative). Where **x** is the sample value and related to RSRP or Throughput, in this case. **Mean** is the arithmetic mean of the distribution represented on table C-1 for this scenario. **standard\_dev** is the standard deviation of the distribution and it is described in the previous table as “Variance”. **cumulative** can assume one of the following options: if **TRUE**, return the cumulative distribution function (CDF); if **FALSE**, returns normal probability distribution function (PDF).





Graphic C - 2. CDF of RSRP; LTE: 796 MHz; Sc: A

In this case, the sector 179 still assumes a distinct behavior when comparing to the adjacent sectors from the same BS. The chance to see a result less than -70 dBm is close to 30% for both adjacent sectors, while in the reference sector is almost null.

The probability to see a result greater than -60 dBm is higher in the reference sector (CDF\_179) when comparing to the other sectors, assuming about 70% chances comparing to 30% and 15% from sector 177 and 178, respectively. Besides that, the sector 179 is the only one where it is possible to verify values greater than -40 dBm assuming a 5% probability.

The following table (table C-2) is able to synthesize all the previous information by describing the chance to be greater than and less than the defined limits for each analyzed sector.

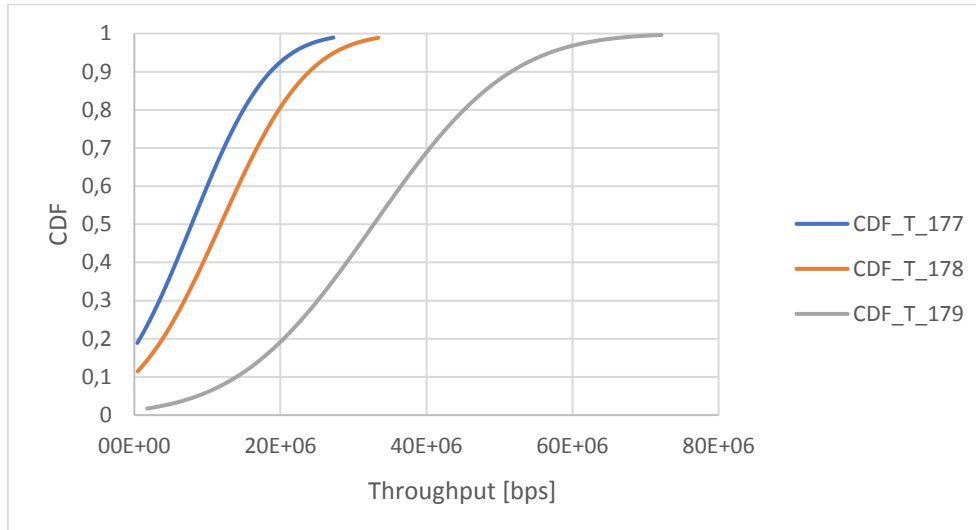
Sectors	RSRP [dBm]					
	177		178		179	
Limits	Greater	Less	Greater	Less	Greater	Less
-70 [dBm]	70%	30%	70%	30%	100%	0%
-60 [dBm]	30%	70%	15%	85%	70%	30%
-40 [dBm]	0%	100%	0%	100%	5%	95%

Table C - 2. Prob. to verify results greater/less than the defined limits; CDF; LTE; Sc: A

Furthermore, “CDF/PDF vs Throughput” graphic analysis is also fundamental, in order to consider the interference factor that might lead to the conclusion that signal strength parameter is not enough to predict a good or bad quality signal.

Sectors	177	178	179
Min. Th. [bps]	1,19E+05	1,20E+05	1,05E+06
Max. Th. [bps]	2,72E+07	3,34E+07	7,22E+07
Mean/Av. Th. [bps]	7,85E+06	1,18E+07	3,28E+07
Standard deviation [bps]	8,43E+06	9,46E+06	1,47E+07

Table C - 3. Main parameters to calculate CDF/PDF of Throughput; LTE; Sc: A



Graphic C - 3. CDF of Throughput; LTE: 796 MHz; Sc: A

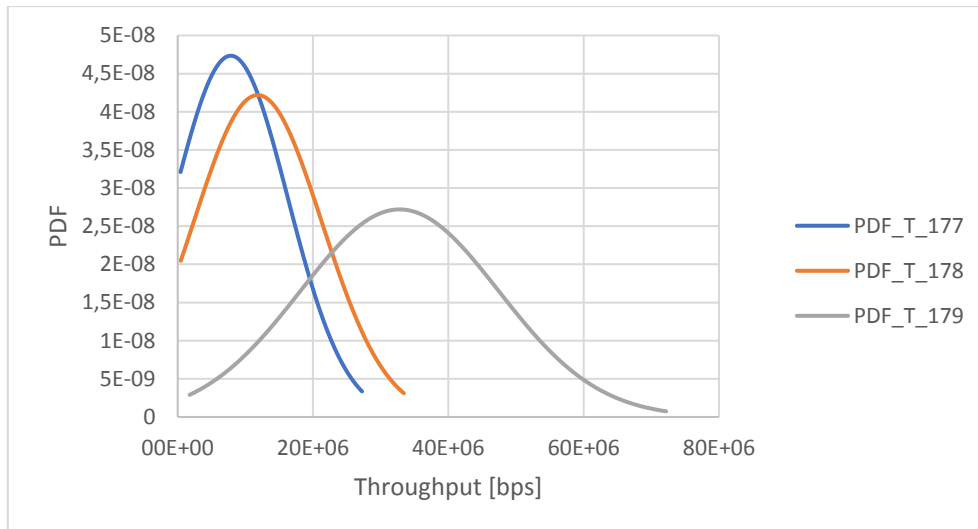
Based on graphic C-3, the reference sector (CDF\_T\_179) still assumes a distinct attitude. However, the adjacent sectors behavior is a bit different by assuming two parallel lines, while in the previous case from graphic C-2, they intercept in a certain point. Besides that, sector 178 has a higher chance to assume greater throughput results when comparing to sector 177 during the whole process. Comparing this to “CDF vs RSRP” graphic, even when sector 178 assume strength results below the ones from sector 177, it assumes a higher quality signal.

The chance to verify a value below 20 Mbps is lower in sector 179, assuming close to 20%, against the 92% and 80% from the sectors 177 and 178, respectively. At this given point, the best results are acquired by the sector 179, followed by 178 and, at last, 177.

Nonetheless, the probability to obtain a value greater than 40 Mbps is about 30% for the reference sector, while the remaining sectors have no chance to reach such high results.

Throughput						
Sectors	177		178		179	
Limits	Greater	Less	Greater	Less	Greater	Less
20 [Mbps]	8%	92%	20%	80%	80%	20%
40 [Mbps]	0%	100%	0%	100%	30%	70%
60 [Mbps]	0%	100%	0%	100%	3%	97%

Table C - 4. Prob. to obtain results greater/less than certain limits; CDF; LTE; Sc: A

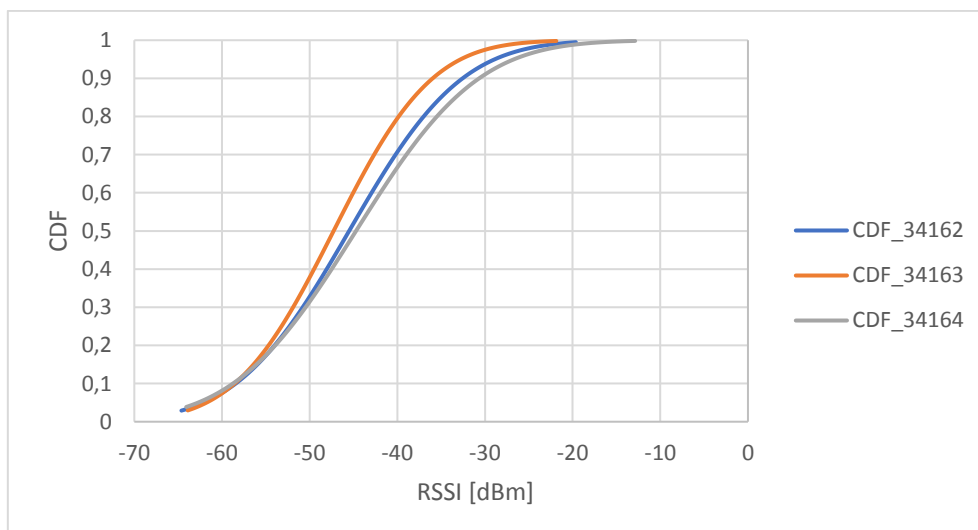


Graphic C - 4. PDF of Throughput; LTE: 796 MHz; Sc: A

Since PDF relates to CDF and vice versa, the reading from the graphic above tends to be approximate to the one from the previous. However, sector 178 assumes the highest probability to obtain results between 0 and 20 Mbps due to the fact that the area based on this interval is larger when comparing to the other sectors from the same BS. Considering the throughput interval from 20 Mbps to 40 Mbps, the sectors 177 and 179 assume the lowest and the highest probability, respectively.

The reference sector assumes the highest mean corresponding to a value of 32.8 Mbps, while the sectors adjacent sectors, 177 and 178, present 7.9 Mbps and 11.2 Mbps, respectively.

## UMTS



Graphic C - 5. CDF of RSSI; UMTS: 2152.4 MHz; Sc: A

Sectors	34162	34163	34164
Minimum [dBm]	-65,04	-64,33	-64,55
Maximum [dBm]	-19,63	-21,86	-12,87
Mean/Average [dBm]	-45,49	-47,27	-44,71
Deviation [dBm]	10,10	8,82	10,96

Table C - 5. Main parameters to calculate CDF/PDF of RSSI; UMTS; Sc: A

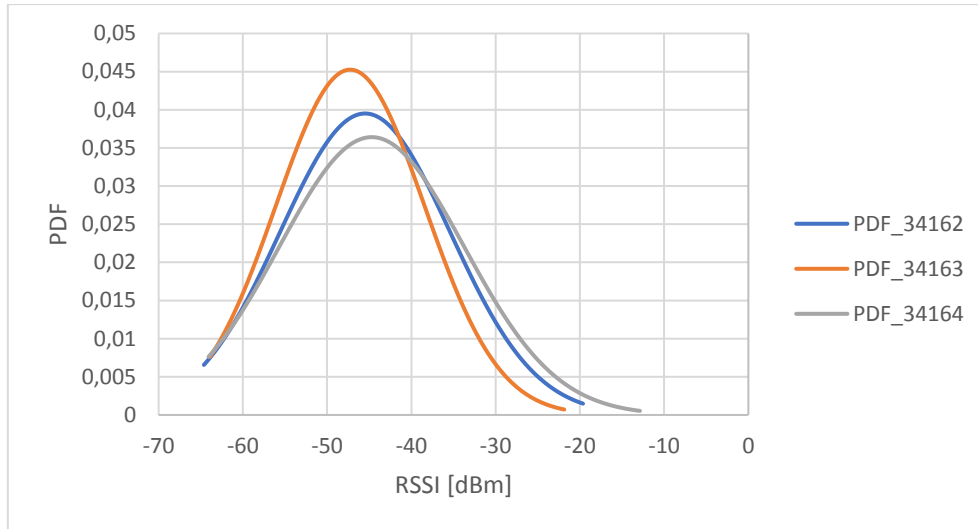
Based on graphic C-5, it is not so noticeable which sector is able to reach the highest signal strength values when comparing to the LTE section, because the lines are almost coinciding. However, from -55 dBm, sector 34163 demonstrates a different relation to the other sectors by achieving a lower probability to assume higher signal strength from that point on.

Close to -45 dBm, the lines corresponding to the sector 34162 and 34164 start to separate from each other and, from that point on, the 34164 assumes the higher probability to achieve higher signal strength results, which leads it to the reference sector role.

Every sector has 20% chance to assume RSSI results less than -55 dBm. Nonetheless, this scenario does not repeat during the whole process. Per example, when considering the probability to assume values greater than -40 dBm, the sector 34163 assumes about 20% chance, while 34162 and 34164 achieve 30% and 33%, respectively.

RSSI						
Sectors	34162		34163		34164	
Limits	Greater	Less	Greater	Less	Greater	Less
-60 [dBm]	90%	10%	90%	10%	90%	10%
-50 [dBm]	70%	30%	60%	40%	70%	30%
-40 [dBm]	30%	70%	20%	80%	33%	67%
-30 [dBm]	7%	93%	3%	97%	10%	90%

Table C - 6. Prob. to obtain values greater/less than certain limits; CDF; UMTS; Sc:A



Graphic C - 6. PDF of RSSI; UMTS: 2152.4 MHz; Sc: A

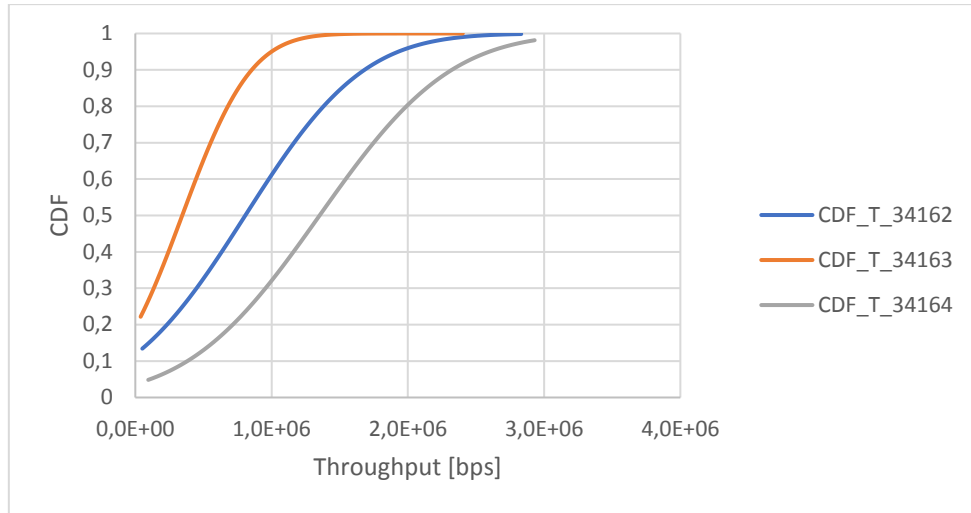
Considering the graphic C-6, all the three sectors have a close mean value occurring between -50 and -40 dBm.

Sector 34163 has a higher chance to obtain values from -60 dBm to -40 dBm, where the three lines coincide. From that event on, sector 34164 has a higher chance between the three sectors and it is able to reach close to -10 dBm but considering a low probability.

Once again, it is crucial to evaluate the throughput parameter but considering UMTS technology, where interference also affect the signal and RSSI is not a reliable parameter to understand whether it is a good or poor-quality signal.

Sector	34162	34163	34164
Minimum [bps]	2,59E+04	1,51E+04	6,90E+04
Maximum [bps]	2,83E+06	2,40E+06	2,93E+06
Average [bps]	8,07E+05	3,44E+05	1,35E+06
Standard deviation [bps]	6,83E+05	3,98E+05	7,57E+05

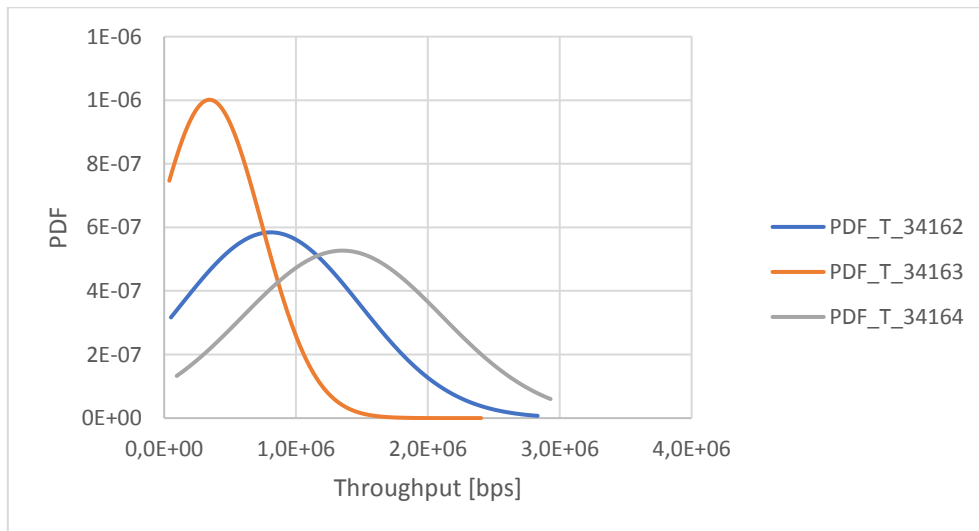
Table C - 7. Main parameters to calculate CDF/ PDF of Throughput; UMTS; Sc: A



*Graphic C - 7. CDF of Throughput; UMTS: 2152.4 MHz; Sc: A*

Comparing graphic C-7 to the previous ones, the lines are not coinciding anymore during the whole process. The sector 34163 assumes a 95% chance to achieve throughput results below 1 Mbps while sectors 34162 and 34164 consider 60% and 30%, respectively.

For throughput greater than 2 Mbps, the sector 34163 has almost no chance to such results due to the fact that its probability to reach values between 1.5 to 2.5 Mbps is below 1%. However, sector 34162 considers a higher probability but still a low one, close to 5%. At last, sector 34164 assumes 20% chance of assuming values greater than 2 Mbps and 5% to be greater than 2.5 Mbps, while the adjacent sectors assume close to 0%.



*Graphic C - 8. PDF of Throughput; UMTS: 2152.4 MHz; Sc: A*

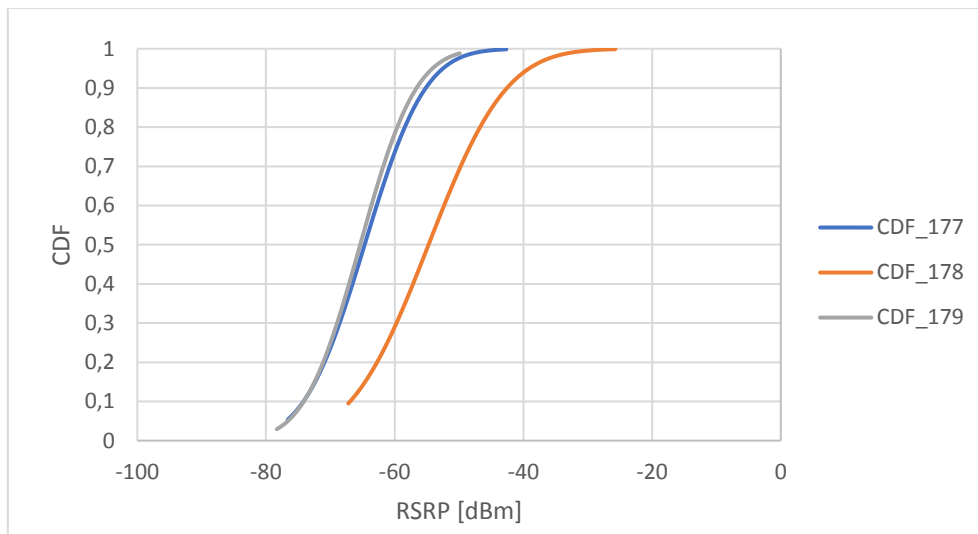
Based on graphic C-8, the adjacent sectors 34162 and 34163 assume the highest and the lowest probability to assume 1 Mbps, respectively. From 2 Mbps on, the reference sector assumes the highest chance, prevailing for greater throughput values as well.

Throughput						
Sectors	34162		34163		34164	
Limits	Greater	Less	Greater	Less	Greater	Less
10 [Mbps]	40%	60%	5%	95%	75%	25%
20 [Mbps]	5%	95%	0%	100%	20%	80%
25 [Mbps]	1%	99%	0%	100%	5%	95%

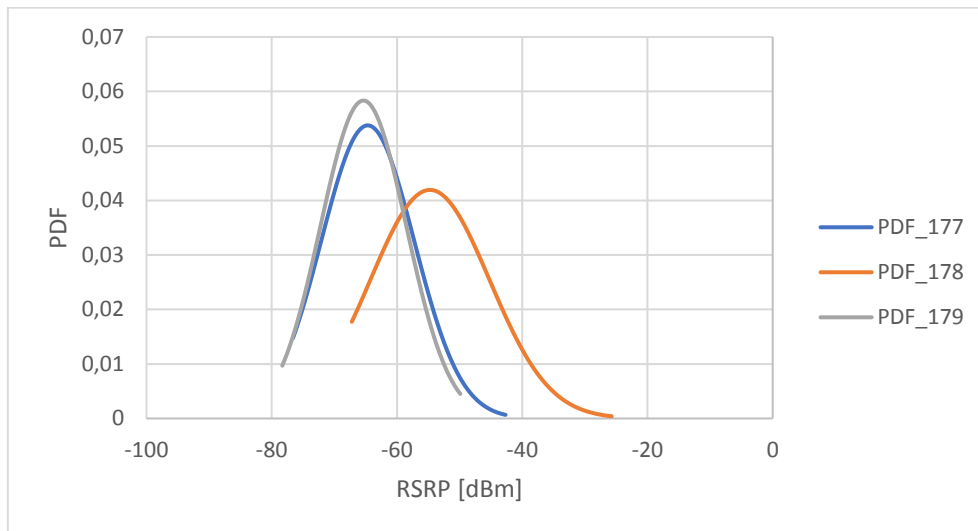
Table C - 8. Prob. to obtain results greater/less than certain limits; CDF; UMTS; Sc: A

## C.2. Scenario B

### LTE



Graphic C - 9. CDF of RSRP, LTE: 796 MHz; Sc: B



Graphic C - 10. PDF of RSRP, LTE: 796 MHz; Sc: B

Sector	177	178	179
Minimum [dBm]	-76,99	-67,68	-78,68
Maximum [dBm]	-46,47	-25,71	-49,88
Average [dBm]	-64,67	-54,73	-65,36
Standard deviation [dBm]	7,42	9,51	6,84

Table C - 9. Main parameters to calculate CDF/PDF for RSRP; LTE; Sc: B

It is predictable that in this scenario one of the adjacent sectors from the scenario A assume now the reference sector role since the measurements took place in a different location where the drone was directed to another antenna from the same BS. Through this, the reference sector role belongs to sector 178 considering the results provided by the two previous graphic, which analysis is in the following paragraph.

Based on the graphic C-9, the adjacent sectors, 177 and 179, assume similar performances since the corresponding lines are coincident during almost the entire trial. However, from -70 dBm to -40 dBm on, the sector 177 reaches a higher probability with a slight difference to the remaining adjacent sector.

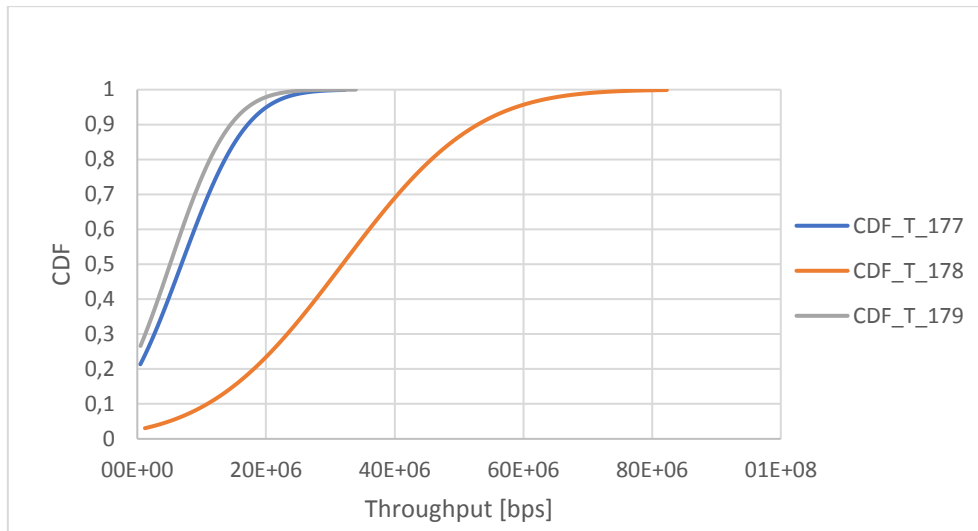
Furthermore, the reference sector is able to reach results greater than -50 dBm, assuming a 20% chance of making this possible, while the other sectors are close to 0%.

RSRP						
Sector	177		178		179	
Limits	Greater	Less	Greater	Less	Greater	Less
-70 [dBm]	80%	20%	100%	0%	80%	20%
-60 [dBm]	25%	75%	70%	30%	20%	80%
-40 [dBm]	0%	100%	5%	95%	0%	100%
-30 [dBm]	0%	100%	1%	99%	0%	100%

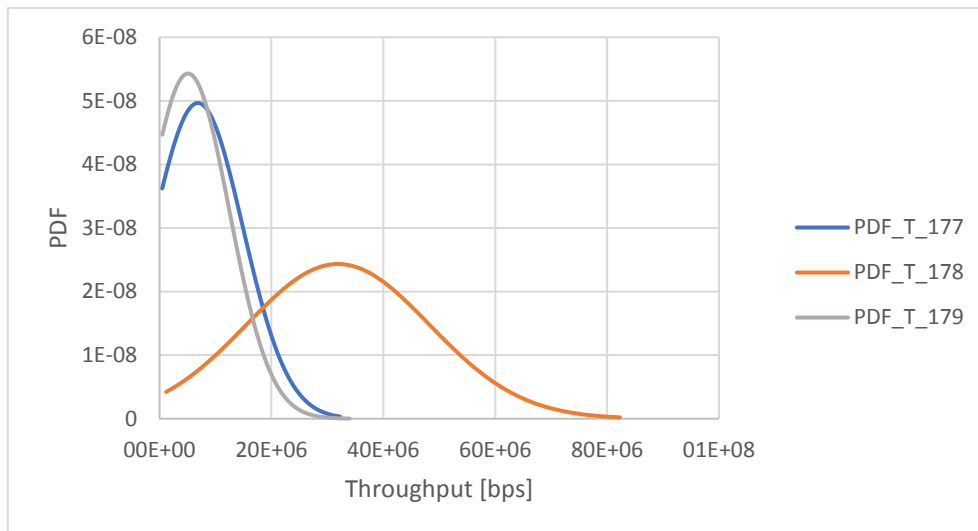
Table C - 10. Prob. to obtain values greater/less than certain limits; CDF; LTE; Sc: B

Based on the graphic C-10, sector 179 assumes the highest probability within the three possibilities to reach results from -80 dBm to -60 dBm. The sector who has more chances to acquire signal strength results between -60 dBm and -30 dBm interval is the reference sector, which is represented by the orange curve. Nonetheless, the three sectors assume almost the same probability of achieving -60 dBm since it is where all the lines intersect with each other.





Graphic C - 11. CDF of Throughput; LTE: 796 MHz; Sc: B



Graphic C - 12. PDF of Throughput; LTE: 796 MHz; Sc: B

Sector	177	178	179
Minimum [bps]	121993,60	370329,75	124251,89
Maximum [bps]	32288637,51	74097650,82	30200816,86
Average [bps]	6859688,56	31888314,69	5089867,84
Standard deviation [bps]	8035120,35	16394454,89	7348273,60

Table C - 11. Main parameters to calculate CDF/PDF of throughput; LTE; Sc: B

Based on graphic C-11, the reference sector prevails with the highest probability to reach higher throughput values throughout the whole process, assuming a 78% chance to achieve throughput results greater than 20 Mbps while the adjacent sectors, 177 and 179, have 3% to 5% chances to get the same results.

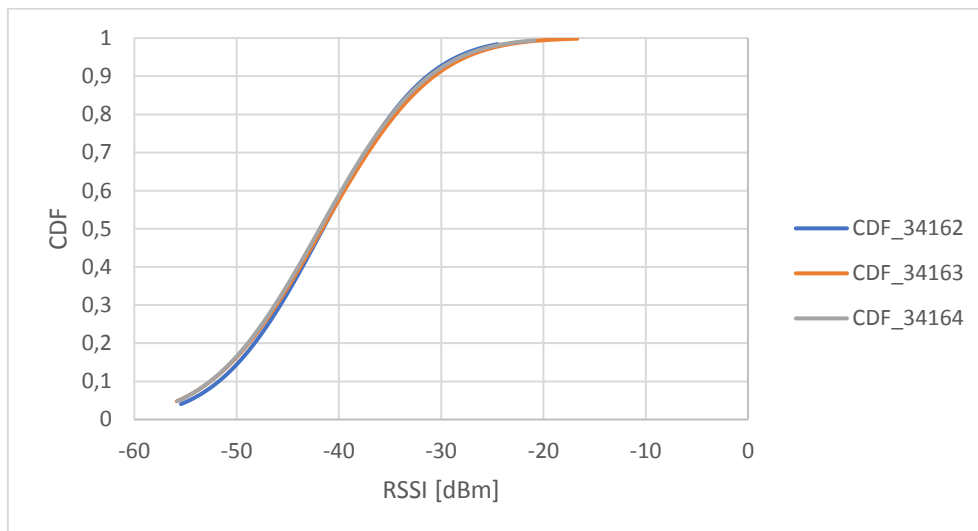
Considering the graphic C-12, the adjacent sector 179 has a higher chance to obtain throughput results between 0 and 20 Mbps, while the reference sector assumes the lowest

probability for the same interval. The adjacent sectors assume the same probability as the reference sector when the its lines intersect with reference's sector line. In this case, the gray line, assumes the same probability as the reference sector for about 16 Mbps, when the gray line intersects with the orange one. The adjacent sector remaining (177) assumes the same chance as the reference sector at about 18 Mbps, when the blue line intersects the orange one.

Throughput						
Sector	177		178		179	
Limits	Greater	Less	Greater	Less	Greater	Less
10 [Mbps]	40%	60%	90%	10%	30%	70%
20 [Mbps]	5%	95%	80%	20%	3%	97%
40 [Mbps]	0%	100%	30%	70%	0%	100%
60 [Mbps]	0%	100%	5%	95%	0%	100%

Table C - 12. Prob. to obtain results greater/less than certain limits; CDF; LTE; Sc: B

## UMTS



Graphic C - 13. CDF of RSSI; UMTS: 2152.4 MHz; Sc: B

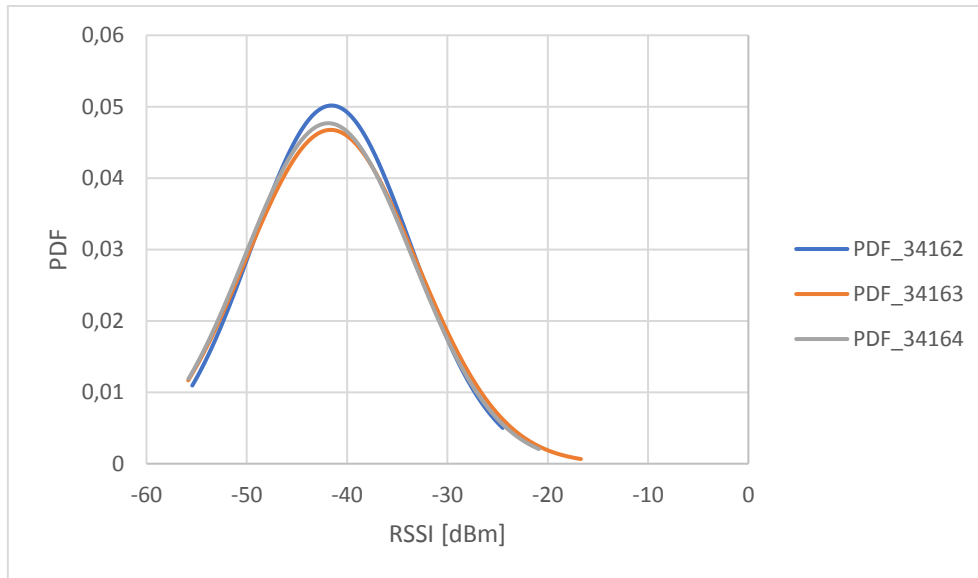
The graphic above demonstrates that the probabilities for every sector considering the same BS are close, based on the coincident lines for every RSSI value. In this case, there is no way to confirm which line assumes the reference sector role so, it is crucial to analyze the graphs related to throughput parameter to get a reliable conclusion.

Sector	34162	34163	34164
Minimum [dBm]	-55,78	-56,24	-56,2
Maximum [dBm]	-27,96	-20,65	-20,88
Average [dBm]	-41,55	-41,63	-41,87
Standard deviation [dBm]	7,95	8,53	8,37

Table C - 13. Main parameters to calculate CDF/ PDF of RSSI; UMTS; Sc: B

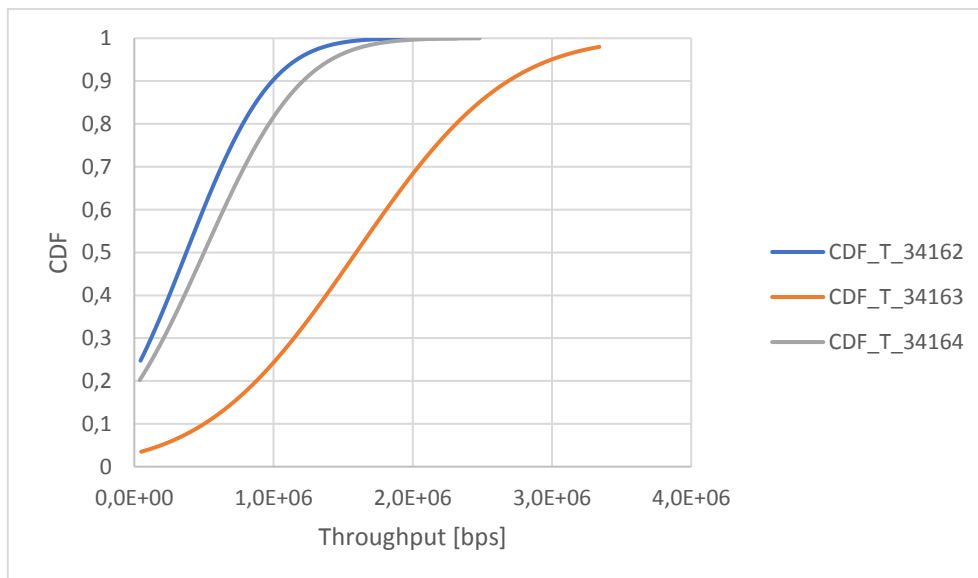
RSSI						
Sector	34162		34163		34164	
Limits	Greater	Less	Greater	Less	Greater	Less
-50 [dBm]	95%	5%	95%	5%	95%	5%
-40 [dBm]	40%	60%	40%	60%	40%	60%
-30 [dBm]	9%	91%	9%	91%	9%	91%
-20 [dBm]	0%	100%	~1%	~99%	0%	100%

Table C - 14. Prob. to obtain values greater/less than certain limits; CDF; UMTS; Sc: B



Graphic C - 14. PDF of RSSI; UMTS: 2152.4 MHz; Sc: B

Based on the fact that CDF and PDF are related, it is expected that graphic C-14 lines assume the same behavior from graphic C-13. However, it is possible to verify that there's a higher chance to obtain results from -60 dBm to -30 dBm in sector 34162 but the difference to the other sectors is not significant.



Graphic C - 15. CDF of Throughput; UMTS: 2152.4 MHz; Sc: B

Sectors	34162	34163	34164
Minimum [bps]	1,92E+04	1,62E+04	1,13E+04
Maximum [bps]	2,32E+06	3,34E+06	2,48E+06
Mean/Average [bps]	3,74E+05	1,59E+06	5,01E+05
Deviation [bps]	4,82E+05	8,52E+05	5,54E+05

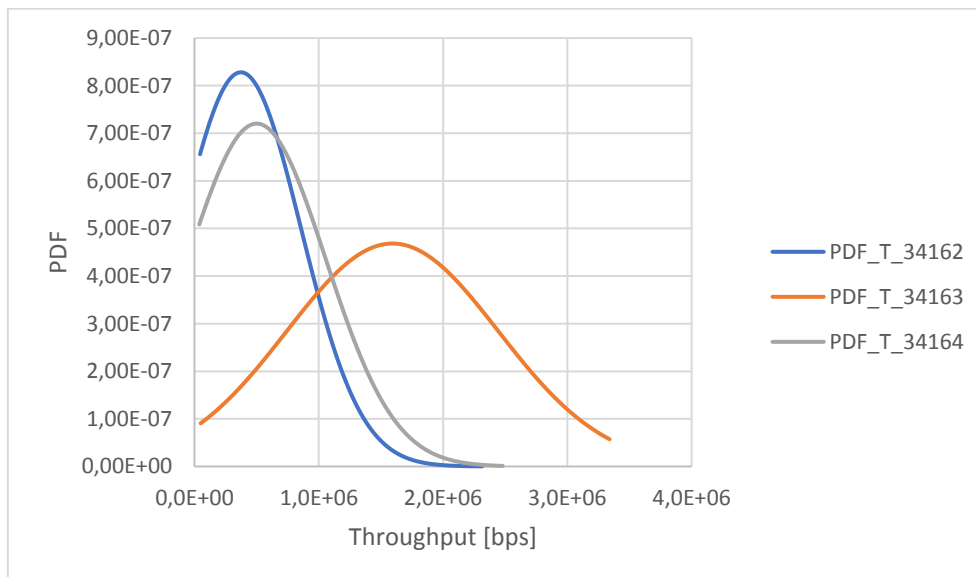
Table C - 15. Main parameters to calculate CDF/PDF of throughput; UMTS; Sc: B

Unlike the previous cases related to RSSI graphs, CDF vs Throughput graphics are able to show which line corresponds to the reference sector. Based on the graphic C-15, the sector 34163 demonstrate a distinct behavior from the remaining sectors during the whole measurement by assuming a higher probability to achieve higher throughput results, which makes it the reference sector.

Throughput						
Sectors	34162		34163		34164	
Limits	Greater	Less	Greater	Less	Greater	Less
1 [Mbps]	10%	90%	75%	25%	20%	80%
2 [Mbps]	1%	99%	30%	70%	1%	99%
3 [Mbps]	0%	100%	5%	95%	0%	100%

Table C - 16. Prob. to obtain results greater/less than certain limits; CDF; UMTS; Sc: B

The probability for reference sector to assume results greater than 1 Mbps is close 75%, while the adjacent sectors, 34162 and 34163, assume 10% and 20%, respectively. For greater than 2 Mbps it assumes about 30%, against 1% from the adjacent sectors.



Graphic C - 16. PDF of Throughput; UMTS: 2152.4 MHz; Sc: B

Based on the graphic C-16, the adjacent sectors assume the same chance about reaching close to 0.75 Mbps, when the blue and gray lines intersect.

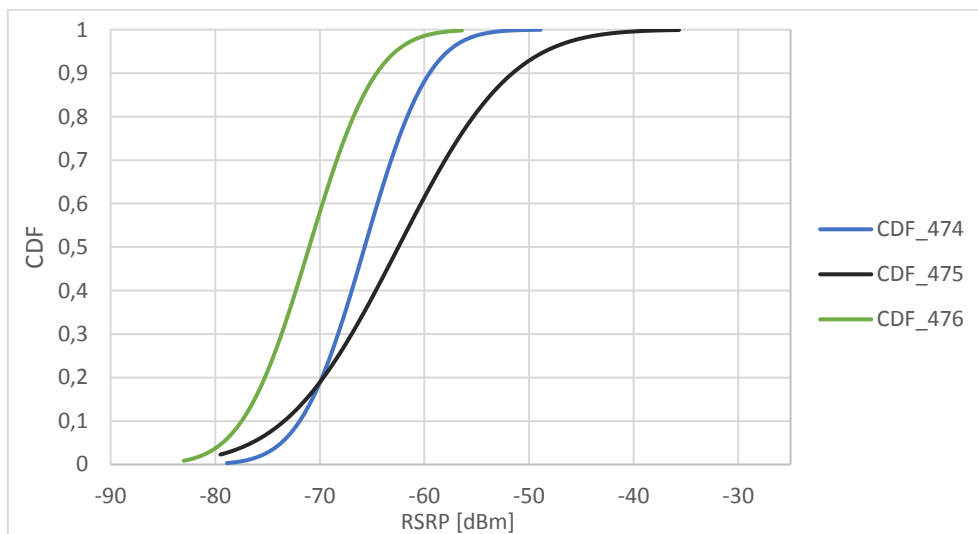
Furthermore, the sector 34162 has the same probability as the reference sector to get 1 Mbps, which is represented by the intersection between the blue line and the orange one. At last, it occurs the same but for the remaining adjacent sector (34164) close to 1.1 Mbps, when the gray line intersects the orange one.

For the interval between 0 and 0.75 Mbps, the sector 34162 has a higher chance to get results within that interval over the others. However, the adjacent sector (34163) overcomes it from 0.75 Mbps until 1.1 Mbps achieving a higher probability. In the end, the reference sector assumes the highest probability of producing a throughput value from 1.1 Mbps to 3.5 Mbps since it assumes a larger area comparing to the areas from the adjacent sectors using the same interval.

### C.3. Scenario C

This scenario considers a different location and base station that belongs to another service provider (Vodafone) and that's one of the reasons why it contemplates other channel frequencies in LTE and UMTS technologies.

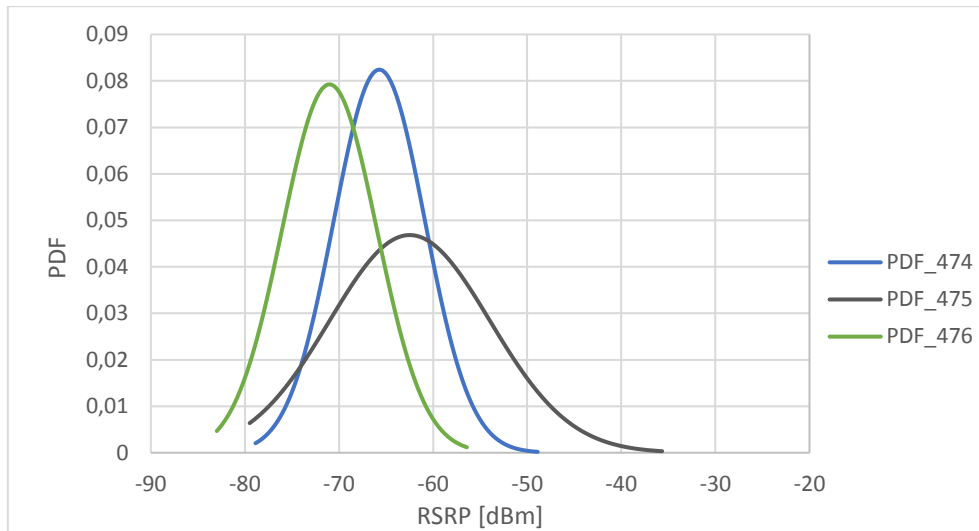
#### LTE



Graphic C - 17. CDF of RSRP; LTE: 806 MHz; Sc: C

Sectors	474	475	476
Minimum [dBm]	-79,18	-79,94	-83,33
Maximum [dBm]	-48,89	-35,66	-56,41
Mean/Average [dBm]	-65,72	-62,49	-71,01
Deviation [dBm]	4,84	8,52	5,03

Table C - 17. Main parameters to calculate CDF/PDF of RSRP; LTE; Sc: C



Graphic C - 18. PDF of RSRP; LTE: 806 MHz; Sc: C

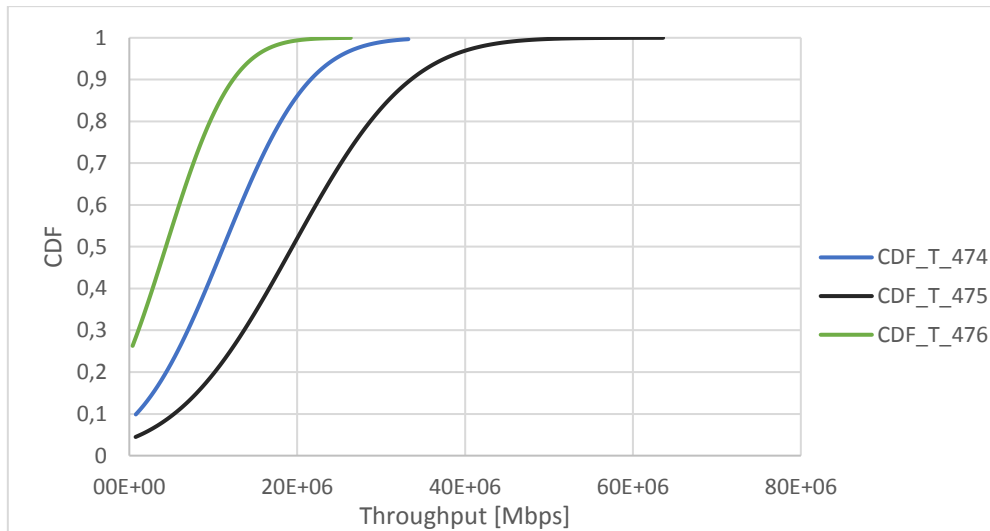
Based on graphic C-17, sector 475 assumes the higher probability of reaching higher RSRP values when comparing to the other two sectors, which makes it the reference sector. This sector corresponds to the coverage area provided by one of the antennas from the BS where measurements take place.

The reference sector has the same chance as the adjacent sector 474 to verify a value greater than -70 dBm and less than -70 dBm when the blue line intersects the black one, where the probabilities correspond to 80% and 20%, respectively. From -70 dBm on, the reference sector assumes the highest probability of reaching greater values, followed by the adjacent sector 474 and, at last, the remaining sector (476).

In graphic C-18, the reference sector has the highest mean between the three leading to a value close to -60 dBm. Nonetheless, the adjacent sector 474 assumes a higher probability to achieve results between -80 dBm and -65 dBm, while the reference sector is able to accomplish higher probabilities for higher RSRP values between -65 dBm to -40 dBm.

RSRP						
Sectors	474		475		476	
Limits	Greater	Less	Greater	Less	Greater	Less
-70 [dBm]	80%	20%	80%	20%	40%	60%
-60 [dBm]	11%	89%	40%	60%	2%	98%
-50 [dBm]	~1%	99%	8%	92%	0%	100%
-40 [dBm]	0%	100%	~1%	99%	0%	100%

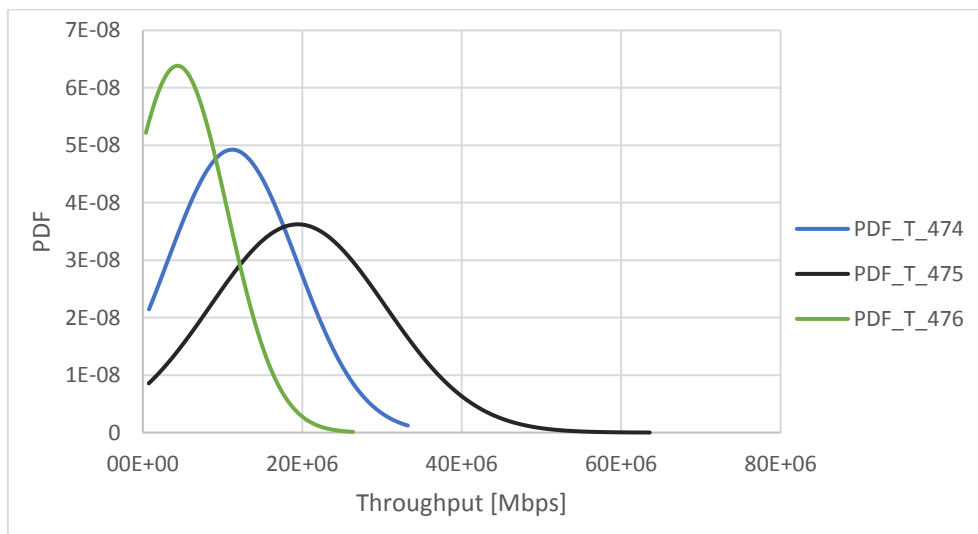
Table C - 18. Prob. to obtain values greater/less than certain limits; CDF; LTE; Sc: C



Graphic C - 19. CDF of Throughput; LTE: 806 MHz; Sc: C

Sectors	474	475	476
Minimum [bps]	4,74E+05	1,69E+05	1,26E+05
Maximum [bps]	3,32E+07	6,36E+07	2,64E+07
Mean/Average [bps]	1,12E+07	1,94E+07	4,36E+06
Deviation [bps]	8,10E+06	1,10E+07	6,25E+06

Table C - 19. Main parameters to calculate CDF/ PDF of throughput; LTE; Sc: C



Graphic C - 20. PDF of Throughput; LTE: 806 MHz; Sc: C

Based on graphic C-19, the black line corresponding to the reference sector has the highest probability to assume the greatest throughput results since the beginning when comparing to the other lines. From -80 dBm to -70 dBm at graphic C-17, the adjacent sector had superior probability than the reference sector. However, the previous two graphs prove that the reference sector, even with lower RSRP values, is capable of

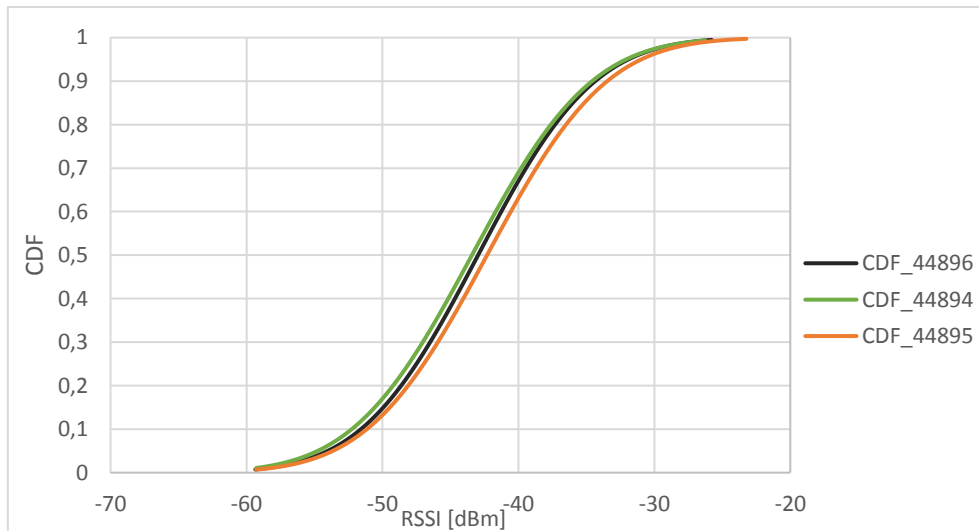
reaching higher throughput values than the adjacent sector 474, due to the interference factor.

In graphic C-20, the area is larger in sector 474 between 0 and 20 Mbps, which corresponds to a higher chance to assume values within that interval. However, from 20 to 40 Mbps, the reference sector assumes the highest probability.

Throughput						
Sectors	474		475		476	
Limits	Greater	Less	Greater	Less	Greater	Less
20 [Mbps]	15%	85%	50%	50%	~1%	~99%
30 [Mbps]	~1%	~99%	20%	80%	0%	100%
40 [Mbps]	0%	100%	3%	97%	0%	100%

Table C - 20. Prob. to obtain values greater/less than certain limits; CDF; LTE; Sc: C

## UMTS

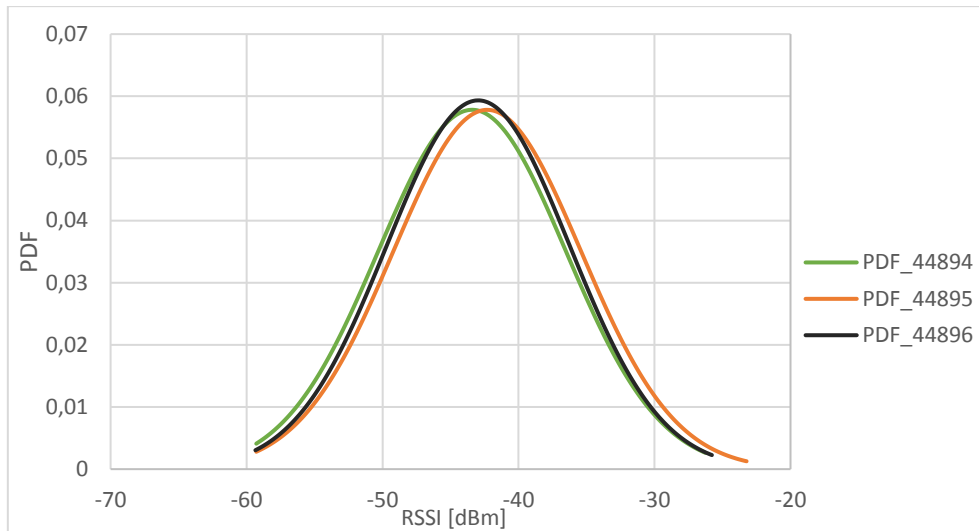


Graphic C - 21. CDF of RSSI; UMTS: 2117.8 MHz; Sc: C

RSSI			
Sectors	44894	44895	44896
Minimum [dBm]	-59,59	-59,41	-59,66
Maximum [dBm]	-26,26	-25,85	-25,78
Mean/Average [dBm]	-43,42	-42,31	-42,97
Deviation [dBm]	6,90	6,90	6,72

Table C - 21. Main parameters to calculate CDF/PDF of RSSI; UMTS; Sc: C



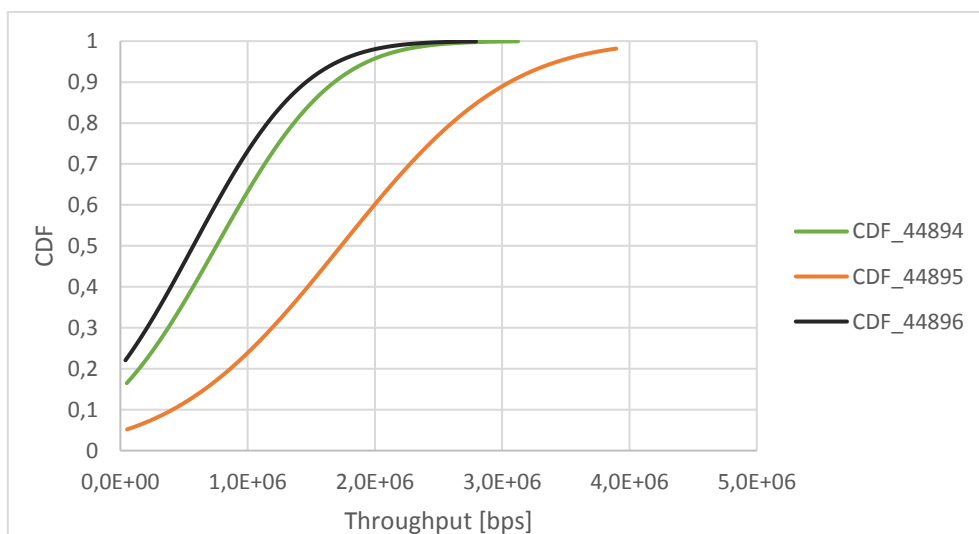


Graphic C - 22. PDF of RSSI; UMTS: 2117.8 MHz; Sc: C

Once again, it is hard to distinguish which line assumes the reference sector role due to the fact that all of them are coincident, which corresponds to equal probabilities to assume a certain value in the same RSSI interval. The following table synthesizes the information from the chart corresponding to “PDF/CDF vs RSSI”:

RSSI						
Sectors	44894		44895		44896	
Limits	Greater	Less	Greater	Less	Greater	Less
-50 [dBm]	17%	83%	12%	88%	15%	85%
-40 [dBm]	30%	70%	39%	61%	35%	65%
-30 [dBm]	3%	97%	5%	95%	3%	97%
-20 [dBm]	0%	100%	0%	100%	0%	100%

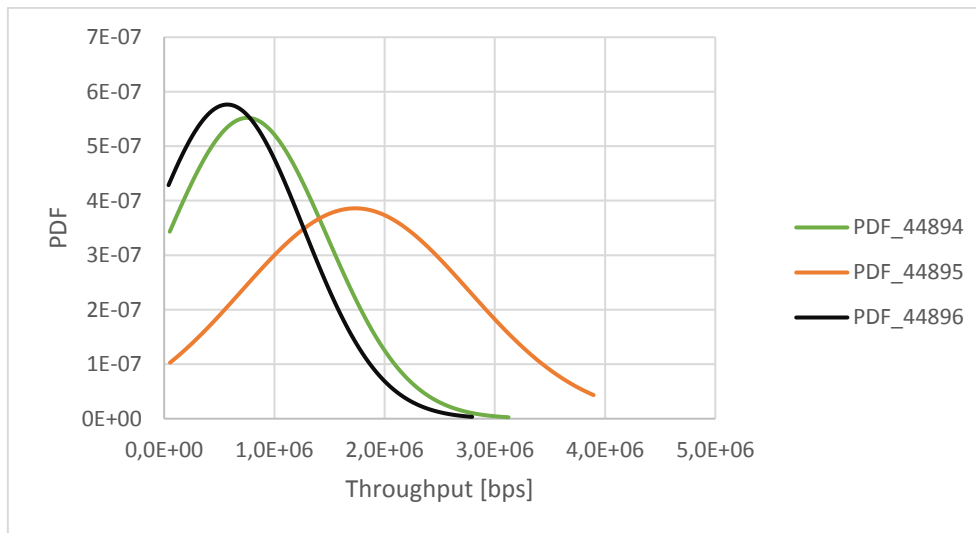
Table C - 22. Prob. to obtain values greater/less than certain limits; CDF; UMTS; Sc: C



Graphic C - 23. CDF of Throughput; UMTS: 2117.8 MHz; Sc: C

Throughput			
Sectors	44894	44895	44896
Minimum [bps]	2,24E+04	2,08E+04	1,45E+04
Maximum [bps]	3,12E+06	3,90E+06	2,79E+06
Mean/Average [bps]	7,55E+05	1,73E+06	5,73E+05
Deviation [bps]	7,23E+05	1,03E+06	6,92E+05

Table C - 23. Prob. to obtain values greater/less than certain limits; CDF; UMTS; Sc: C



Graphic C - 24. PDF of Throughput; UMTS: 2117.8 MHz; Sc: C

In order to verify which one of the lines assume the reference sector role, it is necessary to analyze the throughput parameter by using the graphic C-23 and C-24.

Throughput						
Sectors	44894		44895		44896	
Limits	Greater	Less	Greater	Less	Greater	Less
1 [Mbps]	38%	62%	77%	23%	28%	72%
2 [Mbps]	5%	95%	40%	60%	2%	98%
3 [Mbps]	~0 %	~100%	11%	89%	~0 %	~100%

Table C - 24. Prob. to obtain results greater/less than certain limits; CDF; UMTS; Sc: C

Based on graphic C-23, the orange line is distinct from the others by assuming a higher probability to achieve any throughput value during the whole measurement, which is enough reason to accomplish the reference sector role. It has close to 77% chances to assume a value greater than 1 Mbps, against the 38% and 28% from sector 44894 and 44896, respectively.

In graphic C-24, the adjacent has the same probability to verify a value close to 0.75 Mbps, when the green and the black lines intersect. Both adjacent sectors assume higher probabilities to verify a value between 0 and 1 Mbps when comparing to the reference

one. However, from 1 to 2 Mbps and from 2 to 3 Mbps, the reference sector is consistent about reaching higher probabilities in those intervals.

## REFERENCES

- [1] Tavares, T., Sebastião, P., Souto, N., Velez, F., Cercas, F., Ribeiro, M., & Correia, A. (2015). *Generalized LUI Propagation Model for UAVs Communications Using Terrestrial Cellular Networks* (MSc). ISCTE-IUL.
- [2] Varela, F., Sebastiao, P., Correia, A., Cercas, F., Rodrigues, A., Velez, F., & Robalo, D. (2010). Validation of the unified propagation model for Wi-Fi, UMTS and WiMAX planning. *21st Annual IEEE International Symposium On Personal, Indoor And Mobile Radio Communications*.  
<http://dx.doi.org/10.1109/pimrc.2010.5672049>
- [3] SARAIVA, TIAGO MARTINS, 2017, Reliable air to ground communications for low altitude unmanned aerial vehicles. *Repositorio.iscte-iul.pt* [online]. Available from: <https://repositorio.iscte-iul.pt/handle/10071/11480>
- [4] *Mobile Communications: from 1G to 4G*. Retrieved April 2017, from [http://europa.eu/rapid/exploit/2014/02/MEMO/EN/m14\\_129.eni/Pictures/100000000000E10000006C050D82666.jpg](http://europa.eu/rapid/exploit/2014/02/MEMO/EN/m14_129.eni/Pictures/100000000000E10000006C050D82666.jpg)
- [5] *GSM Coverage*. Retrieved April 2017, from [http://ntrg.cs.tcd.ie/undergrad/4ba2.05/group7/map\\_global.jpg](http://ntrg.cs.tcd.ie/undergrad/4ba2.05/group7/map_global.jpg)
- [6] Sauter, M. (2011). *From GSM to LTE*. Chichester: Wiley-Blackwell.
- [7] Chevallier, C. (2006). *WCDMA (UMTS) deployment handbook* (pp. 1-18). Chichester: Wiley.
- [8] Sanchez, J., & Thioune, M. (2007). *UMTS*. Newport Brach, CA: ISTE Ltd, LAVOISER.
- [9] *Overview of 3GPP Release 99*. (2004). Retrieved from [http://www.3gpp.org/tsg\\_cn/TSG\\_CN/TSGN\\_23/Docs/PDF/NP-040010.pdf](http://www.3gpp.org/tsg_cn/TSG_CN/TSGN_23/Docs/PDF/NP-040010.pdf)
- [10] *3G*. *Pt.wikipedia.org*. Retrieved April 2017, from <https://pt.wikipedia.org/wiki/3G>
- [11] *LTE*. (2017). *3gpp.org*. Retrieved April 2017, from <http://www.3gpp.org/technologies/keywords-acronyms/98-lte>
- [12] Carreira, P. (2011). *Data Rate Performance Gains in UMTS Evolution to LTE at the Cellular Level* (MSc). Instituto Superior Técnico.
- [13] *teleco.com.br*. *Teleco*. Retrieved April 2017, from [http://www.teleco.com.br/tutoriais/tutorial3ghandover/pagina\\_2.asp](http://www.teleco.com.br/tutoriais/tutorial3ghandover/pagina_2.asp)

- [14] 3G UMTS Handover | WCDMA Hard Soft | Radio-Electronics.com. Radio-electronics.com. Retrieved April 2017, from <http://www.radio-electronics.com/info/cellulartelecomms/umts/umts-wcdma-handover-handoff.php>
- [15] Handover Procedures | White Papers | Artiza Networks. Artizanetworks.com. Retrieved April 2017, from [http://www.artizanetworks.com/resources/white/han\\_pro.html](http://www.artizanetworks.com/resources/white/han_pro.html)
- [16] *SPECTRAN HF-60100*. Retrieved from [http://www.aaronia.com/fileadmin/img/spectran-hf/spectrum\\_analyzer\\_aaronia\\_spectran-hf\\_4.jpg](http://www.aaronia.com/fileadmin/img/spectran-hf/spectrum_analyzer_aaronia_spectran-hf_4.jpg)
- [17] *Product Brochure | Version 11.00 R&S@TSME*. (2017). Munich. Retrieved from [https://cdn.rohde-schwarz.com/pws/dl\\_downloads/dl\\_common\\_library/dl\\_brochures\\_and\\_datasheets/pdf\\_1/service\\_support\\_30/TSME\\_bro\\_en\\_3606-7418-12\\_v1100.pdf](https://cdn.rohde-schwarz.com/pws/dl_downloads/dl_common_library/dl_brochures_and_datasheets/pdf_1/service_support_30/TSME_bro_en_3606-7418-12_v1100.pdf)
- [18] Rohde & Schwarz. (2017). *TSME connected to notebook*. Retrieved from [https://cdn.rohde-schwarz.com/pws/product/tsme/TSME\\_img\\_01\\_lightbox\\_landscape.jpg](https://cdn.rohde-schwarz.com/pws/product/tsme/TSME_img_01_lightbox_landscape.jpg)
- [19] *TSMA Product Brochure and Data Sheets*. (2015). Munich. Retrieved from <https://www.rohde-schwarz.com/us/brochure-datasheet/tsma/>
- [20] Rohde & Schwarz. (2015). *TSMA Spectrum Analyzer*. Retrieved from [https://cdn.rohde-schwarz.com/pws/product/tsma/TSMA\\_img\\_03.jpg](https://cdn.rohde-schwarz.com/pws/product/tsma/TSMA_img_03.jpg)
- [21] *Portugal Wireless Frequency Bands and Carriers*. (2017). *Frequencycheck.com*. Retrieved April 2017, from <https://www.frequencycheck.com/countries/portugal>
- [22] *Modelos de Propagação*. (2016). Lisbon. Retrieved from [https://fenix.tecnico.ulisboa.pt/downloadFile/3779571243383/03\\_ModelProp.pdf](https://fenix.tecnico.ulisboa.pt/downloadFile/3779571243383/03_ModelProp.pdf)
- [23] Abuibaid. (2016). OKUMURA, HATA and COST231 Propagation Models. Pt.slideshare.net. Retrieved April 2017, from [https://pt.slideshare.net/M\\_A\\_Abuibaid/okumura-hata-and-cost231-propagation-models](https://pt.slideshare.net/M_A_Abuibaid/okumura-hata-and-cost231-propagation-models)
- [24] *Correction factor for different types of terrain*. Retrieved from [https://upload.wikimedia.org/wikipedia/commons/thumb/8/81/Figure\\_3.24.png/400px-Figure\\_3.24.png](https://upload.wikimedia.org/wikipedia/commons/thumb/8/81/Figure_3.24.png/400px-Figure_3.24.png)

- [25] *Okumura Model*. *Image.slidesharecdn.com*. Retrieved April 2017, from <https://image.slidesharecdn.com/propagationmodelspresentation-160701040815/95/okumura-hata-and-cost231-propagation-models-9-638.jpg>
- [26] Deme, A., Dajab, D., & Nyap, D. (2013). Computer Analysis of the COST 231 Hata Model and Least Squares Approximation for Path Loss Estimation at 900MHz on the Mountain Terrains of the Jos - Plateau, Nigeria. *Iiste.Org*, 4(9), 39-40. Retrieved from: <http://iiste.org/Journals/index.php/CEIS/article/viewFile/7022/7172>
- [27] *3 Radio Propagation Modeling*. (2016). *Morse.colorado.edu*. Retrieved May 2017, from <http://morse.colorado.edu/~tlen5510/text/classwebch3.html>
- [28] Sati, G., & Singh, S. (2014). A review on outdoor propagation models in radio communication. *International Journal Of Computer Engineering & Science*, 4(2), 64-68. Retrieved from [http://www.ijces.org/media/4Iss8-IJCES0402604\\_v4\\_iss2\\_64-68.pdf](http://www.ijces.org/media/4Iss8-IJCES0402604_v4_iss2_64-68.pdf)
- [29] Varela, F., Sebastiao, P., Correia, A., Cercas, F., Rodrigues, A., Velez, F., & Robalo, D. (2010). Validation of the unified propagation model for Wi-Fi, UMTS and WiMAX planning. *21St Annual IEEE International Symposium On Personal, Indoor And Mobile Radio Communications*, 87-92. <http://dx.doi.org/10.1109/pimrc.2010.5672049>
- [30] Varela, F., Sebastiao, P., Correia, A., Cercas, F., Rodrigues, A., Velez, F., & Robalo, D. (2010). Unified propagation model for Wi-Fi, UMTS and WiMAX planning in mixed scenarios. *21St Annual IEEE International Symposium On Personal, Indoor And Mobile Radio Communications*. <http://dx.doi.org/10.1109/pimrc.2010.5672001>
- [31] *Supporting Wireless Video Growth and Trends*. (2013). *5G Americas*. Retrieved March 2017, from [http://www.5gamericas.org/files/5914/0759/2963/4G\\_Americas\\_-\\_Supporting\\_Mobile\\_Video\\_Growth\\_and\\_Trends\\_April\\_2013.pdf](http://www.5gamericas.org/files/5914/0759/2963/4G_Americas_-_Supporting_Mobile_Video_Growth_and_Trends_April_2013.pdf)
- [32] *R&S TSMA Autonomous Mobile Network Scanner - Getting Started*. (2017). Munich. Retrieved from [https://cdn.rohde-schwarz.com/pws/dl\\_downloads/dl\\_common\\_library/dl\\_manu\\_als/gb\\_1/t/tsma\\_1/TSMA\\_GettingStarted\\_en\\_08.pdf](https://cdn.rohde-schwarz.com/pws/dl_downloads/dl_common_library/dl_manu_als/gb_1/t/tsma_1/TSMA_GettingStarted_en_08.pdf)

- [33] *Localização das antenas MEO/NOS/VODAFONE*. (2017). *ZWAME Fórum*. Retrieved March 2017, from <https://forum.zwame.pt/threads/localizacao-das-antenas-meo-nos-vodafone.864418/>
- [34] *Drive Test Software R&S@ROMES 4 Version 4.92 Operating Manual*. (2016). Munich.
- [35] *What is the minimum RSSI needed for 3G or LTE?*. (2015). <https://www.linkedin.com/pulse/what-minimum-rssi-needed-3g-lte-andre-fourie>. Retrieved April 2017, from <https://www.linkedin.com/pulse/what-minimum-rssi-needed-3g-lte-andre-fourie>
- [36] *3G Scrambling Code Planning as part of the RNC databuild (on the Downlink)*. (2017). *Trends-in-telecoms.blogspot.pt*. Retrieved March 2017, from <http://trends-in-telecoms.blogspot.pt/2012/06/3g-scrambling-code-planning-as-part-of.html>
- [37] *Kathrein 742215 Gain Pattern*. (2017). Retrieved from [http://www.raymaps.com/wp-content/uploads/2011/10/radiation\\_pattern1.jpg](http://www.raymaps.com/wp-content/uploads/2011/10/radiation_pattern1.jpg)
- [38] *WCDMA Capacity (Mbps) | RAYmaps*. (2011). *Raymaps.com*. Retrieved April 2017, from <http://www.raymaps.com/index.php/wcdma-capacity/>
- [39] *Shannon Capacity | RAYmaps*. (2015). *Raymaps.com*. Retrieved April 2017, from <http://www.raymaps.com/index.php/tag/shannon-capacity/>
- [40] Donovan, J. (2014). *Cells, Sectors and Antenna Beamforming*. *Commscope.com*. Retrieved May 2017, from <http://www.commscope.com/Blog/Cells--Sectors-and-Antenna-Beamforming/>
- [41] *Most up to date list of MCC and MNC codes: mobile country codes – mobile network codes*. (2017). *Mcc-mnc.com*. Retrieved May 2017, from <http://mcc-mnc.com/>
- [42] *Diário da República, 2.ª série — N.º 238 — 14 de dezembro de 2016*. (2016) (pp. 36613-36622). Retrieved May 2017, from [https://docs.wixstatic.com/ugd/8aa7ba\\_a022d1b08fa7468ca3d8b9f5d4cea4d6.pdf](https://docs.wixstatic.com/ugd/8aa7ba_a022d1b08fa7468ca3d8b9f5d4cea4d6.pdf)
- [43] Drones Portugal. (2017). *Scenario A - Drone's planned route*. Retrieved from <https://www.youtube.com/watch?v=36lVpkVlre0&feature=youtu.be>
- [44] Drones Portugal. (2017). *Scenario B - Drone's planned route*. Retrieved from [https://www.youtube.com/watch?v=2qXA\\_rnJnAU&feature=youtu.be](https://www.youtube.com/watch?v=2qXA_rnJnAU&feature=youtu.be)

- [45] Drones Portugal. (2017). *Scenario C - Drone's planned route*. Retrieved from <https://www.youtube.com/watch?v=02CPAYe1XIA&feature=youtu.be>